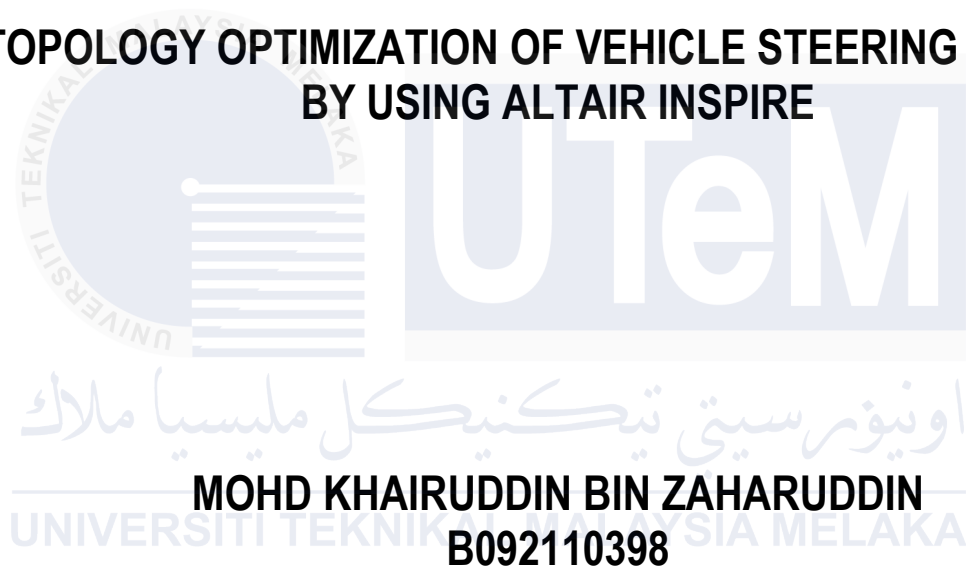




# **TOPOLOGY OPTIMIZATION OF VEHICLE STEERING KNUKLE BY USING ALTAIR INSPIRE**



**MOHD KHAIRUDDIN BIN ZAHARUDDIN**  
**B092110398**

**BACHELOR OF MECHANICAL ENGINEERING  
TECHNOLOGY (AUTOMOTIVE) WITH HONOURS**

**2025**



**Faculty of Mechanical Technology and Engineering**

**TOPOLOGY OPTIMIZATION OF VEHICLE STEERING KNUCKLE  
BY USING ALTAIR INSPIRE**



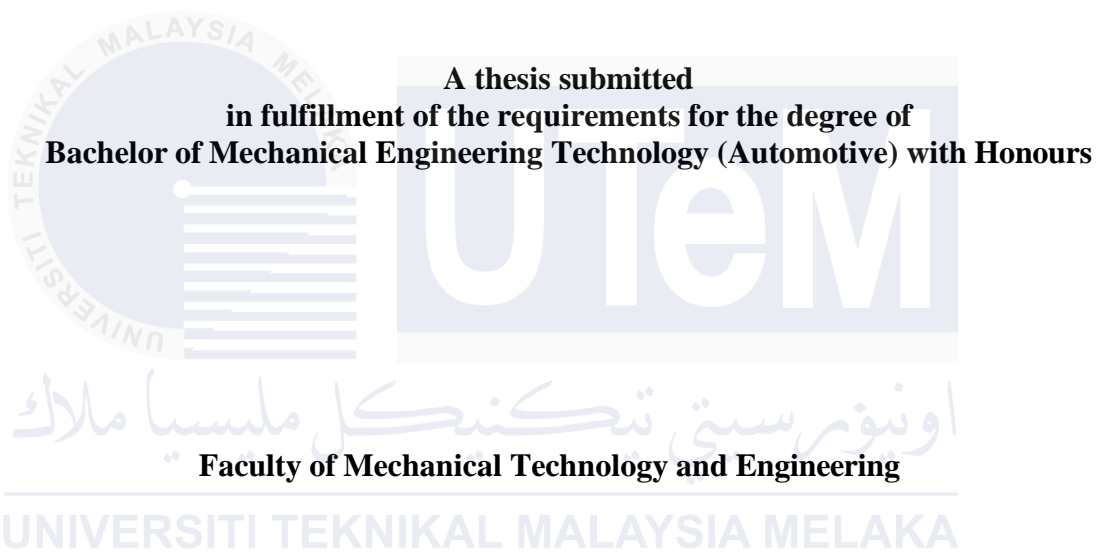
Mohd Khairuddin Bin Zaharuddin

**Bachelor of Mechanical Engineering Technology (Automotive) with Honours**

**2025**

**TOPOLOGY OPTIMIZATION OF VEHICLE STEERING KNUCKLE BY USING  
ALTAIR INSPIRE**

**MOHD KHAIRUDDIN BIN ZAHARUDDIN**



**UNIVERSITI TEKNIKAL MALAYSIA MELAKA**

**2025**

**BORANG PENGESAHAN STATUS LAPORAN PROJEK SARJANA MUDA**

**TAJUK: TOPOLOGY OPTIMIZATION OF VEHICLE STEERING KNUCKLE BY USING ALTAIR INSPIRE**

**SESI PENGAJIAN: 2024-2025 Semester 1**

Saya **MOHD KHAIRUDDIN BIN ZAHARUDDIN**

mengaku membenarkan tesis ini disimpan di Perpustakaan Universiti Teknikal Malaysia Melaka (UTeM) dengan syarat-syarat kegunaan seperti berikut:

1. Tesis adalah hak milik Universiti Teknikal Malaysia Melaka dan penulis.
2. Perpustakaan Universiti Teknikal Malaysia Melaka dibenarkan membuat salinan untuk tujuan pengajian sahaja dengan izin penulis.
3. Perpustakaan dibenarkan membuat salinan tesis ini sebagai bahan pertukaran antara institusi pengajian tinggi.
4. \*\*Sila tandakan (✓)

☐

TERHAD

(Mengandungi maklumat yang berdarjah keselamatan atau kepentingan Malaysia sebagaimana yang termaktub dalam AKTA RAHSIA RASMI 1972)

☐

SULIT

(Mengandungi maklumat TERHAD yang telah ditentukan oleh organisasi/badan di mana penyelidikan dijalankan)

☒

TIDAK TERHAD

Disahkan oleh:

Alamat Tetap:

**AHMAD ZUL HUSNI BIN CHE MAMAT**  
Cop Rasmi: **Jurutera Pengajar**  
**Fakulti Teknologi Dan Kejuruteraan Mekanikal**  
**Universiti Teknikal Malaysia Melaka (UTeM)**

Tarikh: 9 JANUARY 2025

Tarikh: 10 FEBRUARY 2025

**\*\* Jika tesis ini SULIT atau TERHAD, sila lampirkan surat daripada pihak berkuasa/organisasi berkenaan dengan menyatakan sekali sebab dan tempoh laporan PSM ini perlu dikelaskan sebagai SULIT atau TERHAD.**

## DECLARATION

I declare that this bachelor's degree project entitled "Topology Optimization of Vehicle Steering Knuckle By Using Altair Inspire" is the result of my own research except as cited in the references. The bachelor's degree project has not been accepted for any degree and is not concurrently submitted in candidature of any other degree.

Signature

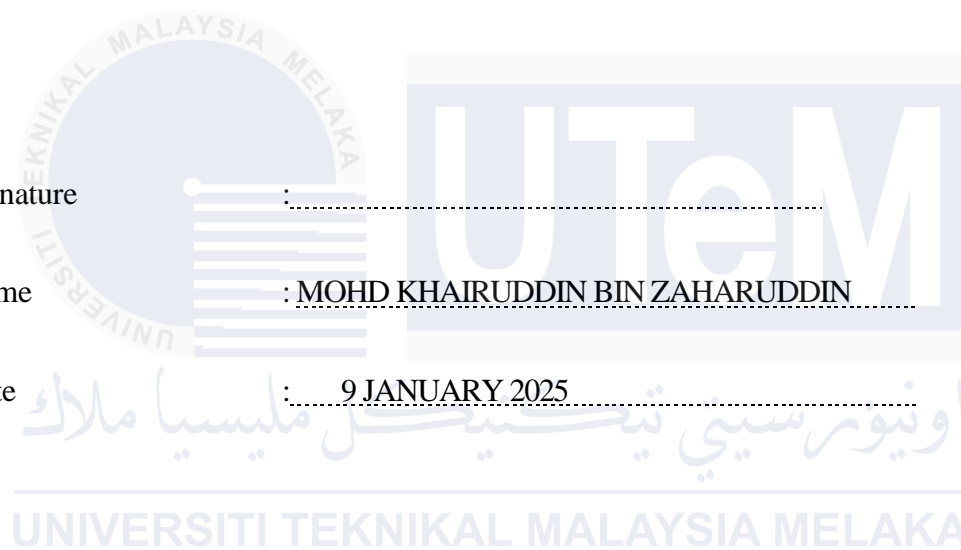
Name

Date

.....

: MOHD KHAIRUDDIN BIN ZAHARUDDIN

: 9 JANUARY 2025



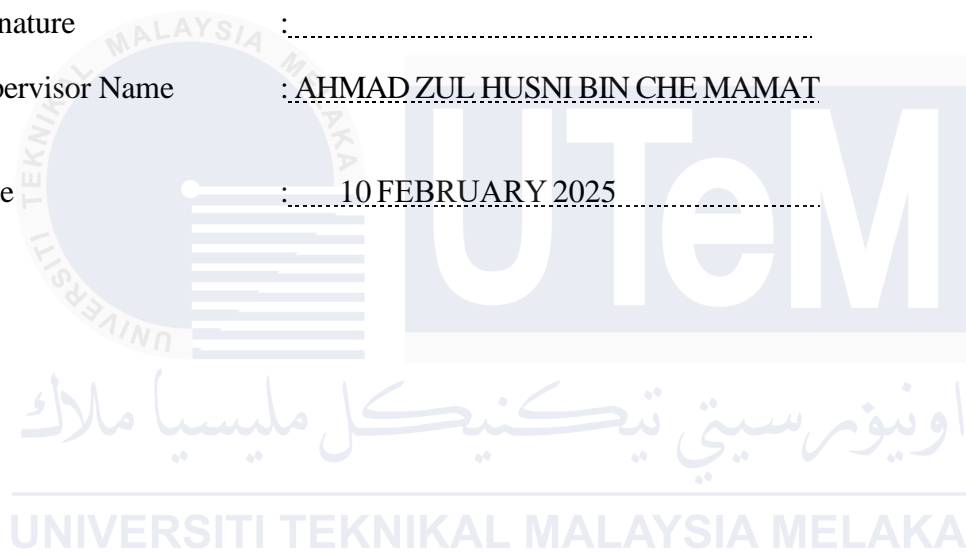
## APPROVAL

I hereby declare that I have checked this thesis and in my opinion, this thesis is adequate in terms of scope and quality for the award of the Bachelor of Degree Engineering Technology (Automotive) with Honours.

Signature : .....

Supervisor Name : AHMAD ZUL HUSNI BIN CHE MAMAT

Date : 10 FEBRUARY 2025



## DEDICATION

I hereby dedicate this here piece of work to my precious parents and my trusty supervisor, Ahmad Zul Husni Bin Che Mamat. They have been my rock, offering me love and support through thick and thin. I couldn't have done it without them. Much obliged for giving me the grit to wrap up my Bachelor's Degree Project.



## ABSTRACT

Steering knuckles are important components of the steering system, essential for maintaining vehicle stability as well as controlling steering. This research analyses the topological optimization of a vehicle steering knuckle with Altair Inspire to optimize structural performance, weight, and improve fuel efficiency. The steering knuckle, a necessary component connecting suspension, steering, and braking systems, has to possess an optimal combination of strength, durability, and lightweight characteristics according to safety and operational requirements. The analysis begins with the reverse engineering process by using the EX-Scan Pro system to scan the component, followed by complex CAD modelling in CATIA V5. Structural analysis, including stress distribution and displacement analysis, is conducted with Finite Element Analysis (FEA). Topology optimization methodologies are used to improve geometry and reduce weight while maintaining structural integrity. Furthermore, lattice structures are used to improve mechanical performance. The results show that optimizing topology and lattice structures significantly decreases component weight without compromising strength, hence enhancing fuel efficiency and supporting sustainable automotive methods of design.

UNIVERSITI TEKNIKAL MALAYSIA MELAKA



## ABSTRAK

Buku jari stereng adalah komponen penting dalam sistem stereng, yang berperanan utama dalam mengekalkan kestabilan kenderaan serta kawalan stereng. Penyelidikan ini menganalisis pengoptimuman topologi buku jari stereng kenderaan menggunakan Altair Inspire untuk mengoptimumkan prestasi struktur, mengurangkan berat, dan meningkatkan kecekapan bahan api. Buku jari stereng, komponen penting yang menghubungkan sistem suspensi, stereng, dan brek, perlu mempunyai kombinasi kekuatan, ketahanan, dan ciri ringan yang optimum mengikut keperluan keselamatan dan operasi. Analisis bermula dengan proses reverse engineering menggunakan sistem EX-Scan Pro untuk mengimbas komponen tersebut, diikuti dengan pemodelan CAD yang kompleks dalam CATIA V5. Analisis struktur, termasuk pengagihan tegasan dan analisis anjakan, dijalankan menggunakan Finite Element Analysis (FEA). Kaedah pengoptimuman topologi digunakan untuk menambah baik geometri dan mengurangkan berat sambil mengekalkan integriti struktur. Selain itu, struktur kekisi digunakan untuk meningkatkan prestasi mekanikal. Hasil kajian menunjukkan bahawa pengoptimuman topologi dan struktur kekisi secara signifikan mengurangkan berat komponen tanpa menjejaskan kekuatan, seterusnya meningkatkan kecekapan bahan api dan menyokong amalan reka bentuk automotif yang mampan.

UNIVERSITI TEKNIKAL MALAYSIA MELAKA

## ACKNOWLEDGEMENTS

In the Name of Allah, the Most Gracious, the Most Merciful

Bissmillahirrahmanirrahim, Alhamdulillah. Thank you to Allah SWT, whom with His willing giving us the opportunity to complete our research thesis. This final year project report was prepared for University of Technical Malaysia Melaka (UTeM). I just wanted to take a moment to thank everyone who helped make this research project a success. Your contributions are greatly appreciated. This project would not have been possible without the help, advice, and motivation they provided.

At the outset, I would like to express my gratitude to Ahmad Zul Husni bin Che Mamat, from University of Technical Malaysia Melaka (UTeM) for all of the help, advice, and encouragement they've given me throughout this study project. The course and quality of this research have been greatly influenced by their intelligent comments, critical feedback, and ready availability. Furthermore, I would like to extend my gratitude to Mohd Rafi bin Omar and Ts. Mohd Hafizi Bin Abdul Rahman, from University of Technical Malaysia Melaka (UTeM) for assisting and providing me with invaluable feedback and suggestions.

Thank you so much for giving me with the opportunity to do this research at University of Technical Malaysia Melaka (UTeM). The research funding, database access, and laboratory resources have all been important for gathering and analysing the necessary data.

I'd like to give thanks to the people who helped me during my studies and at work. The project greatly benefited from their openness to sharing information, participating in conversations, and lending assistance. Their input improved the quality of the research as a whole. I would want to express my sincere appreciation to everyone who took part in this research and offered their time, energy, and expertise. The research results and conclusions offered here would not be possible without their assistance.

I'd like to thank my parents and loved ones for their unending encouragement, tolerance, and understanding as I've worked on this study. Their unending support, affection, and faith in me had kept me going whenever I felt down.

In closing, I would like to express my deep appreciation to everyone who has helped bring this study to fruition. Thank you for all of your help, advice, and input as we developed this piece. We appreciate your help, support, and confidence in the importance of this study.

## TABLE OF CONTENT

<b>ABSTRACT .....</b>	<b>i</b>
<b>ABSTRAK.....</b>	<b>ii</b>
<b>ACKNOWLEDGEMENTS .....</b>	<b>iii</b>
<b>TABLE OF CONTENT .....</b>	<b>iv</b>
<b>LIST OF TABLES.....</b>	<b>vi</b>
<b>LIST OF FIGURES.....</b>	<b>vii</b>
<b>LIST OF SYMBOLS AND ABBREVIATIONS.....</b>	<b>x</b>
<b>LIST APPENDIX .....</b>	<b>xi</b>
<b>INTRODUCTION .....</b>	<b>1</b>
1.1 Background.....	1
1.2 Problem Statement .....	2
1.3 Research Objective.....	3
1.4 Scope of Research .....	3
1.5 Rational of Study.....	4
<b>LITERATURE REVIEW .....</b>	<b>5</b>
2.1 History of the Steering Knuckle Mechanism .....	5
2.2 Types of Steering Knuckle .....	6
2.3 Steering Knuckle: Function and Design Considerations.....	8
2.4 Materials for Steering Knuckles.....	10
2.4.1 Aluminium Alloy .....	11
2.4.2 Mild Steel .....	13
2.4.3 Cast Iron .....	14
2.5 Manufacturing Methods for Steering Knuckles .....	16
2.5.1 Forging .....	17
2.5.2 CNC Machining .....	19
2.6 Computer Aided Design (CAD).....	20
2.6.1 CATIA V5 Generative Shape Design (GSD) .....	21
2.6.2 CATIA V5 Part Design .....	21
2.7 Computer Aided Engineering (CAE).....	22
2.7.1 ANSYS.....	23
2.7.2 Altair Inspire .....	24
2.7.3 Meshing and Type of Elements.....	25
2.7.4 Topology Optimization .....	27
2.7.5 Topography Optimization .....	28
2.7.6 Lattice Structure .....	29
2.8 Applications of Topology Optimization in Automotive Design.....	30
2.9 Applications of Lattice Structure in Automotive Design.....	32
2.10 Impact of Topology Optimization on Vehicle Performance .....	33
2.11 Summary .....	34

<b>METHODOLOGY .....</b>	<b>35</b>
3.1 Introduction.....	35
3.1.1 Flow Chart.....	36
3.2 Scanning Part.....	37
3.2.1 Scanner .....	39
3.2.2 Mode of Alignment .....	40
3.2.3 Generate Points Cloud.....	42
3.2.4 Alignment.....	43
3.2.5 Mesh Optimization and Editing .....	44
3.3 CATIA V5 Generative Shape Design (GSD) .....	47
3.4 CATIA V5 Part Design .....	50
3.5 Design Validation.....	51
3.6 Altair Motion View .....	53
3.6.1 Setup Model Front Suspension Vehicle .....	53
3.6.2 Setup Analysis Static Load .....	55
3.7 Altair Inspire .....	61
3.7.1 Static Structural Analysis .....	61
3.7.2 Topology Optimization .....	65
3.7.3 Lattice Structure Optimization .....	71
3.8 Summary .....	76
<b>RESULTS AND DISCUSSION.....</b>	<b>77</b>
4.1 Introduction.....	77
4.2 Static Structural Analysis Base Model.....	77
4.3 Topology Analysis and Optimization .....	80
4.3.1 Topology Optimized 30% .....	80
4.3.2 Topology Optimized 40% .....	83
4.3.3 Topology Optimized 50% .....	86
4.4 Comparison Analysis Between Base Model And 3 Topology Model .....	89
4.5 Lattice Structure Analysis .....	92
4.6 Comparison Between Base Model, Optimized and Lattice Structure.....	95
4.7 Summary .....	97
<b>CONCLUSION &amp; RECOMMENDATION.....</b>	<b>98</b>
5.1 Conclusion.....	98
5.2 Recommendations .....	99
5.2.1 Future Research.....	99
<b>REFERENCES .....</b>	<b>100</b>
<b>APPENDICES.....</b>	<b>106</b>

## LIST OF TABLES

Table 2.1: Mechanical Properties of type Aluminium alloy (Sathishkumar & Kanna, 2019)	12
Table 2.2: Property specification type of Mild Steel (Velmanirajan & Anuradha, 2020)	13
Table 2.3: Property specification type of Cast Iron (Georgantzia et al., 2021)	15
Table 3.1: Weight Model	52
Table 3.2.: Design parameters for setting up the Front Vehicle Suspension	54
Table 3.3: Calculation Vehicle Parameter	56
Table 3.4: Calculation Force X, Y, Z	58
Table 3.5: Data Hardpoint on Left Side	60
Table 3.6: Data for Structural analysis for all designs	62
Table 3.7: Run Optimization Parameter	67
Table 4.1: Result of Base Model	78
Table 4.2: Result of WRM 30%	81
Table 4.3: Result of WRM 40%	83
Table 4.4: Result of WRM 50%	86
Table 4.5: Comparison for all WRM	89
Table 4.6: Result Data of LSM	93
Table 4.7: Comparison Analysis Data of Base Model, WRM 40% and LSM	96

## LIST OF FIGURES

Figure 2.1: Steering Kuuckle (Kashyzadeh, 2023).....	7
Figure 2.2: Steering knuckle of FSAE2018 vehicle. (Gupta et al., 2021).....	7
Figure 2.3: Nomenclature used for Forged Steel Steering Knuckle (Jhala et al., 2010) .....	7
Figure 2.4: The Steering Knuckle and Suspension Assembly (Lee & Rahman, 2021) .....	8
Figure 2.5: Application of the Steering Knuckle ( <a href="https://en.wikipedia.org/wiki/Steering_knuckle">https://en.wikipedia.org/wiki/Steering_knuckle</a> ).....	9
Figure 2.6: Methods of Forging ( <a href="https://shorturl.at/f8fDf">https://shorturl.at/f8fDf</a> ).....	17
Figure 2.7: CNC Knuckle Steering ( <a href="https://shorturl.at/fRii5">https://shorturl.at/fRii5</a> ) .....	19
Figure 2.8: Elements of Computer Aided Design (CAD) (Terrile et al., 2004) .....	20
Figure 2.9: The Elements of CAE ( <a href="https://shorturl.at/lyCez">https://shorturl.at/lyCez</a> ).....	23
Figure 2.10: Type of Mesh 3D Elements( <a href="https://shorturl.at/l2R0a">https://shorturl.at/l2R0a</a> ).....	26
Figure 2.11: Structural planning of knuckle prototype. (Mailapalli et al., 2023).....	27
Figure 2.12: A topography optimized sheet metal (Sun et al., 2023).....	28
Figure 2.13: A topologically optimized solid-lattice hybrid structure (Zhu et al., 2021) .....	29
Figure 2.14: Configuration of the design space (Matsimbi et al., 2021).....	30
Figure 2.15: Lightweight components with lattice structure for helicopters and racing cars. (Tao & Leu, 2016).....	32
Figure 3.1: Flowchart for Shape Optimization in Automotive Engineering .....	36
Figure 3.2: EXScan Pro .....	38
Figure 3.3: EinScan Pro HD .....	39
Figure 3.4: Steering Knuckle.....	39
Figure 3.5: Selection Scan Mode.....	40
Figure 3.6: Selection Mode of Alignment .....	41
Figure 3.7: Data Editing / Meshing for Top View .....	42
Figure 3.8: Data Editing / Meshing for Bottom View .....	42
Figure 3.9: Alignment Top view and Bottom View .....	43
Figure 3.10: Mesh Parameter.....	44
Figure 3.11: Mesh Editing Manual Hole Filling .....	45
Figure 3.12: Mesh Editing Smooth Section.....	45
Figure 3.13: Mesh Editing Process Completed .....	46
Figure 3.14: Generative Shape Design .....	47
Figure 3.15: Fill Surface Definition .....	48
Figure 3.16: Split Definition.....	48
Figure 3.17: Steering Knuckle Before Fill Surface .....	49

Figure 3.18: Steering Knuckle After Fill Surface.....	49
Figure 3.19: The Steering Knuckle Part Design.....	50
Figure 3.20 : (a) Actual Steering Knuckle (b) Base Model.....	51
Figure 3.21: Vehicle Parameter .....	55
Figure 3.22: Load Case.....	57
Figure 3.23: Load Case for Each Axis .....	57
Figure 3.24: Run Static Load Analysis.....	59
Figure 3.25: Result Animation of Assembly Front Wheel Drive.....	59
Figure 3.26: Design Base Model and Boundary Conditions .....	62
Figure 3.27: Setup to run the structural simulation analysis .....	63
Figure 3.28: Analysis Explorer.....	64
Figure 3.29: Partition on Steering Knuckle .....	65
Figure 3.30: Design Space on Steering Knuckle.....	66
Figure 3.31: Shape Explorer .....	68
Figure 3.32: Optimized Steering Knuckle.....	69
Figure 3.33: PolyNURBS Shape After Optimized.....	69
Figure 3.34: Lattice Icon (Altair Inspire, 2023) .....	71
Figure 3.35: Strut Lattice Body Selection .....	72
Figure 3.36: Sturt Lattice Outer Body .....	72
Figure 3.37: Steering Knuckle With lattice body .....	73
Figure 3.38: Run Analysis Model of Lattice Structure .....	74
Figure 3.39: Analysis Process Completed.....	74
Figure 4.1: Base Model Analysis .....	77
Figure 4.2: Displacement of Base Model .....	79
Figure 4.3: Von Mises Stress of Base Model .....	79
Figure 4 4 : Factor of Safety of Base Model .....	79
Figure 4.5: Steering Knuckle 30% .....	80
Figure 4.6: WRM 30% Displacement .....	81
Figure 4.7: WRM 30% Von Mises Stress .....	82
Figure 4.8: WRM 30% Factor of Safety.....	82
Figure 4.9: Steering Knuckle 40% .....	83
Figure 4.10: WRM 40% Displacement .....	84
Figure 4.11: WRM 40% Von Mises Stress .....	84
Figure 4.12: WRM 40% Factor of Safety.....	85
Figure 4.13: Steering Knuckle 50% .....	86
Figure 4.14: WRM 50% Displacement .....	87

Figure 4.15: WRM 50% Von Mises Stress .....	87
Figure 4.16: WRM 50% Factor of Safety.....	88
Figure 4.17: Comparison Analysis Data (a) Von Mises Stress (b) Displacement (c) Factor of Safety .....	90
Figure 4.18: Steering Knuckle Lattice Structure Analysis .....	92
Figure 4.19: LSM Displacement .....	94
Figure 4.20: LSM Von Mises Stress .....	94
Figure 4.21: LSM Factor of Safety.....	94
Figure 4.22: (a) Base Model (b) WRM 40% (c) LSM .....	96





## LIST OF SYMBOLS AND ABBREVIATIONS

$\rho$	-	Density
E	-	Young' Modulus
$\nu$	-	Poisson's Ratio
$\sigma_u$	-	Ultimate strength
$\sigma_y$	-	Yield Stress
$\sigma_f$	-	Fatigue Limit
SUV	-	Sport Utility Vehicle
ATSM	-	American Society for Testing and Materials
CNC	-	Computer Numerical Control
AM	-	Additive Manufacturing
GSD	-	Generative Shape Design
AISI	-	American Iron and Steel Institute
FEA	-	Finite Element Analysis
CAE	-	Computer Aided Engineering
CAD	-	Computer Aided Design
FSAE	-	Formula Society of Automotive Engineers
ANSYS	-	Analysis System
CATIA	-	Computer Aided Three-dimensional Interactive Application
3D	-	3 Dimensions
WRM	-	Weight Reduction Model
LSM	-	Lattice Structure Model
Kg	-	Kilograms
MPa	-	Mega Pascal
Mm	-	Millimeter

## LIST APPENDIX

Appendix A Graph Wheel Centre Left.....	108
Appendix B Graph Lower Arm Left .....	108
Appendix C Graph Absorber Left .....	109
Appendix D Graph Tie Rod Left.....	109
Appendix E Graph For 4 Parts in Left Side.....	110
Appendix F Technical Drawing of Base Model (Load Case 1) .....	111
Appendix G Base Model .....	112
Appendix H WRM 30% .....	112
Appendix I WRM 40% .....	113
Appendix J WRM 50%.....	113
Appendix K Model (Lattice Structure).....	114
Appendix L Base Model Fabrication.....	114
Appendix M WRM 40% Fabrication .....	115
Appendix N Lattice Structure Model Fabrication .....	115

# CHAPTER 1

## INTRODUCTION

### 1.1 Background

A variety of steering knuckles can be obtained, each fitted to a particular suspension configuration. A spindle is a common component in non-drive suspension systems; it functions as a hub to which braking components are attached and as a means of sustaining the weight of the wheel assembly. By contrast, direct drive suspension systems use a hub housing bearing system and a drive shaft instead of a spindle, which influences wheel rotation depending on drive shaft engagement.

The design of the steering knuckle varies depending on the type of suspension system used in the vehicle. In a conventional suspension configuration, the steering knuckle is commonly linked to the lower control arm, upper control arm, and tie rod end. In contemporary designs, such as MacPherson strut suspensions, the steering knuckle is incorporated into the strut assembly.

For the steering knuckle to withstand the forces applied to it in everyday driving situations and unexpected collisions like potholes or bumps in the road, it must be resilient and durable. Typically, it is constructed from an aluminum alloy or high-strength steel to maintain structural integrity and minimize weight. For a vehicle to operate safely and effectively, the steering knuckle must be properly maintained and inspected. It is important to take quick action in case of any damage, such as fractures or excessive wear, to avoid steering problems and possible accidents.

Weight reduction is an important goal in engineering, specifically inside the automotive industry. By using advanced strategies like optimization, it can design additives that maintain strength while the use of much less material. This not only reduces the overall weight of the car, enhancing its overall performance and fuel efficiency, but additionally contributes to decreasing emissions and advanced sustainability.

The study of steering knuckles involves several techniques, such as the use of finite element analysis (FEA) to evaluate displacement and stresses under actual load circumstances, fatigue life comparisons between various materials, and racing car optimization to provide lightweight designs. The research highlights the significance of optimizing steering knuckles to enhance performance and efficiency.

## **1.2 Problem Statement**

The automobile industry is placing a growing focus on improving vehicle performance by reducing the weight of important components, such as the steering knuckle. The steering knuckle is an important part that connects the suspension, steering system, brake, and wheel hub. It can handle a wide range of loads and driving situations while maintaining the best possible steering performance. A thorough strategy is required to do this, beginning with structural analysis to evaluate the effects of static and dynamic loads and identify regions susceptible to stress concentration and deformation.

The issue is to ensure the steering knuckle's durability and performance is crucial as this component must sustain repeated stress and strains during the vehicle's lifetime without substantial wear or failure. However, present steering knuckle designs are too heavy, resulting in increased overall vehicle weight, which affects fuel efficiency and increases emissions. To improve vehicle performance and environmental sustainability, steering knuckle designs must be developed that can withstand a wide range of loads and strains while being lightweight. (Kumar et al., 2020).

### 1.3 Research Objective

The objectives of this project are stated below:

1. To remodel the actual part of steering knuckle into a CAD format.
2. To analyze the maximum stress and maximum displacement of a based model.
3. Comparison study of weight, maximum stress, and maximum displacement of optimized vs-based model steering knuckle.

### 1.4 Scope of Research

The scope of research on vehicle steering knuckles involves several problems such as design, and integration with the vehicle's suspension and steering systems.

- a) To do a reverse engineering of part steering knuckle and model in CATIA V5.
- b) Applying shape optimization methods to reduce the component's weight by 50% to 30%, ensuring a significant decrease in its overall mass.
- c) To increase the strength of steering knuckle by 25%.
- d) CAE will be performed using Static Structural analysis.
- e) Applications of lattice structure in enhancing vehicular maneuverability and structural integrity.

## 1.5 Rational of Study

The rationale for studying topology optimization of a vehicle steering knuckle using Altair Inspire or similar software is multifaceted and encompasses.

- 1) Topology optimizations enhance steering knuckle stiffness, strength, and durability. The knuckle's material distribution may be optimized to better handle vehicle forces and loads, improving handling, and safety.
- 2) Topology optimization aims to minimize structural component weight while boosting performance. A lighter steering knuckle can reduce vehicle weight, improving fuel efficiency, emissions, and performance.
- 3) Topology optimization eliminates waste and concentrates material where it is needed, reducing material use and manufacturing costs. This can reduce production costs while achieving steering knuckle performance and safety standards.
- 4) Advanced algorithms for optimization allow engineers to investigate innovative design combinations that standard design methods might overlook. Engineers can experiment with different steering knuckle designs using Altair Inspire or comparable software to create new, more efficient ones.

## CHAPTER 2

### LITERATURE REVIEW

#### 2.1 History of the Steering Knuckle Mechanism

The steering knuckle mechanism has a long and interconnected records that intently follows the development of car engineering. Steering knuckles saw substantial trends with the introduction of cars within the late 19th and early twentieth centuries. Engineers along with Karl Benz and Henry Ford acknowledged the importance of a sturdy and accurate steering system to guarantee stable and powerful automobile management. The preliminary designs mounted the idea for cutting-edge steering knuckle era by integrating substances and geometries that could endure the higher speeds and stresses of motor motors (Yang & Zhao, 2020).

During the 20th century, the design and capability of steering knuckles improved because of breakthroughs in substances technology and production strategies. The advancement of excessive-power metal and next aluminium alloys facilitated the manufacturing of knuckles that are both lighter and longer lasting, resulting in greater automobile performance and elevated gasoline efficiency. The durability and precision of those additives had been similarly stepped forward via advancements in casting and forging tactics. The implementation of Computer Aided Design (CAD) and Finite Element Analysis (FEA) introduced approximately a good-sized transformation inside the method, allowing to decorate the geometry and cloth distribution to reap superior overall performance. The development on this field has resulted in the development of rather advanced steering knuckles which might be employed in cutting edge cars (Chen et al., 2021).

## 2.2 Types of Steering Knuckle

The steering knuckle is a vital component of a vehicle's suspension and steering systems, serving as the pivotal connection between the wheel and the suspension and steering linkage. Conventional steering knuckles are often designed for different vehicle constructions, possessing extreme features to withstand high pressures and tensions while in use. These knuckles, ordinarily made of solid iron or solid metal, are generally solid for the reason of high durability and good power-to-weight ratio. The conventional steering knuckle consists of attachment elements for the tie rod, lower control arm, and upper control arm or strut. It allows for accurate control of the wheel alignment and promotes smooth steering dynamics (Gupta et al., 2021).

Besides that, the steering knuckles used in Formula SAE have a radically different design than the ones in FSAE2018, specifically tailored to suit performance needs. These knuckles happen to be designed in such a manner to optimize weight, power and stress. This is, however, of utmost importance in race conditions. Generally, these FSAE2018 steering knuckles are made of lightweight yet robust materials such as high-strength aluminium or composite materials. A good level of handling and responsiveness results from this. When talking about forged steel steering knuckles, one is referred to by terms such as "hub flange, steering arm, and ball joint mount". These terms define the various sections of the knuckle that connect specifically to other suspension and steering components. Proper terminology used ensures effective production and assembly of these critical components (Gupta et al., 2021).





Figure 2.1: Steering Kuuckle (Kashyzadeh, 2023)

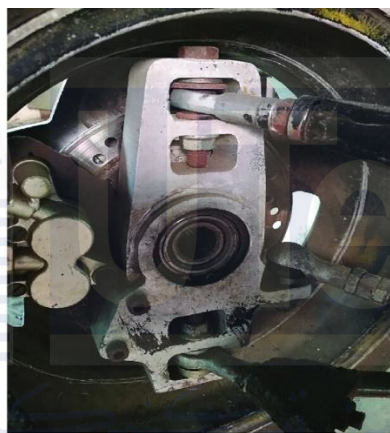


Figure 2.2: Steering knuckle of FSAE2018 vehicle. (Gupta et al., 2021)

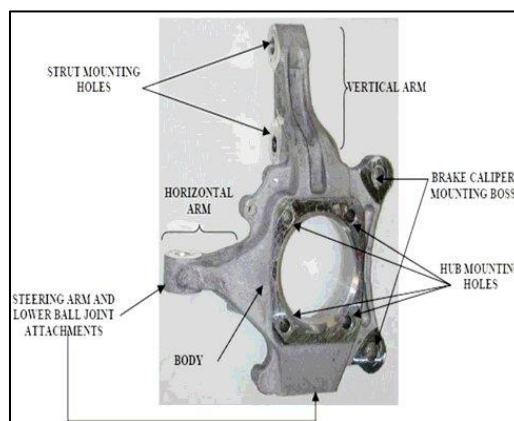


Figure 2.3: Nomenclature used for Forged Steel Steering Knuckle (Jhala et al., 2010)

### 2.3 Steering Knuckle: Function and Design Considerations

The most important element of a car's steering system is the steering knuckle, which attaches the wheel and tire assembly to the suspension system and enables wheel rotation and pivoting at steering (Heißing & Ersoy, 2011). Effective steering and vehicle protection depend on its robust structure and suitable setup. Ensuring safety, preventing steering control issues, and saving costs are critical components of performing routine damage and wear checks. Critical procedures such as greasing and alignment testing should be performed to ensure clean operation and prolong the life span of the steering knuckle (Pugazhenthir et al., 2021).

An inspection for corrosion, cracks, and undue wear is critical, as these factors could negatively influence steering operation. Regular lubrication prevents wear and friction and makes it possible for the steering gear to serve longer effectively (Pugazhenthir et al., 2021). Regular maintenance ensures a good vehicle life along with steering knuckle longevity with safety assurance and better steering performance. Any alterations made to enhance vehicle performance, commonly in suspension or tire length, should warrant the close examination of the steering knuckle to guarantee overall efficiency and safety (Chen et al., 2021).

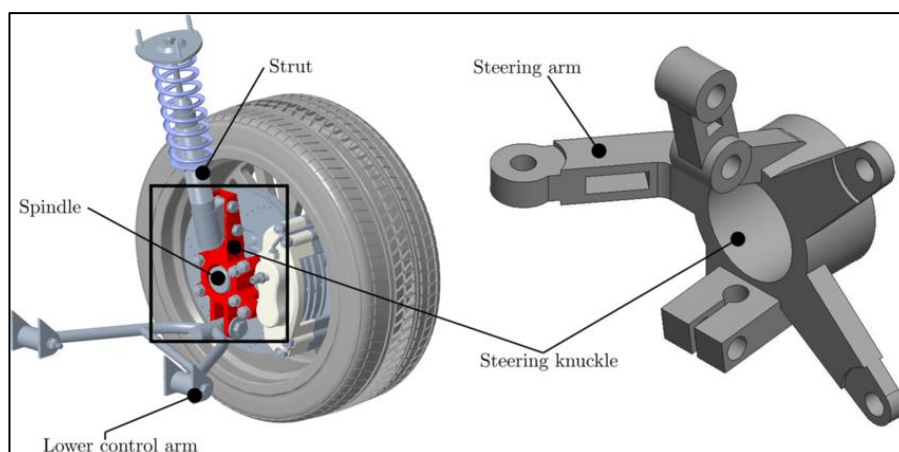


Figure 2.4: The Steering Knuckle and Suspension Assembly (Lee & Rahman, 2021)

Designing a steering knuckle requires comprehensive examination of numerous components to ensure the vehicle's maximum performance and safety. The selection of materials is of paramount significance since the chosen material must be able to endure the stress and loads experienced during steering and suspension, while also achieving a balance between power, durability, and weight. Ensuring the structural integrity of the knuckle is essential for preserving its shape and operation in various settings (A Review on Steering Knuckle Analysis, 2019).

To maximize performance, besides the consideration of materials, it is essential to also focus on other design aspects, like strength, service life, and weight. This is a point that must be analyzed thoroughly for the function of the steering knuckle to be optimized and overall, the vehicle steering system improved. Thus, the focus during structural design will be on achieving a weight reduction balanced with achieving desired optimum levels of strength and durability. (Tyflopoulos et al., 2021).

An ideally engineered steering knuckle should focus on features related to robustness, longevity, and light weight for assured high performance and functioning of the steering system. (Deshpande et al., 2020).

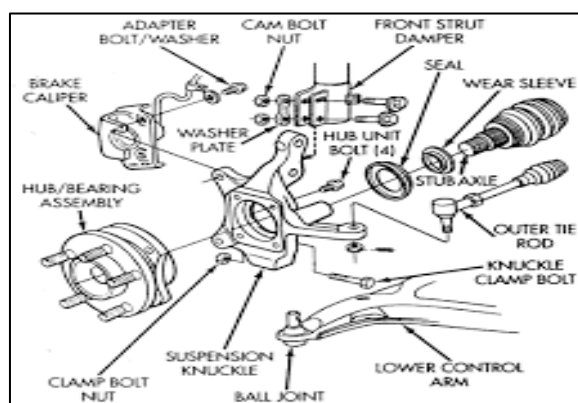


Figure 2.5: Application of the Steering Knuckle ( [https://en.wikipedia.org/wiki/Steering\\_knuckle](https://en.wikipedia.org/wiki/Steering_knuckle) )

Figure 2.5 shows the application of the steering knuckle, an advanced engineering solution designed to address common issues found in traditional steering knuckles.

## 2.4 Materials for Steering Knuckles

Steering knuckles are often made of cast iron, aluminum, or steel, all of which have specific advantages and disadvantages. Ductile iron is a suitable contender for these difficult and demanding applications due to its reliability and high stress tolerance. However, aluminum's lightweight property gives rise to the benefit of lower overall vehicle weight and effective fuel efficiency. Steel, with an incredible strength-to-weight ratio, can withstand the extreme operating conditions (Santana et al., 2024).

In automobile manufacturing, steering uprights tends to be made of grey cast iron or weight cast iron. The materials are selected based on certain criteria that include strength, weight specifications, and cost concerns. Furthermore, ductile iron and composite materials are also used in the construction of steering knuckles. Aluminium alloy is preferred owing to its superior physical and mechanical qualities (Gupta et al., 2021).

Furthermore, manufacturing techniques allow steering knuckles to be made from lightweight alloys and main-side technologies. Using techniques such as topology optimization and the capability of Aluminium alloys ensures the fabrication of lightweight knuckles while retaining other important parameters such as strength, stiffness, and frequency. (Srivastava et al., 2020).

### 2.4.1 Aluminium Alloy

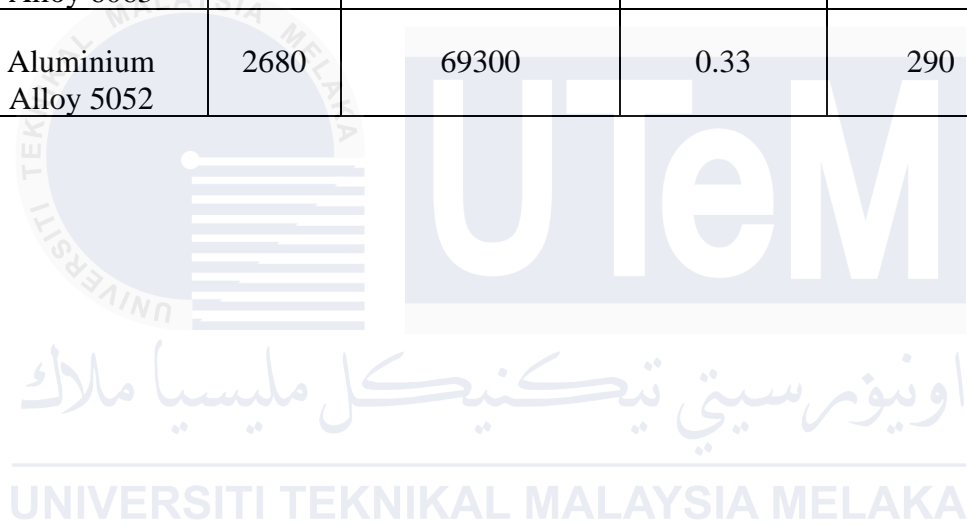
The selective of materials would, therefore, be important in steering knuckle manufacturing since it affects performance and durability, as well as safety. The advantages of aluminum alloy are modernized features, ease of machining, and wear resistance, keeping up with the need in the automotive industry for lightweight materials geared towards sustainability (Blatnický et al., 2020). The manufacturing process allowed a certain uniqueness and complexity in design, enhancing the performance of the component. Use of lightweight materials such as aluminum alloy indicates a reduction in vehicle weight, fuel consumption, and emissions.

Moreover, the use of aluminium alloy for steering knuckles fits technical requirements and the industrial sustainability agenda. Its availability, widespread usage in other industrial and automotive applications, and efficiency (Tisza & Czinege, 2018). The automotive industry should, strictly, choose suitable materials fostering sustainability and future business prosperity (Ghungarde et al., 2019). Therefore, choosing aluminium alloy assumes a commitment to technological evolution and proficient eco-responsibility.

Table 2.1 presents an overview of the mechanical properties of aluminium alloy. These properties include Density, Young's Modulus, Poisson's Ratio, Yield Stress, Ultimate Strength. Such comprehensive exposition helps acquire in-depth knowledge of the material features important in the engineering application and choosing materials.

Table 2.1: Mechanical Properties of type Aluminium alloy (Sathishkumar & Kanna, 2019)

Materials, Symbol, Unit	Density $\rho$ (kg/m <sup>3</sup> )	Young's Modulus E (MPa)	Poisson's Ratio $\nu$	Ultimate strength $\sigma_u$ (MPa)	Yield Stress $\sigma_y$ (MPa)
Aluminium Alloy 6061-T6	2700	68900	0.33	310	276
Aluminium Alloy 7075-T6	2810	71700	0.33	540	480
Aluminium Alloy 6063	2690	68900	0.33	190	160
Aluminium Alloy 5052	2680	69300	0.33	290	250



### 2.4.2 Mild Steel

The steering knuckles are mostly made of mild steel because of its more favorable mechanical properties and low cost. Mild steel possesses strength, sturdiness, flexibility, weldability, and excellent impact resistance, capable of withstanding the loads and stress of the operating conditions under which the steering system must function safely and maintain integrity (Qaralleh et al., 2024).

However, iron and aluminium alloy provide certain properties, especially in terms of very high wear resistance and being good enough for the most arduous loading conditions. Also, aluminum alloys may be able to improve fuel economy by lessening the weight on the bearing structure of the steering knuckle. The material of the steering knuckle should be selected, keeping in consideration the load conditions and manufacturing requirements (Shirsat & More, 2021). Besides, mechanical characteristics plus values such as corrosion resistance and workability for the most secure performance of the steering system.

Table 2.2 shows detailed information about the mechanical properties of mild steel. These properties include Density, Young's Modulus, Poisson's ratio, Yield stress, and Ultimate strength. This comprehensive data is essential to predict the performance of this material and its applicability in different structural engineering applications.

Table 2.2: Property specification type of Mild Steel (Velmanirajan & Anuradha, 2020)

Materials, Symbol, Unit	Density $\rho$ ( $\text{kg/m}^3$ )	Young's Modulus E (MPa)	Poisson's Ratio $\nu$	Ultimate strength $\sigma_u$ (MPa)	Yield Stress $\sigma_y$ (MPa)
AISI 1008	7870	210,000	0.29	340	285
AISI 1010	7870	210,000	0.29	365	305
AISI 1020	7870	210,000	0.29	420	350

### 2.4.3 Cast Iron

Cast iron is often used in steering knuckles due to its durability and resistance to wear. These characteristics enable it to endure significant pressures and impacts while in operation. Its cost-effectiveness and suitability for high-volume manufacturing make it an attractive choice for the automotive industry. Corrosion resistance and endurance in harsh operating conditions contribute to a material's long-term performance potential (Sun et al., 2019).

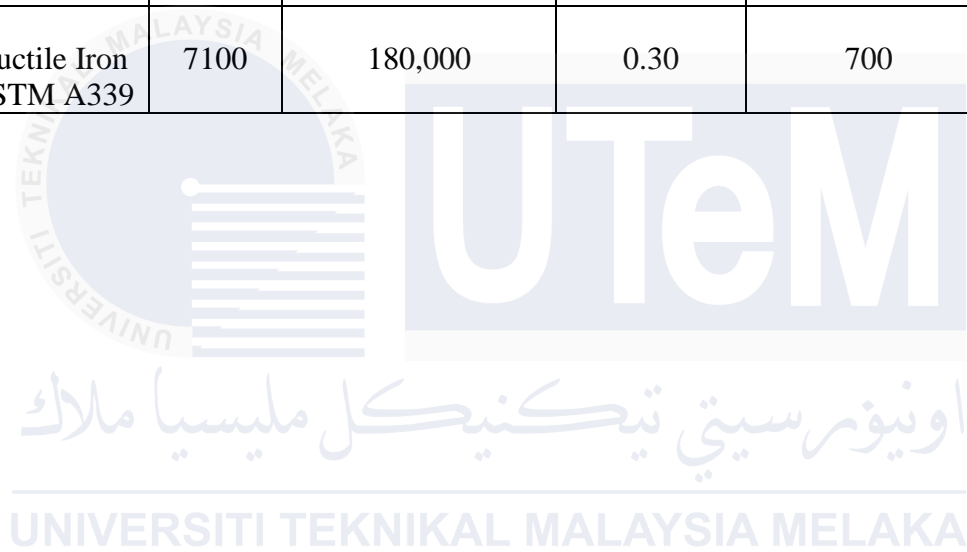
The mechanical properties of cast iron make it an appropriate material for constructing steering knuckles. Its amazing compressive strength allows it to withstand the loads and stresses of steering and suspension actions. The wear resistance of cast iron ensures that the steering knuckle can maintain structural integrity and dimensional stability even after prolonged use ultimately ensuring vehicle safety and reliability (Jeon et al., 2018). Cast iron steering knuckles are used extensively in commercial vehicles, enduring the unforgiving conditions of commercial trucks, SUVs, and heavy-duty vehicles working off-road or in demanding applications (Deshpande et al., 2020).

Table 2.3 focuses on the mechanical properties of cast iron, such as density, Young's modulus, Poisson's ratio, yield stress, and ultimate strength. This data set really matters for choosing properties pertaining to the performance and use of cast iron in engineering and industrial applications.



Table 2.3: Property specification type of Cast Iron (Georgantzia et al., 2021)

Materials, Symbol, Unit	Density $\rho$ ( $\text{kg/m}^3$ )	Young's Modulus E (MPa)	Poisson's Ratio $\nu$	Ultimate strength $\sigma_u$ (MPa)	Yield Stress $\sigma_y$ (MPa)
Grey Cast Iron ASTM A48	7000	150,000	0.30	400	400
Malleable Iron ASTM A47	7200	172,000	0.26	450	300
Ductile Iron ASTM A339	7100	180,000	0.30	700	500



## 2.5 Manufacturing Methods for Steering Knuckles

The manufacturing methodologies applied to steering knuckles vary significantly in terms of complexity and capabilities as each method has its own unique advantages intended for certain production requirements. One method involves the application of a careful machining process to precisely alter the location of the steering-knuckle. This process is the reallocation of the surplus material and further lubrication for precision production in the lathe reproduction process, thus providing excellent tolerance and product quality (Liu et al., 2023). An additional technical solution includes a manufacturing machine comprising heating, roll forging and edge cutting. This configuration provides uninterrupted automated manufacturing, ensuring quality stability, Meanwhile, improves production efficiency greatly by optimizing the process.

Furthermore, a thorough machining procedure for steering knuckle rod components encompasses multiple phases initial rough turning, subsequent semi-finish turning, drilling of cross-shaped holes, and final finish turning. This technique enhances accuracy and preserves the strengthening of borders mainly with additives that fulfil stringent mechanical standards. These various strategies emphasize the continuous advancement and refinement inside the manufacturing of steering knuckles demonstrating the industry's willpower to improve the fine and efficiency of producing procedures.

### 2.5.1 Forging

Steering knuckles are mostly forged to increase strength and durability, hence ensuring vehicle safety and performance. Forging is a process of imparting concentrated compressive energy to heated material resulting in steering knuckles that are mechanically superior and reduced in weight. This procedure is suitable for providing components with a high strength to weight ratio. The precision of forging allows components with outstanding mechanical properties and complex geometries improving performance and reliability while incurring negligible material waste and adhering to sustainable manufacturing norms (Jeon et al., 2018).

The requirements dictate that the steering knuckle must be lightweight but not at the of safety, which is why there is development of new design and production technology (Yunjun et al., 2020). Precision forging has eliminated these concerns by manufacturing lightweight strong steering knuckles that withstand extreme conditions and yet provide for safe and dependable performance. Furthermore, precision forging affects the production of steering knuckles through improving mechanical properties, reducing weight, and surpassing the safety and performance expectations for commercial vehicles.

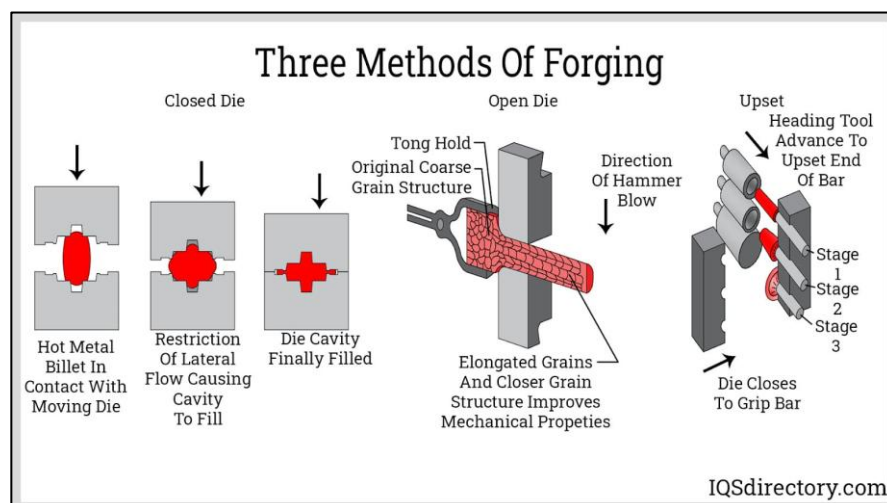


Figure 2.6: Methods of Forging ( <https://shorturl.at/f8fDf> )

As can be seen in figure 2.6, there are 3 methods for forging closed die, open die, and ring rolling. A precision technique that produces complex shapes closed forging is performed by working metal between shaped dies. Open die forging makes use of flat or easy dies to create large parts, such as shafts, and it complements more than one blows and repositioning. Ring rolling reduces a metal ring's thickness and expands its diameter with rollers, producing strong components like bearings and gears.



### 2.5.2 CNC Machining

The recommendation for CNC machining arises from its precision and adaptability a method through which material can be removed accurately and structures can be kept intact, extremely vital for weight optimization (Kumar et al., 2020). Various metals such as aluminium, steel, and titanium can be used in this method, allowing for a great deal of design and performance flexibility. However, it may result in longer production schedules and higher upfront costs (Product Re-Engineering by Topology Optimization for Forged Component, 2021). Proper programming, tool path optimization, and cutting tool selection are essential for efficient, high-quality production, while firm quality control standards ensure compliance with safety and performance parameters.

Combining forging and CNC machining can improve the properties of materials and produce complex shapes. Forging realigns the metal structure, improving strength, whilst CNC machining improves dimensions and delicate features. Despite potentially higher manufacturing costs due to additional tooling and setup needs (Kumar & Mondal, 2021), maintaining perfect control over both processes maintains consistency and optimizes grain structure for peak performance.

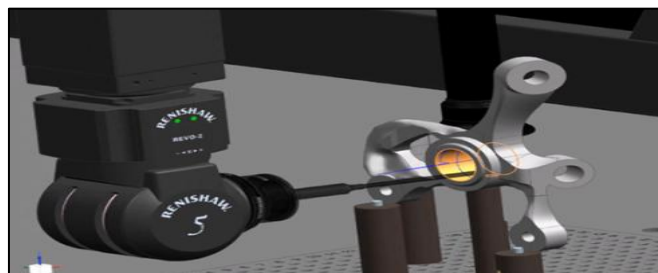


Figure 2.7: CNC Knuckle Steering (<https://shorturl.at/fRii5>)

Figure 2.7 illustrates a CNC-machined steering knuckle. The steering knuckle is a critical component in a vehicle's suspension system, connecting the wheel to the steering and suspension mechanisms.

## 2.6 Computer Aided Design (CAD)

The engineering and manufacturing fields have been revolutionized by CAD by developing advanced software for creating accurate of actual products. CAD technologies will enhance the design process the components and assemblies can be created, modeled, and simulated in a digital environment. These methods enhance accuracy and efficiency and allow the study of complex geometries that would be difficult to produce with conventional drafting methods. CAD software has enabled designers to rapidly iterate on designs, optimize the parts for performance and manufacturability, and identify potential problems early in the development process. (Lee & Yan, 2016).

There are advantages of the CAD to such an touch the complete life cycle of a product. CAD models become a framework for Finite Element Analysis and all other subsequent analyses as evolve. Such integration shortens the manufacturing process, shortens the cycle of activity, reduces errors, and guarantees that the final product is as close in performance to the original intent of design as possible. Computer-aided design has certainly become a crucial tool within modern engineering allowing for efficiency, creativity, and quality in the realization of a product.

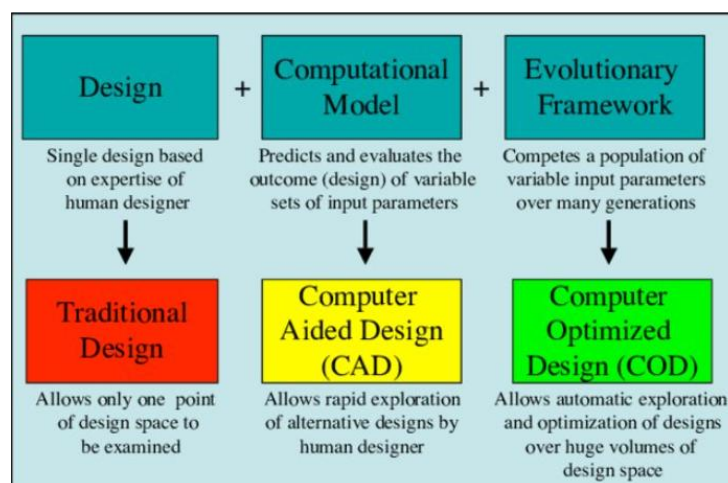


Figure 2.8: Elements of Computer Aided Design (CAD) (Terrile et al., 2004)

### **2.6.1 CATIA V5 Generative Shape Design (GSD)**

Generative shape design is an effective method in the field of computer-aided design (CAD) software. CATIA V5's GSD feature offers numerous options to generate complex 3D shapes and surfaces. Its simple interface and extensive compilation of features enable it to easily construct and change complex shapes, making it a useful feature for product design and engineering. The GSD workbench gives the flexibility and precision required to bring innovative ideas, ensuring the experiment with a wide range of options for design and optimize final solutions. Furthermore, the workbench has an extensive selection of surfacing features for designing complicated and complex designs with ease. Generative Shape Design in CATIA V5 allows to create smooth, sweeping curves as well as complex, sculpted surfaces. The demands of many industries such as automotive, consumer products, and aerospace engineering (Gulanová et al., 2018).

### **2.6.2 CATIA V5 Part Design**

Part design is important in modern engineering because it provides great tools for developing complicated and precise 3D models of specific components. The part design workbench makes it easier to create complex solid models using parametric methods. Flexibility is an important quality in iterative design processes because it enables quick adaptation to new requirements without having to start from scratch (Ioana & Oancea 2019).

The module places a high value on precision and efficiency, effectively integrating with other modules such as Assembly Design, Surface Design, and Drafting to ensure that revisions are applied consistently to related files. Advanced capabilities such as feature-based modelling and design history management improve the ability to create complicated parts. Furthermore, CATIA V5 may be used to resemble actual situations and sketch new parts to enhance designs for optimal performance and ease of manufacture. This highlights CATIA V5's important importance in current engineering design methods.

## 2.7 Computer Aided Engineering (CAE)

CAE has changed the way engineering design optimization is done. It incorporates new software and simulation capabilities for the analysis and optimization of designs. Computer-Aided Engineering allows efficient testing and comparisons between alternative design iterations, allowing for less time in design decisions and more solutions to be explored. Furthermore, it allows simultaneous consideration of various performance criteria of different states. (Sathishkumar & Kanna, 2019).

In addition, Computer Aided Engineering (CAE) can accurately simulate real-international running situations, presenting substantial insights into the performance of a layout in lots of situations. It can make use of this predictive functionality to optimize designs and meet specific typical performance targets and requirements. ANSYS are software program applications used for the modelling of structures, analyzing stress, and optimizing topology. This equipment facilitates the improvement of aircraft, vehicles, and production designs that own more electricity and decreased weight (Zhu et al., 2021). Altair Inspire is a professional-level product analysis toolkit designed by Altair Engineering, which is designed to simulate industry-level products in the manufacturing processes found in automotive construction, shipbuilding and other fields. It also offers a few tools that help to address several steps of the engineering process, from preliminary design and modeling to optimization and verification. Some of its elements are topology optimization that assists engineers in minimizing on the amount of material needed as well as enhancing on structure performance, this is valuable in automotive, aerospace industries and manufacturing. (Srivastava et al., 2020).



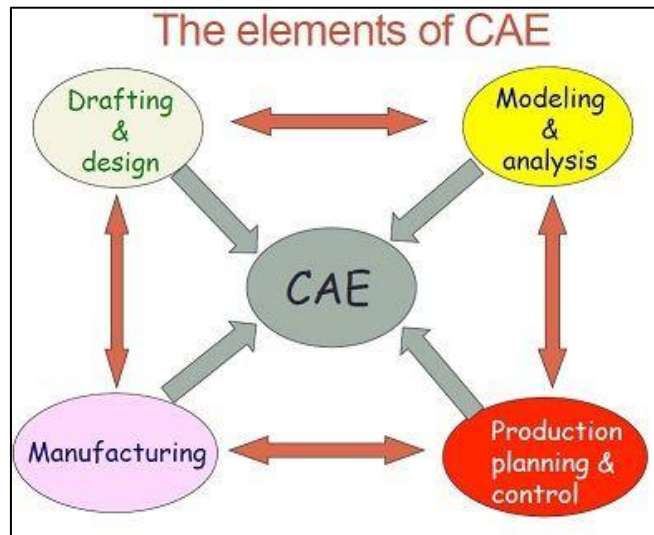


Figure 2.9: The Elements of CAE (<https://shorturl.at/lyCez>)

Figure 2.9 shows the elements of CAE that have significantly enhanced the accuracy and efficiency of design and analysis processes in various engineering fields.

### 2.7.1 ANSYS

The ANSYS has become commonly utilized for the have a look at and optimization of vehicle parts, that are crucial additives in automotive structures. ANSYS's superior finite element analysis (FEA) skills allow to generate correct simulations under distinctive load occasions for the reason of assessing their structural integrity, strain distribution, and fatigue existence. ANSYS allows the detection of feasible locations of failure, bearing in mind iterative improvements in layout that enhance durability and decrease weight whilst nonetheless preserving the required electricity and stiffness. The use of this thorough analytical technique ensures that steering knuckles may fulfil traumatic overall performance and protection standards, making a massive contribution to the advancement of safer and greater efficient automobiles (Chen et al., 2019).

### 2.7.2 Altair Inspire

There are ways in which Altair Inspire contributes to the automotive industry through being an avenue through which design is made more efficient through simulation and optimization solutions with advanced simulation and optimization techniques. It provides topology optimization which helps in dispersion of materials within the automotive parts and can bring significant reduction in weight which can be up to 65.9% in some cases and yet increases stiffness and decreases stress (Ferede, 2020). Moreover, Altair Inspire Form extends in the simulation of sheet metal forming processes inclusive of that using Aluminium alloy AA6061 where it gives a formability analysis and factors defining behavior of such material to eliminate lapse in manufacturing which leads to such defects like excessive thinning and material tearing (Tharazi et al., 2024). In addition, the software facilitates casting simulations and means that one can be able to view mold filling and the solidification processes and ultimately trace likely defects without having to rely on physical models (Kuangdi, 2022). These capabilities exert positive effects on the automobile costs reduction as well as the product quality and efficiency in automobile design and production processes (Amarnath et al., 2023).

### 2.7.3 Meshing and Type of Elements

Meshing in finite element analysis (FEA) is an essential process that requires reducing a complex geometry into smaller, more manageable pieces to accurately represent physical occurrences. It reduces a model's continuous geometry to a finite set of elements and nodes, enabling numerical solutions to physical issues like stress, heat transfer, and fluid dynamics. Proper meshing ensures that the model adequately represents the geometry and that the analytical conclusions are reliable (Kendli, 2020).

The number of elements and nodes used to model a steering knuckle greatly depends on the geometry's complexity and the level of information required in the analysis. A high-fidelity model of a steering knuckle may include thousands of elements and tens of thousands of nodes. This guarantees that the mesh is small enough to capture detailed stress distributions and deformation properties precisely (Santana et al., 2024). The exact number of elements and nodes is chosen by a trade-off between processing resources and desired result accuracy.

The element type used in finite element analysis is defined by the analysis's specific requirements as well as the component's geometry. For structural analysis, 3D solid elements such as tetrahedral or hexahedral elements are commonly used. Tetrahedral elements are versatile and can fit into diverse geometries, however hexahedral elements are preferred for computational efficiency and accuracy in regular geometries (Pan et al., 2020). Higher-order elements, which have more nodes and can better represent curved geometries, are commonly used to improve analytical precision.

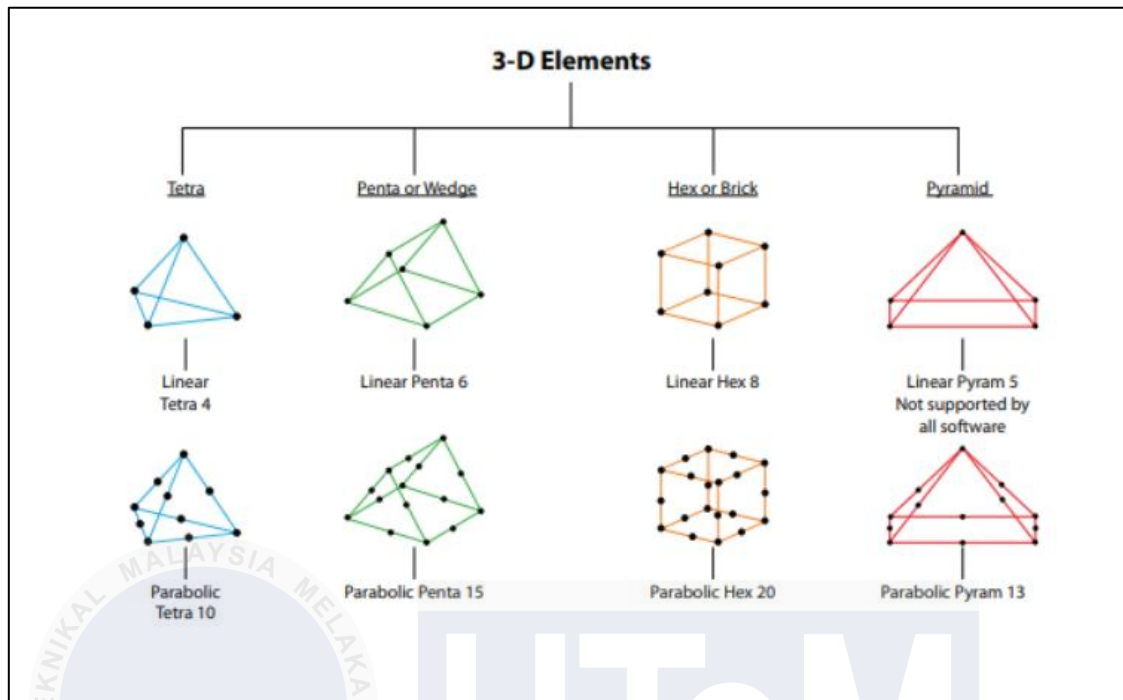


Figure 2.10: Type of Mesh 3D Elements(<https://shorturl.at/12R0a>)

#### 2.7.4 Topology Optimization

Topology optimization is a crucial aspect of engineering design that involves redistributing material inside a given space in order to achieve optimal performance while minimizing material usage. By iteratively modifying material distribution, this technique produces new and efficient designs that meet specific performance and structural requirements, frequently outperforming traditional ones. Advanced algorithms, based on performance measurements and structural limitations, allow to discover new methods to enhance various engineering systems. (Vlah et al., 2020). Topology optimization can be accomplished using methods such as density-based approaches, which repeatedly update material density fields, and level set methods, which apply functions to describe material boundaries and are applicable for a variety of issues (Kentli, 2020).

Topology optimization aids car designers design steering knuckles by identifying the suitable material distribution to balance weight reduction with strength and durability (Remigio-Reyes et al., 2022). To endure maximum stresses and effects during vehicle operation, this analytical approach develops steering knuckles with minimal material utilization and structural integrity. Reducing unsprung mass increases handling, fuel efficiency, and overall performance (Rashwan, 2019). Topology optimization in steering knuckle design can clear up complex design issues and make automotive components lighter, less costly, and more durable (DeFelice, 2023).

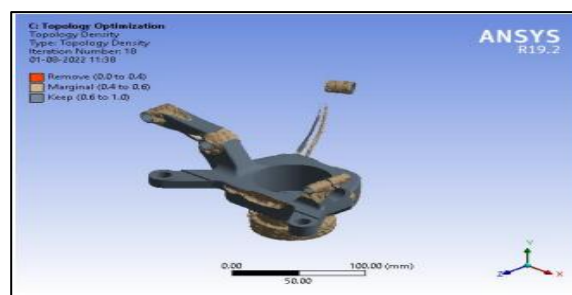


Figure 2.11: Structural planning of knuckle prototype. (Mailapalli et al., 2023)

### 2.7.5 Topography Optimization

Topography optimization is a critical technique for enhancing the architecture and efficiency of automotive components, such as the steering knuckle. Based on Finite Element Analysis, surface deformation is iteratively performed on the surface of the object. The overall objective is to improve its efficiency under flavorful loads while minimizing its associated weight (Srivastava et al., 2020). This is by far a lighter and stronger form by finding the regions where material can be removed without losing structural integrity. Optimizing this configuration gives greater maneuverability to the vehicle and an enhanced economy thereafter (Rajesh kumar et al., 2020).

Furthermore, going toward topographical optimization is beneficial in operating efficiently towards stress distributions and improving fatigue life for the steering knuckle. This approach allows meticulous shape adjustments, making sure that the knuckle can resist the tricky masses encountered at some point of vehicle operation. Preliminary optimization can perceive feasible troubles, permitting them to be resolved before production, for this reason reducing the chance of highly redesigning (Srivastava et al., 2020). This approach now not only improves the protection and dependability of the car.

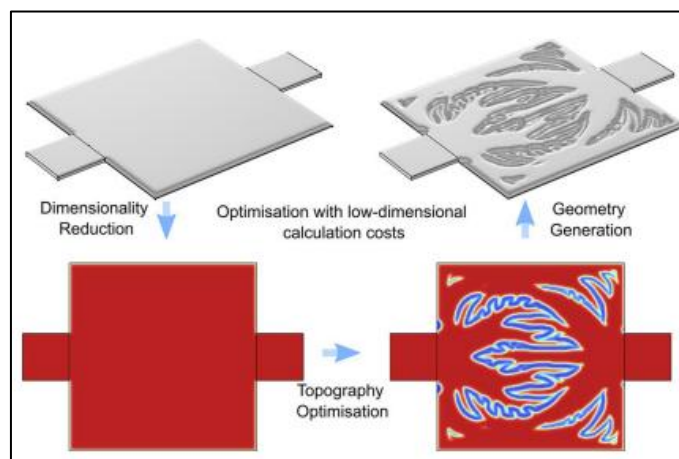


Figure 2.12: A topography optimized sheet metal (Sun et al., 2023)

### 2.7.6 Lattice Structure

In the automobile industry, lattice structure applications in the design of steering knuckles result in performance-enhancing and durability improving features towards a vehicle. In turn, this means optimum balance for strength, weight, and requisite stiffness characteristics. The process entails slight modification of the structure and design of lattice components to avoid areas of maximum stress, achieve increased load-bearing capacity, decrease material consumption, and sustain, at the very least, structural integrity (Chen and Zhang, 2022).

The use of Finite Element Analysis (FEA) simulations and optimization methods allows for the evaluation of various lattice configurations and the determination of the most efficient design parameters. The lattice structure was optimized by iteratively refining and determining stress distribution under various loading circumstances, resulting in improved performance and reduced weight and material expenses. This development in optimizing the lattice structure of steering knuckles signifies an important achievement in the automotive industry. By employing analytical methodologies and new design approaches, it is possible to enhance the structural efficiency and performance of important parts such as steering knuckles. This not only simplifies the process of making automobiles that are lighter and consume fuel efficiency but also minimizes the negative effects on the environment by optimizing material usage and enhancing overall vehicle performance (Pan et al., 2020).

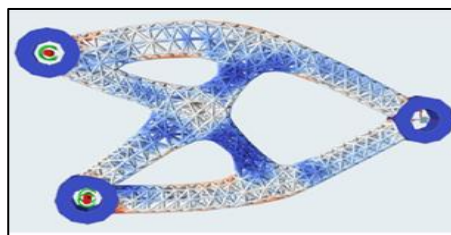


Figure 2.13: A topologically optimized solid-lattice hybrid structure (Zhu et al., 2021)



## 2.8 Applications of Topology Optimization in Automotive Design

Topology optimization determines the optimal material layout in a design based on loads, boundary conditions, and restrictions, minimizing material use while meeting performance standards. In automotive design, it plays a key role in reducing weight, improving fuel efficiency, and lowering emissions by identifying areas for material reduction or reinforcement. Other than that, this process ensures components meet strict strength and stiffness requirements to withstand static, dynamic, and impact loads without excessive material usage, contributing to efficient, high-performing, and environmentally friendly vehicle designs (Remigio-Reyes et al., 2022; Research on Aluminum Alloy Materials and Application Technology for Automotive Lightweighting, 2023).

Topology optimization combined with additive manufacturing (AM) technologies like 3D printing. It enables the creation of complex, lightweight, and efficient geometries that traditional manufacturing cannot achieve. Besides that, this approach enhances vehicle suspension systems, wheel rims, chassis components, and engine pistons by reducing weight, improving strength, and increasing fuel efficiency, ultimately supporting sustainability efforts in modern automobile design (DeFelice, 2023; Dalpadulo et al., 2021).

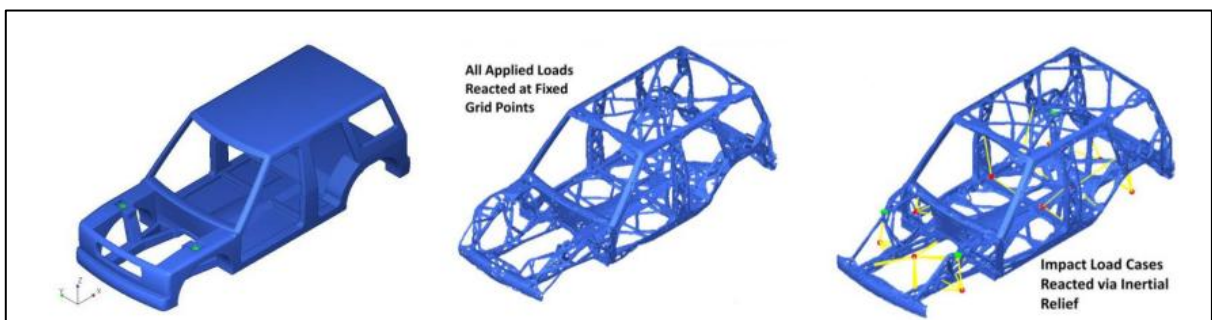


Figure 2.14: Configuration of the design space (Matsimbi et al., 2021).

In automotive vehicle design, ensuring structural integrity while minimizing weight is crucial, particularly in safety-critical components like steering knuckles. The safety factor,



which quantifies the margin between the maximum stress a component can withstand and the actual operating stress, plays a key role in this balance. According to Hoffenson (2012), for most automotive parts, the range for the safety factor should be between 1.0 and 3.0 to have an adequate margin against failure under operational loads. A safety factor of less than 1.0 means that the hinge parts are at the risk of failures, whereas when the safety factor is more than 3.0, that is regarded as an over-engineering and would result in unnecessary weight and material usage. Insight into new safety factors has helped to optimize automotive components so that performance and durability can be maintained, whereas regulatory demands on safety are still satisfied (Hoffenson, 2012).



## 2.9 Applications of Lattice Structure in Automotive Design

The automotive industry is inducing lattice systems to respond to the demand for lighter, fuel-efficient vehicles that emit less carbon. Components such as engine mounts, seat frames, and structural panels contribute to increased fuel efficiency, safety, and lifespan. This improvement comes about by different lattices that lead to a decrease in weight (Srivastava et al., 2020). The introduction of lattice in automotive design significantly boosts the overall performance and sustainability of cars through a reduction in vehicle weight (Li et al., 2019). Lattice structures thus provide high strength to weight ratios, leading to tremendous loss of weight without compromising structural integrity and allowing innovative engineering and tailor-made structural solutions in the automotive landscape (Tyflopoulos et al., 2021).

However, producing complex geometries with precision and consistency, it introduces lattice structures into vehicle design and creates production issues (Nguyen, 2019). A complex procedure requires significant research and development to provide optimal performance and durability while minimizing weight. Furthermore, optimizing the design requires suitable material and parameter selection, (Farhatnia et al., 2019).



Figure 2.15: Lightweight components with lattice structure for helicopters and racing cars. (Tao & Leu, 2016)

## **2.10 Impact of Topology Optimization on Vehicle Performance**

Topology optimization is important in automotive design because it uses complex geometric and modelling methodologies to improve performance, reduce weight, and increase fuel efficiency (Mantovani et al., 2020). This technique optimises component composition, removing unnecessary material and reducing structural weight. The main advantage of topology optimization is weight reduction, which immediately improves fuel efficiency and overall performance. This method results in lighter vehicles that use less energy to function by decreasing extra material while maintaining structural integrity, which is crucial for components such as chassis frames, wheels, and plastic elements in electric vehicles. Enhancing system safety and performance, optimized chassis systems become lighter and stronger for example (Remigio-Reyes et al., 2022).

Hybrid cellular automation is an advanced computational method used in topology optimization to deal with complex, nonlinear, and dynamic conditions. This approach enables designers to correctly recreate actual situations, ensuring that optimized components function effectively under stress and strain (Rashwan, 2019). Furthermore, topology optimization improves the cost-effectiveness of electric vehicles. Lighter vehicles consume less energy, resulting in improved fuel efficiency and lower pollutants. Increased structural strength and load distribution help to increase stability and reliability, resulting in smoother driving experience and better overall vehicle performance.

## 2.11 Summary

In general, it explores the development and function of steering knuckles, highlighting their importance in maintaining vehicle stability and managing steering. It examines the origins of steering knuckle systems and discusses several kinds used in automobile design. The discussion eventually turns to the function and structural characteristics of steering knuckles, highlighting the importance of selecting suitable substances such as aluminum alloy, mild steel, and cast iron, each offering different benefits in terms of strength, weight, and durability.

The review looks at manufacturing methods to make steering knuckles, with special emphasis on forging and CNC machining, which are all required for the fabrication of accurate parts. It explores the use of CAE methods for complex analyses, specifically in Altair Inspire, in topology optimization for finding the most effective distribution of material, topography optimization to optimize surface properties, and the inclusion of lattice structures to improve mechanical efficiency. The application of topology optimization and lattice structures in automotive design to highlight the very key effect that have on vehicle performance, as it increases the strength-to-weight ratio and enhances fuel efficiency.

## **CHAPTER 3**

### **METHODOLOGY**

#### **3.1 Introduction**

This chapter describe the approach used to complete this project successfully. This chapter shows the flow process starting from process scan part until optimize and analyses the steering knuckle. This chapter includes the project planning flow chart, the process of selecting component and testing the circuit, and the final product outcome. This chapter also includes a detailed process for each section. Detailed procedure on how selecting component is made design a comprehensive and detailed scan, simulation modelling in term of development, performance, and testing of the product.

The first step in the methodology for scanning the steering knuckles vehicles involves understanding the vehicle specifications and requirements. This includes analysing the load conditions, operating environment, and performance expectations. Once the requirements are defined, the design process begins with creating CAD models and conducting finite element analysis to ensure structural integrity and performance.

The method to be employed for the retrieval of relevant primary and secondary data for this research project will be very much a combination. Primary data will, in this instance, be collected with the assistance of scanning parts. Secondary data will be collected from the literature review of existing scholarly articles, industry reports, and suitable websites.

### 3.1.1 Flow Chart

The general setup used in this project is being discussed in the section. Figure 3.1 shows the general flow chart of this project.

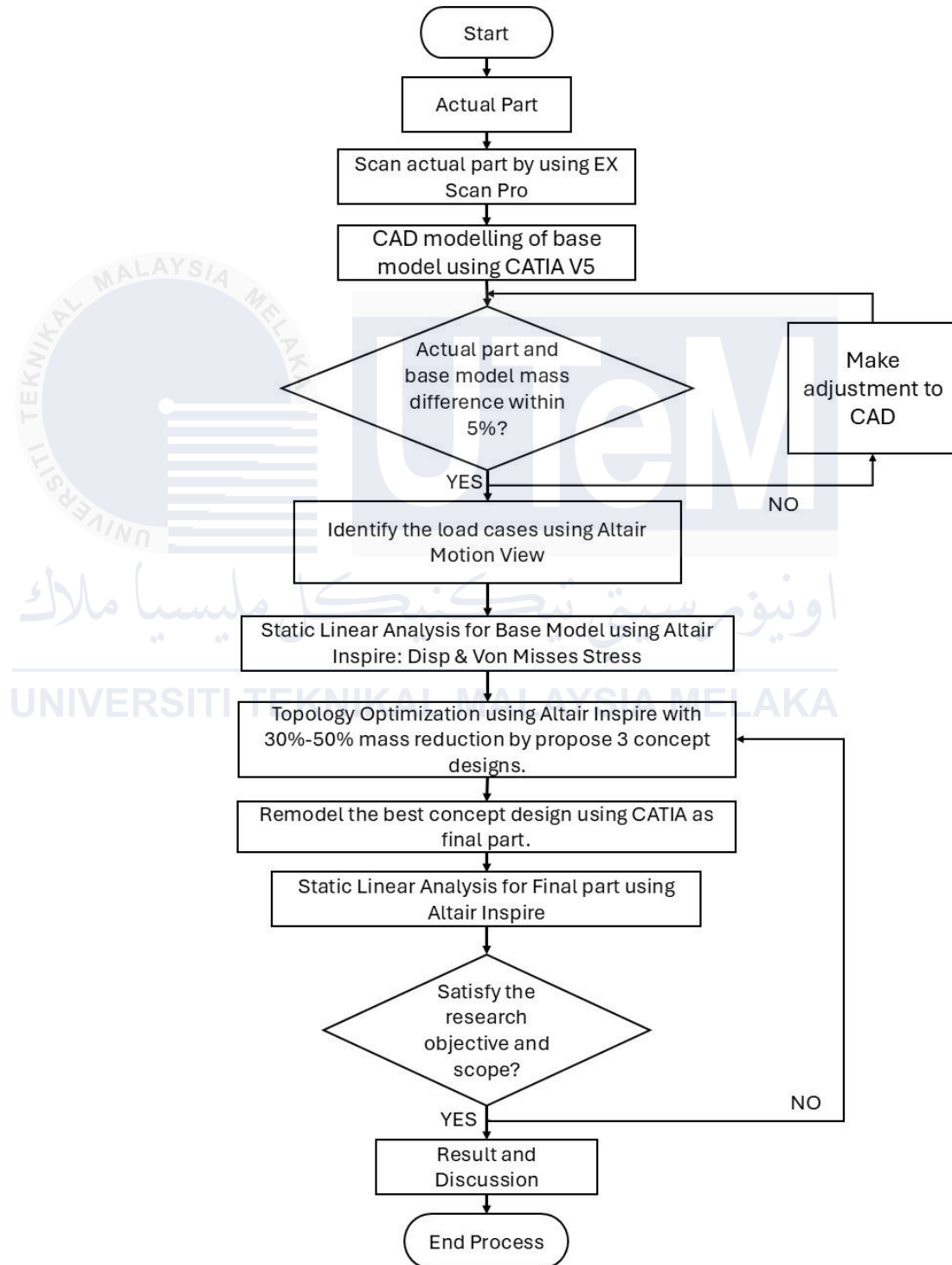


Figure 3.1: Flowchart for Shape Optimization in Automotive Engineering

The flowchart shown in figure 3.1 outlines a systematic workflow for optimizing a mechanical part through CAD modeling, simulation, and topology optimization. This usually begins with taking the actual part into consideration and scanning it with EX-Scan Pro for geometry capturing. This scanned data is then used to create a base model in CATIA V5. Mass comparison is conducted to make sure that the mass difference between the actual part and the CAD model should not exceed 5%. In case actual and CAD model differences in mass turn to be more than 5%, changes in CAD model for further refinement of the design are introduced. Once verified, the load cases of the part are specified using Altair Motion View. Static linear analysis is then carried out using Altair Inspire on the base model to determine displacement and von Mises stress. The next step is topology optimization via Altair Inspire to yield three conceptual designs for improved mass reduction of between 30 and 50%. The best concept design is then remodeled in CATIA to create the final part. Another round of static linear analysis is conducted on the final part to ensure it satisfies the research objectives and scope. If the objectives are met, the process concludes with results and discussion; otherwise, adjustments are made, and the optimization cycle is repeated.

### **3.2 Scanning Part**

Recent advances in automotive engineering, The introduction of the EX-Scan Pro system have led to a revolution in the precision scanning and digitization of complicated mechanical parts such as steering knuckles. The purpose of this method is to evaluate the EX-Scan Pro system's dependability and efficacy in this domain, which has significance for ensuring the accuracy and safety of automotive vehicles. By thoroughly this method, its capabilities not only improves understanding about of this technology by method of cutting-edge. The findings demonstrated potential for expediting automotive design and production processes, which could lead to considerable advances in the region.



Figure 3.2: EXScan Pro

The EXScan Pro system uses cutting-edge scanning technology to accurately capture and digitise complicated mechanical elements such as steering knuckles. Figure 3.2 shows the software's simple to operate interface, which allows for fast selection of scanning parameters and settings. It can specify resolution, alignment characteristics, and other parameters for precise scanning, while real-time data display assists in monitoring and modifications during the operation.



### 3.2.1 Scanner



Figure 3.3: EinScan Pro HD

Shining 3D manufactures it for detailed scanning processes and can be applied in multiple areas including industrial design, reverse engineering, quality control, and preservation. The EinScan Pro HD is a 3D Scanner that captures high resolution 3D scans. It comes with a handheld design that allows scanning flexibility and mobility, thereby allowing scanning of objects in different surroundings. The EinScan Pro HD uses advanced scanning technology to give high-resolution, accurate scans, and manufacturers.



Figure 3.4: Steering Knuckle

In figure 3.4, the setup of the steering knuckle for scanning using the EXScan Pro system is demonstrated. The steering knuckle part is securely positioned within the scanning area, ensuring stability and accuracy during the scanning process.

### 3.2.2 Mode of Alignment

The mode of alignment for the EXScan Pro HD system, when scanning steering knuckle parts, has been instrumental in ensuring digitization of utmost precision and accuracy.

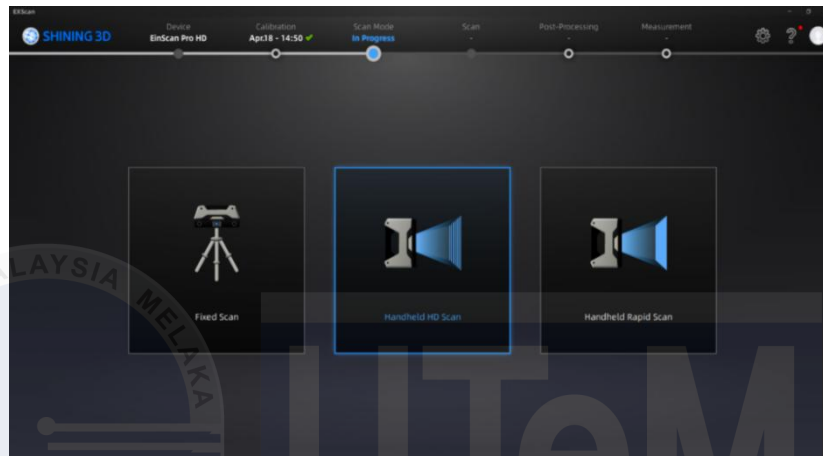


Figure 3.5: Selection Scan Mode

In figure 3.5 shows the selection of Fixed Scan, Handheld HD Scan, and Handheld Rapid Scan. For this project, the scan part chooses the Handheld HD Scan.

The handheld HD scanning mode requires the scanner to be held in a handheld configuration, which allows the operator to move around the object at will. It gives a high level of detail and accuracy developing the fine features of the object. Handheld HD scanning is usually used for scanning large objects or parts that are impossible or hard to move. It allows flexibility in scanning in different environments and angles, hence its wide range of uses in reverse engineering, detailed inspection, and custom manufacturing. The high-definition capability will capture minute details accurately.

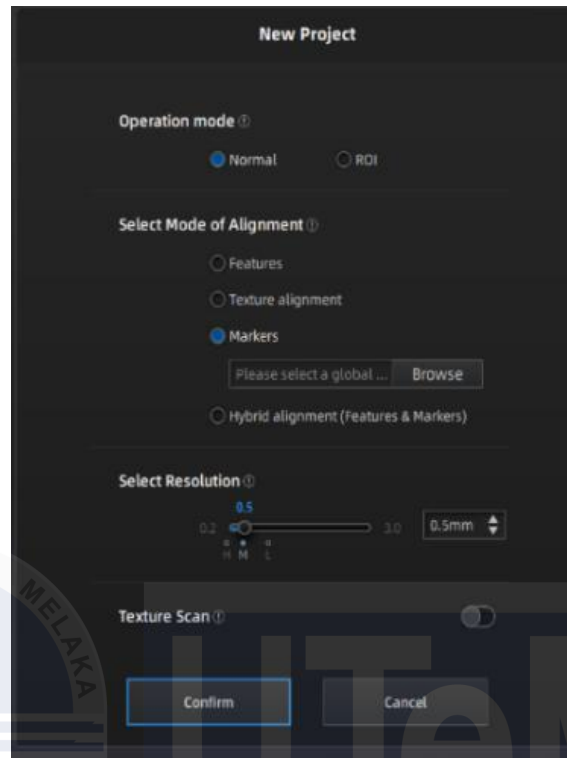


Figure 3.6: Selection Mode of Alignment

In figure 3.6 shows that type of mode of alignment that includes features, texture alignment, markers, and hybrid alignment (Features & Alignment).

Marker-based alignment involves the attachment or placement of physical markers near or on the object to be scanned. As the scanner acknowledges, the markers act as landmarks for aligning multiple scans. The scanning software will always detect these markers since it come with individual patterns when are often just small stickers or dots. This method is particularly powerful in aligning the scans of objects with smooth or repetitive surfaces on which geometric features or textures might not be enough to provide precise alignment. Marker-based alignment assures accuracy in scanning large or complex objects.

### 3.2.3 Generate Points Cloud

Creating point clouds with an EinScan Pro HD requires reflected structured light on a part and record the reflected shapes with webcams using EXScan Pro software. This method, repeated from multiple angles obtains the whole geometry. The software then interprets the reflections and produces a dense point cloud with millions of exact spatial coordinates. These thorough point clouds are necessary for building accurate 3D models for reverse engineering, quality inspection, and digital archiving, capturing even the smallest details, as illustrated in Figures 3.7 and 3.8.

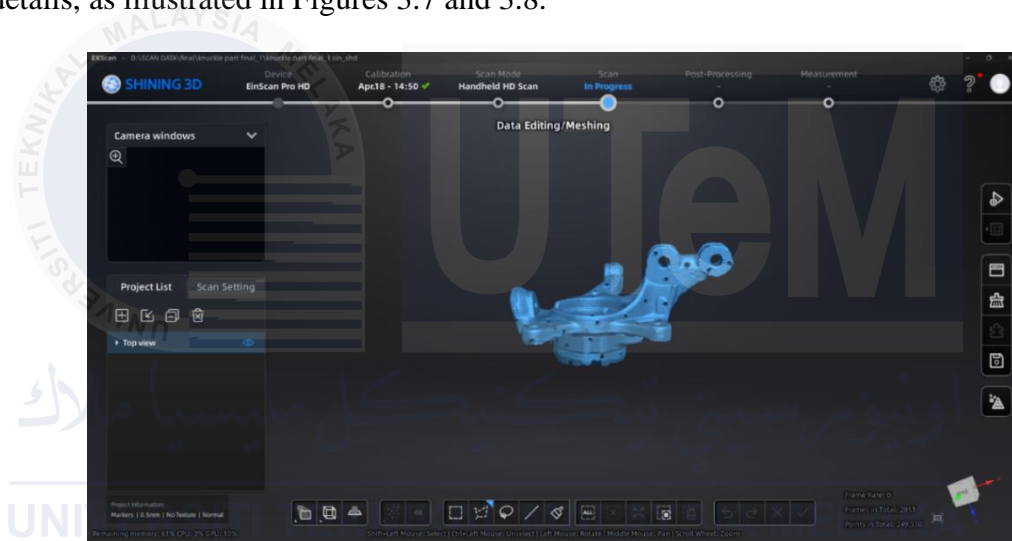


Figure 3.7: Data Editing / Meshing for Top View

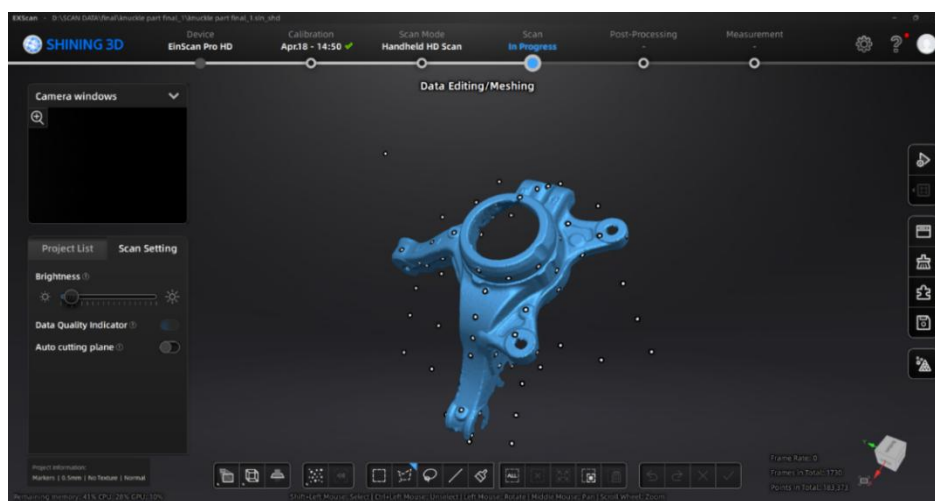


Figure 3.8: Data Editing / Meshing for Bottom View

### 3.2.4 Alignment

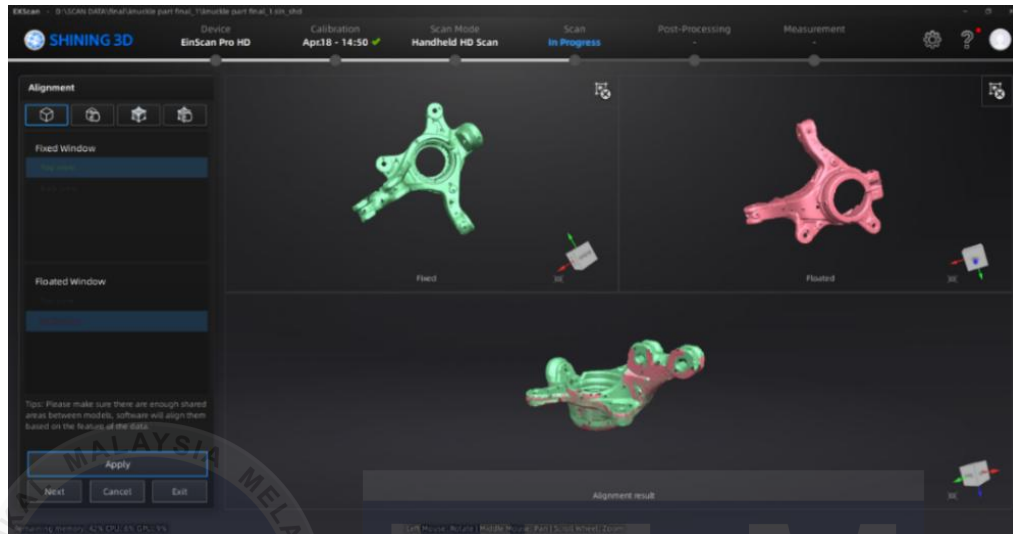


Figure 3.9: Alignment Top view and Bottom View

In Figure 3.9, the green product shows top view alignment in the EinScan Pro HD scanning process, it enables fix scan alignment by matching visible features or markers. The EXScan Pro set enables this operation either automatically or manually resulting in precise scan overlap and detailed geometry capture in the final 3D model.

On the other hand, the red product displays a bottom view alignment which focuses on aligning scans from the bottom view. This procedure ensures that features or marks on the lower surface are exactly aligned, capture details that might otherwise be invisible from other perspectives. The software enables these alignments, producing a full 3D model with detailed views from all sides.

### 3.2.5 Mesh Optimization and Editing

Mesh optimization and editing with the EinScan Pro HD using the EXScan Pro software involve refining the captured point cloud data to create a high-quality 3D mesh model. Once the point cloud is generated, the software converts these points into a mesh, consisting of interconnected triangles that represent the surface of the object as shown in figure 3.10.

An optimization process that includes triangle reduction minimizes the mesh complexity while still maintaining most of the details and accuracy of the model, as illustrated in figure 3.10. This is very important when making the model more manageable for various applications, including 3D printing, CAD modelling, and simulation.



Figure 3.10: Mesh Parameter

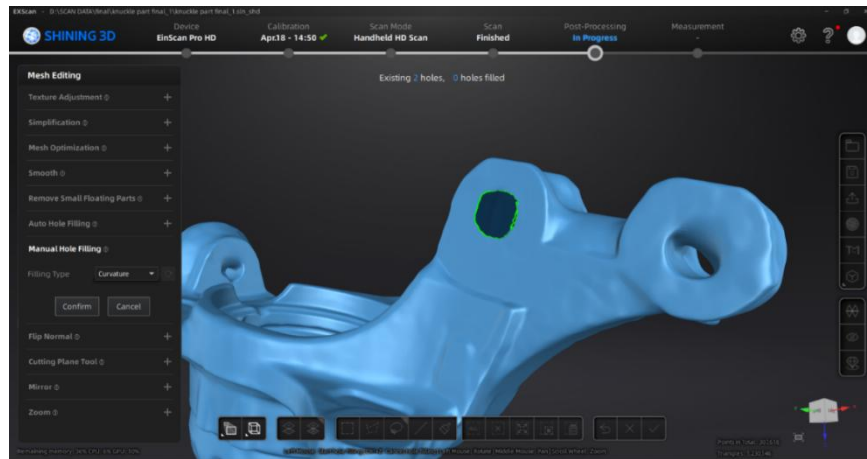


Figure 3.11: Mesh Editing Manual Hole Filling

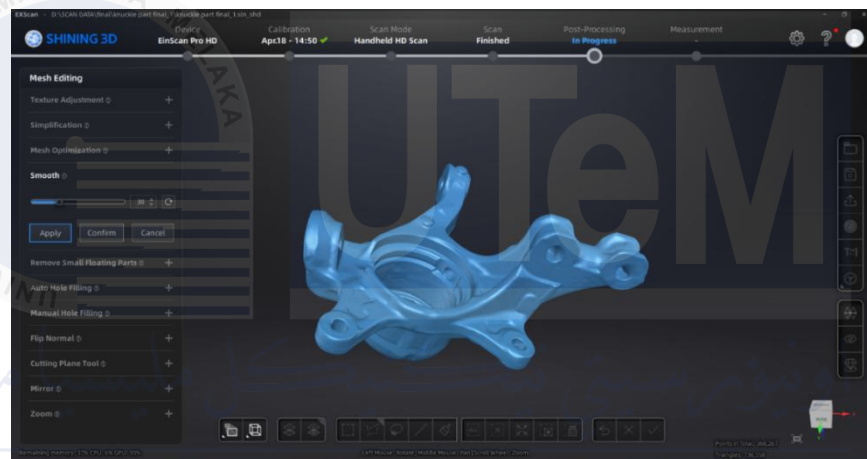


Figure 3.12: Mesh Editing Smooth Section

Editing the mesh involves numerous operations: filling holes, smoothing surfaces, and removing noise or any disturbed artifacts. Filling holes ensures that the mesh is watertight, which is especially important for applications requiring a solid, continuous surface as illustrated in figure 3.11. Smoothing leads to a clearer, more aesthetic model by removing undulations and sharp edges as shown in figure 3.12.

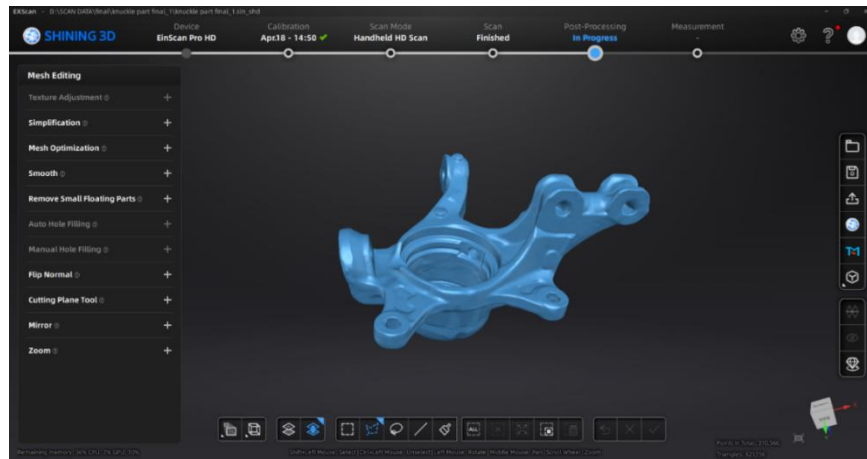


Figure 3.13: Mesh Editing Process Completed

Overall, mesh optimization and editing enhance the quality and usability of the 3D model, making it ready for further processing, analysis, or manufacturing as shown in figure 3.13. The advanced capabilities of the EinScan Pro HD and the EXScan Pro software provide users with powerful tools to achieve precise and professional-grade 3D models.



### 3.3 CATIA V5 Generative Shape Design (GSD)

Generative Shape Design (GSD) in CATIA enhances the digital design process by using 3D scanning data of a component. After importing the processed scan data into the GSD workbench, it's created precise surface models by following the contours of the scanned element. This method is critical for opposite engineering, converting physical items into correct CAD models for additional use. GSD gear like surface advent, sweeping, lofting, and filleting make sure the final virtual version stays real to the original, enhancing layout accuracy and performance in engineering and manufacturing.

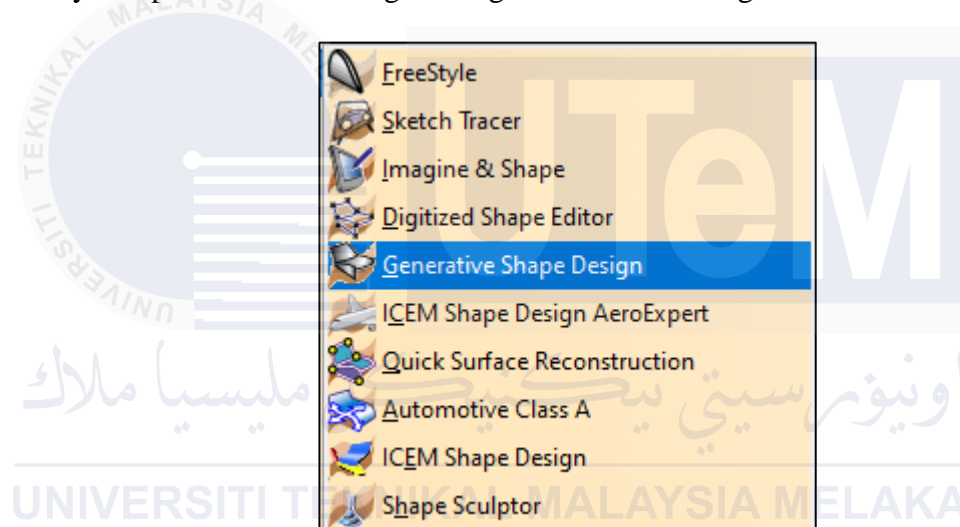


Figure 3.14: Generative Shape Design

Figure 3.14 shows the method for selecting the Generative Shape Design (GSD) icon in CATIA. When picking this icon, it will launch the GSD workbench, which offers specialized tools for generating and altering intricate surfaces and curves. This workbench enables the replication of geometric details from scanned components, ensuring a very accurate digital representation.

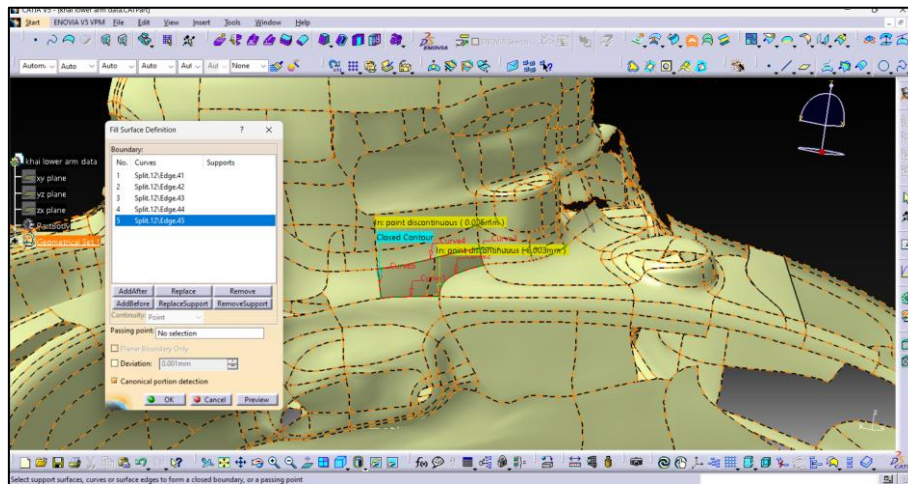


Figure 3.15: Fill Surface Definition

Figure 3.15 shows that the steering knuckle fills the surface by using fill tool by following the boundary line for the new surface to exist. The new surface requires deviation because the boundary got the edge or chamfer.

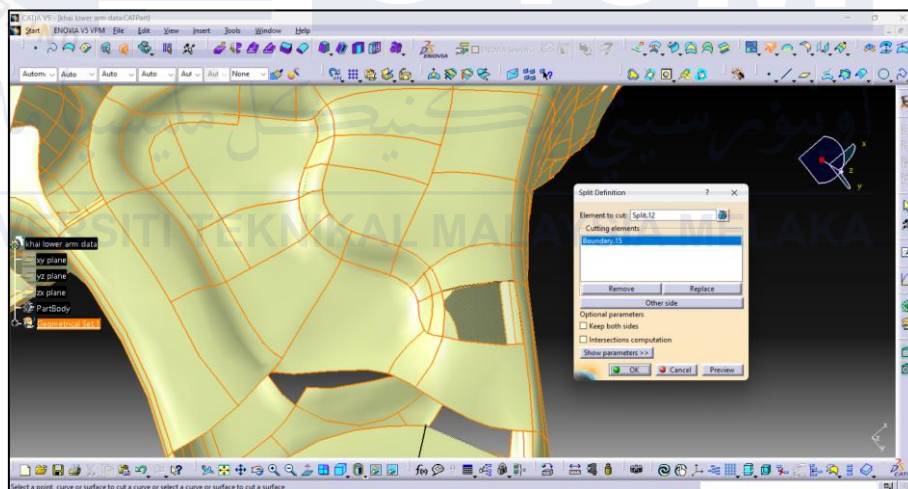


Figure 3.16: Split Definition

Figure 3.16 shows that the steering knuckle trims the strange surface by using trim tool by following the surface. The surface has been trimmed and will create a smooth surface.

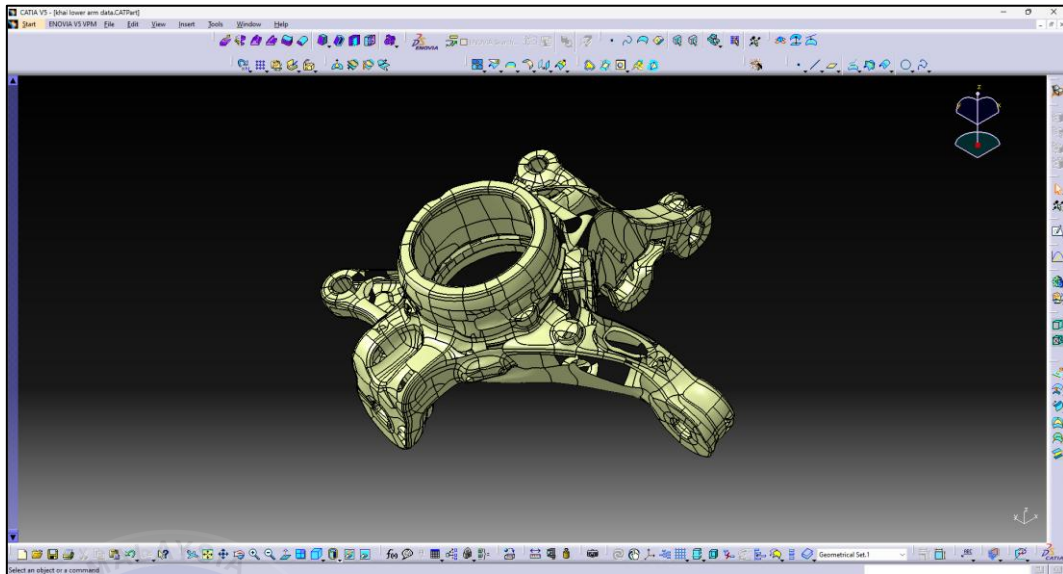


Figure 3.17: Steering Knuckle Before Fill Surface

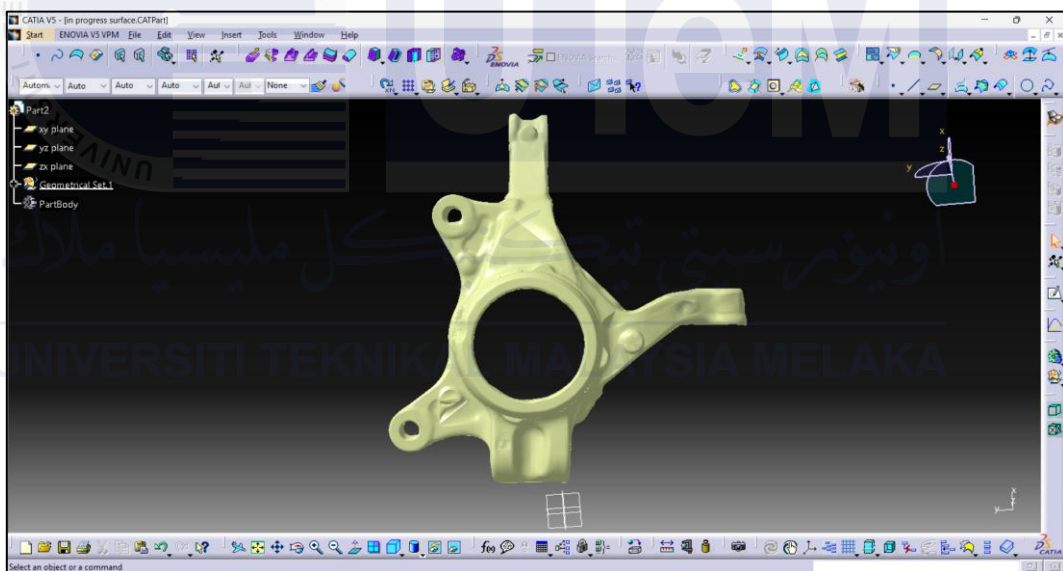


Figure 3.18: Steering Knuckle After Fill Surface

Figures 3.17 and 3.18 show the surface of the steering knuckle before and afterwards the filling method, respectively. The contrast of these two figures highlights the successful result of the filling process in attaining a smoother and more homogeneous surface. Enhancing this aspect is crucial for optimizing the efficiency and longevity of the steering knuckle, as it guarantees more effective distribution of loads and mitigates the likelihood of material fatigue.

### 3.4 CATIA V5 Part Design

Once the Generative Shape Design phase in CATIA has been completed, the next step is to connect the dimensions for the part design to make it compatible for use in Altair Inspire. This involves checking the geometric parameters to ensure they are correct and modifying them to make the model ready for simulation or finding the best way to do this. Accurate dimensions are important in any analysis performed in Altair Inspire to yield reliable results and insights into how the part will perform under various conditions.

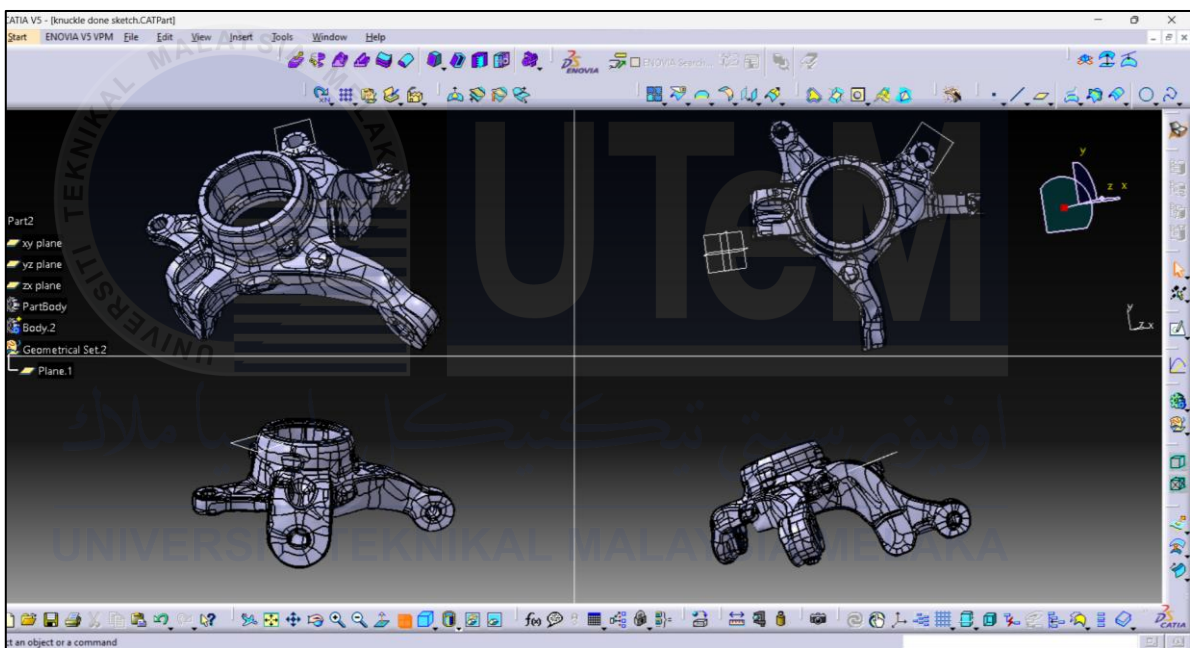


Figure 3.19: The Steering Knuckle Part Design

In this figure 3.19 shows that the steering knuckle after the all surface is closed and joined. The next step is to convert the scan part to part design. And recreate the new dimension for easy analysis.

### 3.5 Design Validation

Design validation is an important stage in the product analysis method that ensures a steering knuckle matches with the specifications provided and maintains well in real-world application. It involves several types of tests and evaluations to ensure that the design performs the purpose it was developed for and satisfies quality standards. A steering knuckle design validation is to make sure that mass is within 5% of the base model mass, which is critical for sustaining performance and efficiency. The design validation method focused on assuring congruence between the real mass and the base model mass, with a key tolerance threshold of 5%. Using Cast iron based on the actual steering knuckle and applied the same material in the base design with the same density  $7870\text{kg/m}^3$  in CATIA V5 as shown in figure 3.20. Ensures high structural integrity as well as predictable mass properties. This standardized approach allows consistent evaluation of mass distribution and overall component weight throughout multiple design iterations.



Figure 3.20 : (a) Actual Steering Knuckle (b) Base Model



Table 3.1: Weight Model

Model	Mass (Kg)
Actual Model	3.118 Kg
Base Model	2.982 Kg

Table 3.1 shows the weight of two models, which is the Actual Model and the Base Model. The Actual Model has a mass of 3.118 kg, while the Base Model weighs 2.982 kg.

Calculation Mass Difference:

$$\begin{aligned}
 \text{Mass Difference (\%)} &= \frac{\text{Actual Model} - \text{Base Model}}{\text{Base Model}} \times 100 \\
 &= \frac{3.118 - 2.982}{2.982} \times 100 \\
 &= 4.56\%
 \end{aligned}$$

The result shows that the Actual Model is only 4.56% heavier than the Base Model, which is within the acceptable range, because it is less than the 5% threshold. This slight rise in mass shows that the base model performance and compliance with design limitations have been maintained by successfully managing design modifications to prevent a major weight increase.

After design validation, it is verified that the design is applicable to any material. Although both the Actual Model and the Base Model are made of Cast Iron, the design is flexible enough to work with materials of different densities, such as Aluminum Alloy or Steel, depending on the required properties of the final component. This material adaptability allows optimization based on weight and strength.

### **3.6 Altair Motion View**

Altair Motion View is a fully integrated multi-body dynamics modelling and analysis environment for complex mechanical systems. It allows create a virtual model by defining bodies, joints, and forces and adding inputs such as loads or motion profiles. The software runs simulations and examines the system's operation to predict its performance under a variety of scenarios. Generating data such as animations, graphs, and reports gives valuable insight into validating and increasing design efficiency. As a result, it is critical for optimizing mechanical systems in industries such as automotive, aerospace, and machinery.

#### **3.6.1 Setup Model Front Suspension Vehicle**

The setup of the front suspension model in Motion View involves a series of steps to accurately simulate the vehicle's suspension system. Initially, the model type is selected, typically starting with a front-end vehicle configuration. The driveline configuration is then defined, such as choosing the front-wheel-drive system, followed by the selection of primary systems like the vehicle body, front subframe, and powertrain. Key components, including the front suspension, steering linkages, and stabilizer bars, are chosen, with options for spring and damper setups like front struts and stabilizer bars. Additionally, the appropriate steering subsystems, such as the steering column and boost, are configured. Finally, the assembly wizard guides the user through completing the setup, ensuring that all necessary elements are in place for an accurate simulation of the front suspension system in motion.

## DESIGN PARAMETERS

Table 3.2.: Design parameters for setting up the Front Vehicle Suspension

Assembly Wizard	Selection Setup
Model Type	Front end of vehicle
Driveline Configuration	Front wheel drive
Primary Systems	<ul style="list-style-type: none"> <li>- Vehicle body &gt; body to fixed ground</li> <li>- Instrumentation &gt; Instrumentation</li> <li>- Front subframe &gt; None</li> <li>- Front suspension &gt; front MacPherson susp (1pc. LCA)</li> <li>- Steering linkages &gt; Rack pin steering</li> <li>- Powertrain &gt; None</li> </ul>
Steering Subsystems	<ul style="list-style-type: none"> <li>- Steering column &gt; Steering column 1 (not for Abaqus)</li> <li>- Steering boost &gt; None</li> </ul>
Spring, dampers and stabilizer bars	<ul style="list-style-type: none"> <li>- Front struts &gt; front strut with inline jts</li> <li>- Front stabilizer bars &gt; None</li> </ul>
Jounce and Rebound dampers	<ul style="list-style-type: none"> <li>- Front Jounce Dampers &gt; None</li> <li>- Front Rebound Dampers &gt; None</li> </ul>
Driveline systems	<ul style="list-style-type: none"> <li>- Front driveline &gt; independent Front Wheel Drive</li> </ul>
Assembly wizard	Finish

Table 3.2 Configuration settings in the Assembly Wizard at time of setup Model Type set to the front end of the vehicle and driveline configuration to be front-wheel drive. Primary systems: the vehicle body set to body-to-fixed-ground, instrumentation on, front subframe to none, front suspension to a front MacPherson suspension with a one-piece lower control arm, steering linkages to rack and pinion steering, and no powertrain is specified. In steering subsystems: steering column to Steering Column 1 (not for Abaqus), and no steering boost is applied. For spring, dampers, and stabilizer bars, the front struts are set as front struts with inline joints while there is no selection for front stabilizer bars. Furthermore, there is no selection for front jounce dampers and front rebound dampers. The driveline system is set as an independent front-wheel drive, and the Assembly Wizard setup is complete.



### 3.6.2 Setup Analysis Static Load

Static load analysis in Motion View is a simulation process used to evaluate the structural response of a system or component under steady-state loads. This type of analysis focuses on determining how forces, such as weight, external loads, or constraints, affect a model in a non-dynamic environment, meaning there are no time-dependent effects like acceleration or vibrations. In Motion View, the analysis involves defining the system's geometry, assigning material properties, applying relevant boundary conditions, and introducing static forces, such as the curb weight of a vehicle or loads at specific contact points. The software computes displacements, stresses, and reactions within the structure, providing insights into its performance under the applied loads.

Vehicle Parameters	
Front gvm - includes unsprung mass (Kg)	624.0000
Rear gvm - includes unsprung mass (Kg)	416.0000
Front SLR (mm)	247.8200
Rear SLR (mm)	300.0000
Acceleration due to gravity (mm/s <sup>2</sup> )	9810.0000

Figure 3.21: Vehicle Parameter

In Figure 3.21, the setup for the static load analysis is shown where the vehicle parameters are required to be input. These parameters include the Front GVM (which includes the unsprung mass in kilograms), Rear GVM (which includes the unsprung mass in kilograms), Front SLR (Static Load Radius) in millimeter, Rear SLR (Static Load Radius) in millimeter, and the acceleration due to gravity, set as 9.81 m/s<sup>2</sup>. Here, by using these inputs, calculations are performed to determine the static load distribution across the vehicle. These calculations help analyze the load-bearing performance of the front and rear sections of the vehicle under static conditions, ensuring accurate simulation results.

### Calculation For Vehicle Parameter

According to the data of Toyota Vios specifications, it indicates a vehicle mass of 1040 kg, with a tire size of 175/65 R14. The tire dimensions include a width of 175 mm, an aspect ratio of 65% of the width, and a rim diameter of 14 inches (355.6 mm). Before calculating the SLR, the formula requires the sidewall height and rim radius to be determined first. Then SLR can be calculated. A weight distribution of 60:40 front and rear are assumed, as shown in Table 3.3.

#### Calculate the Sidewall Height (SH):

$$\text{Sidewall Height} = W \times \left(\frac{AR}{100}\right) = 175 \times \left(\frac{65}{100}\right) = 113.75 \text{ mm}$$

Rim radius (D):

$$\frac{D}{2} = \frac{355.6}{2} = 177.8 \text{ mm}$$

Approximate SLR by accounting for tire compression under load (100-15% reduction):

Table 3.3: Calculation Vehicle Parameter

Formula	Calculation	Value
Front GVM = $0.6 \times \text{mass of vehicle}$	$0.6 \times 1040 \text{ Kg}$	624 Kg
Rear GVM = $0.4 \times \text{mass of vehicle}$	$0.4 \times 1040 \text{ Kg}$	416 Kg
SLR = (Sidewall height + Rim radius) $\times$ 0.85	$(113.75\text{mm} + 177.8 \text{ mm}) \times 0.85$	247.82mm

State	Loadcase #	Title	Location	Direction	Load Type	Mult.	Value	Steps
<input checked="" type="checkbox"/>	1	Vert load	WC -left	Z	LOAD	1.0000	3060.7200	10
<input checked="" type="checkbox"/>	1	Vert load	WC -right	Z	LOAD	1.0000	3060.7200	10

Figure 3.22: Load Case

After the values were calculated and entered the Vehicle Parameters, as illustrated in Figure 3.21, the next step is detailed in Figure 3.22. In Figure 3.22, the load case is presented, showing the locations of the left and right wheel centers. The direction for each load case is aligned with the z-axis, and the values were derived from the Vehicle Parameters.

Record	Label	Variable	Type	Value
<input type="checkbox"/> 0	Load case number	num[0]	Integer	1
	Steps	steps[0]	Integer	10
	Multiplier	mult[0]	Real	1.0000
	Expression	expr[0]	Real	3060.7200
	Load case title	title[0]	String	Vert load
	State of loadcase	active_flag[0]	Boolean	<input checked="" type="checkbox"/>
	Load/Disp location	loc[0]	Option	WC -left
	Load/Disp direction	dir[0]	Option	Z
	Load type	type[0]	Option	LOAD
<input type="checkbox"/> 2	Load case number	num[2]	Integer	2
	Steps	steps[2]	Integer	10
	Multiplier	mult[2]	Real	1.0000
	Expression	expr[2]	Real	7651.8000
	Load case title	title[2]	String	
	State of loadcase	active_flag[2]	Boolean	<input checked="" type="checkbox"/>
	Load/Disp location	loc[2]	Option	WC -left
	Load/Disp direction	dir[2]	Option	X
	Load type	type[2]	Option	LOAD
<input type="checkbox"/> 3	Load case number	num[3]	Integer	3
	Steps	steps[3]	Integer	10
	Multiplier	mult[3]	Real	1.0000
	Expression	expr[3]	Real	7651.8000
	Load case title	title[3]	String	
	State of loadcase	active_flag[3]	Boolean	<input checked="" type="checkbox"/>
	Load/Disp location	loc[3]	Option	WC -left
	Load/Disp direction	dir[3]	Option	Y
	Load type	type[3]	Option	LOAD

Figure 3.23: Load Case for Each Axis

Figure 3.23 shows that the load case was added to the front-end task to incorporate the new directions for the left wheel centre along the x and y axis. The force values for the x and y axis are the same, calculated using a formula for wheel centre. This step ensures the accuracy and consistency of the force distribution, which is essential for the proper analysis and optimization of vehicle performance.

### Calculation For Force at Wheel Center Left and Bracket Brake Caliper

The curb weight of the vehicle is 1040 kg. To calculate the weight on each tire, divide the vehicle's weight by 4. Therefore, calculating the force acting on the wheel center, we require the following loading conditions, which are calculated as shown in the table below (Tagade et al., 2015):

Table 3.4: Calculation Force X, Y, Z

Force	Calculation	Value
Force X	$3 \times 260 \text{ kg} \times 9.81 \text{ m/s}^2$	7651.8 N
Force Y	$3 \times 260 \text{ kg} \times 9.81 \text{ m/s}^2$	7651.8 N
Force Z	$260 \text{ kg} \times 9.81 \text{ m/s}^2$	2550.6 N

To calculate the moment at the brake caliper:

$$\text{Braking force} = 1.5mg = 1.5 \times 260 \times 9.81 = 3825.9 \text{ Nm}$$

Moment at brake caliper = braking force \* bolts perpendicular distance

$$= 3825.9 \text{ N} \times 0.03 \text{ m} = 114.777 \text{ Nm}$$

Since this value represents total for two points on the brake caliper, the moment needs to be divided by two:

$$= \frac{114.777}{2} = 57.39 \text{ Nm}$$

Thus, the force moment at the brake calliper is:

57.39 Nm for Fx, Fy, and Fz.

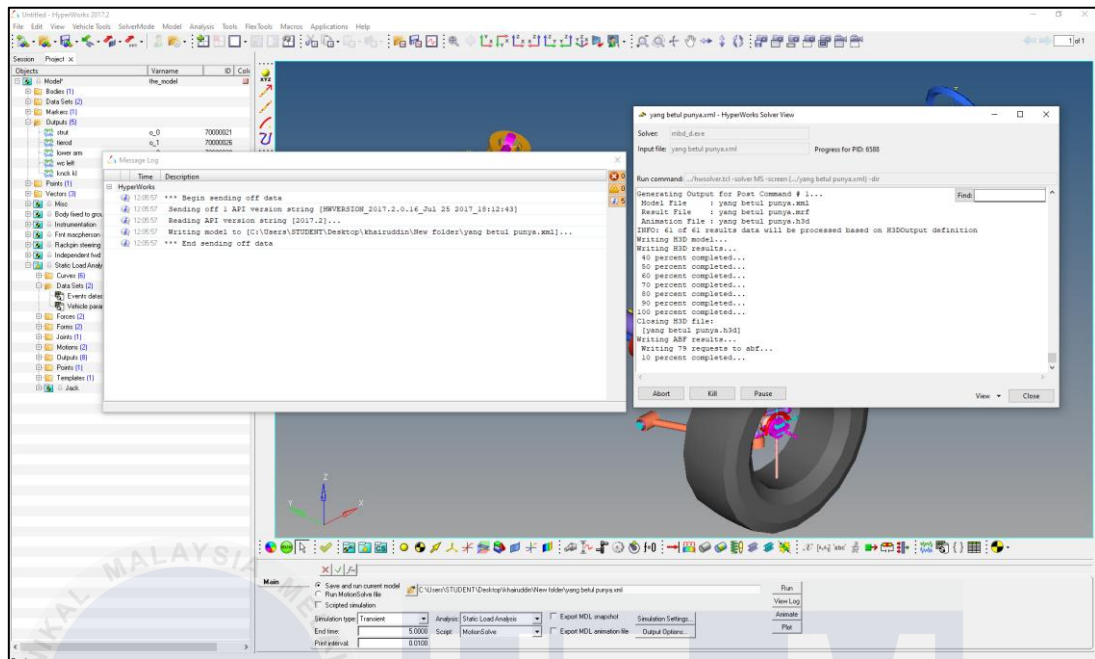


Figure 3.24: Run Static Load Analysis

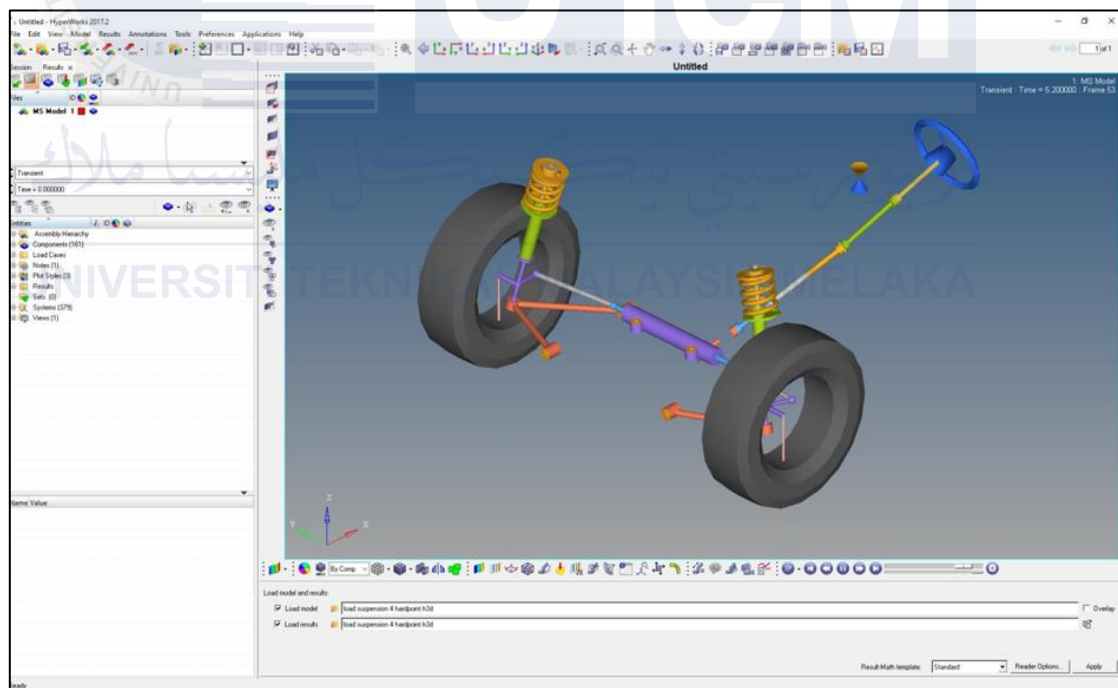


Figure 3.25: Result Animation of Assembly Front Wheel Drive

Figure 3.24 shows the assembly of the front-wheel drive system with the load cases for each force applied along the x, y, and z axes under the running analysis conditions. Before the analysis can be run, the file needs to be saved in the appropriate

format (.abf). Result Animation of Assembly Front Wheel Drive is shown in Figure 3.25. The front-wheel drive system may be animated in this output, allowing to determine whether the static load circumstances create reasonable and perform as expected. The analysis assists in verifying the precision and dependability of the system's operation under varied loading conditions.

Table 3.5: Data Hardpoint on Left Side





Load For Each Point on Left Side				
Hardpoint	Symbol Representation on Graph	Fx	Fy	Fz
Wheel Centre		7651.79 N	7651.79 N	3060.71 N
Tie rod End		5975.35 N	671.464 N	328.35 N
Lower Arm		5770.50 N	544.07 N	171.06 N
Absorber		1209.83 N	1132.367 N	2219.42 N
Bracket Calliper Brake		57.39 Nm	57.39 Nm	57.39 Nm

Table 3.5 shows the significant hard points on the left side of the vehicle. The wheel center, tie rod end, lower arm, absorber, and brake caliper bracket for these hard points. Analyzing the load distribution and structural of these essential parts requires that the data be expressed in terms of the force components (Fx, Fy, and Fz) acting at each position.

### 3.7 Altair Inspire

Altair Inspire simulation driven framework for designing and optimizing critical automotive components like the steering knuckle. The process begins by importing a CAD of the steering knuckle and material properties, load cases, and real scenarios with appropriate boundary conditions. This approach combines static structural analysis, topology optimization, and lattice optimization for performance improvements, losing weight, and safety. the evolutionary workflow that scales up to lightweight yet durable enough for a manufacturing design.

#### 3.7.1 Static Stuctural Analysis

The first stage of static structural analysis of a steering knuckle performed in Altair Inspire includes assigning material properties. The material chosen is Aluminium 6061-T6, which has excellent strength-to-weight ratio, good corrosion resistance, and compatible for automotive applications. As stated in the literature review table2.1 , Aluminium 6061-T6 has typical mechanical properties of: Young's modulus 68.9 GPa, yield strength 276 MPa, and Poisson's ratio 0.33. These values ensure the material can withstand the operational loads expected in the steering knuckle design while maintaining optimal weight for vehicle performance.

Once the material properties are defined, the relevant forces and boundary conditions are applied to simulate real-world operating conditions in Components mode, with the magnitudes specified in  $F_x$ ,  $F_y$ , and  $F_z$  by clicking the icon “Loads”. Boundary conditions are defined at the attachment points, such as where the knuckle connects to the lower control arms, Absorber, bracket brake calliper, and tie rod to prevent unnecessary movement and simulate the constraints in the system are illustrated in Figure 3.26.



Figure 3.26: Design Base Model and Boundary Conditions

Table 3.6: Data for Structural analysis for all designs

Components	Magnitude $F_x, F_y, F_z$
Wheel centre	$1.125 \times 10^4 N$
Absorber Point 1 & 2	2769.796 N
Lower arm	5798.616 N
Tie rod end	6021.917 N
Brake calliper Bracket point 1 & 2	$9.94 \times 10^4 Nmm$

Table 3.6 summarizes the components, and the corresponding magnitudes applied during the simulation, defined in terms of components along the x, y, and z axis ( $F_x, F_y, F_z$ ). These forces are derived from the methodology of Motion View outlined in Table 3.5, ensuring accurate representation of real-world operating conditions. At the wheel center, a force of  $1.125 \times 10^4 N$  is applied. For Absorber Points 1 and 2, a force of 2769.796 N is applied. The lower arm is subjected to a force of 5798.616 N, while the tie



rod ends up experiencing a force of 6021.917 N. Finally, the brake caliper bracket points 1 and 2 are subjected to a moment of  $9.94 \times 10^4 \text{ Nmm}$ , simulating the torque experienced during operation.

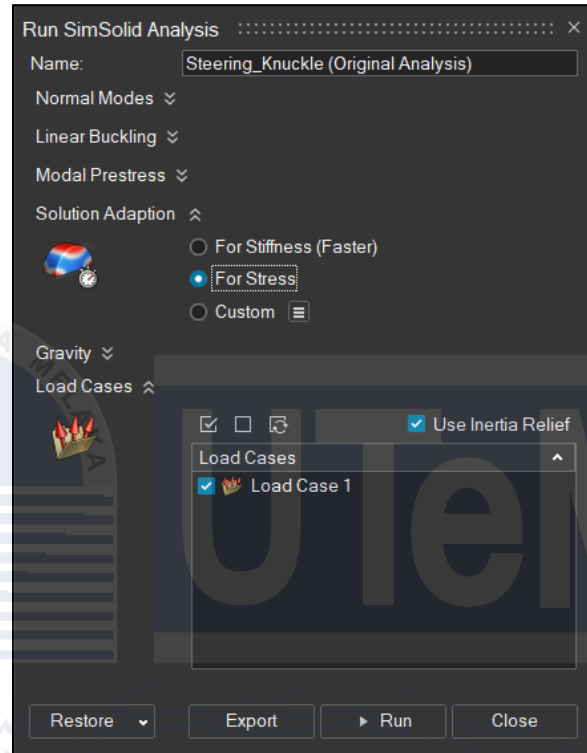


Figure 3.27: Setup to run the structural simulation analysis

Figure 3.27 illustrates the setup for running the structural simulation analysis. The configuration shown is for analysing the steering knuckle under specific conditions. The analysis type is selected as "Normal Modes," while options such as "Linear Buckling" and "Modal Prestress" remain unselected. For solution adaptation, the "For Stress" option is chosen to prioritize stress analysis. Gravity is not accounted for in the simulation, and "Load Case 1" is specified as the applied loading condition. Additionally, the "Use Inertia Relief" option is enabled, ensuring that inertial effects are considered during the analysis. After selected the requirements from the analysis setup then click button Run to running the analysis.

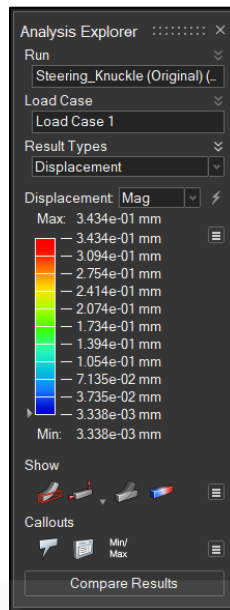


Figure 3.28: Analysis Explorer

After setting up the forces, supports, and material properties, the static structural analysis is run to evaluate the steering knuckle's performance. Altair Inspire calculates important results such as Von Mises stress, displacement, and factor of safety (FOS) as shown in Figure 3.28. Von Mises stress indicates regions on the knuckle that experience high stresses for possible failure detection. Displacement analysis should give insight into any deformation taking place in the steering knuckle under load and that the deformation experienced does not surpass the limits. Last, the factor of safety is calculated to ascertain whether the design has adequate safety margins. A factor of safety greater than 1 indicates that the component can withstand the applied loads without failure.

Upon completing the analysis, Altair Inspire will generate a report that contains the findings from the static analysis in full detail. The report includes plots showing distributions of Von Mises stress, displacement, and factors of safety, along with numerical details that help direct further design improvement and ensure that the steering knuckle is meeting safety and performance specifications.

### 3.7.2 Topology Optimization

The topology optimization process within a reduction range of 30% to 50% on the shape of the design, weight optimization was carried out based on maintaining structural integrity. This selected range is, in this analysis, balanced between the harnessing of maximizing strength and achieving lightweight. Certain conditions were given to the model without shape controls during optimization, and the load case value was taken directly from the standard design.

Before beginning the topology optimization run, the partition icon was selected for defining the boundary conditions and the design space. This was important for dividing the model into distinct regions, thereby offering a focused and controlled optimization phase. The design space was partitioned in such a way as to enable optimization to occur in the relevant regions of the structure while leaving unaffected other regions outside the purview of the optimization. This would ensure a more effective redistribution of material with mass reduction, thus ensuring that the final design would meet the weight-saving objectives while ensuring structural strength and stability.

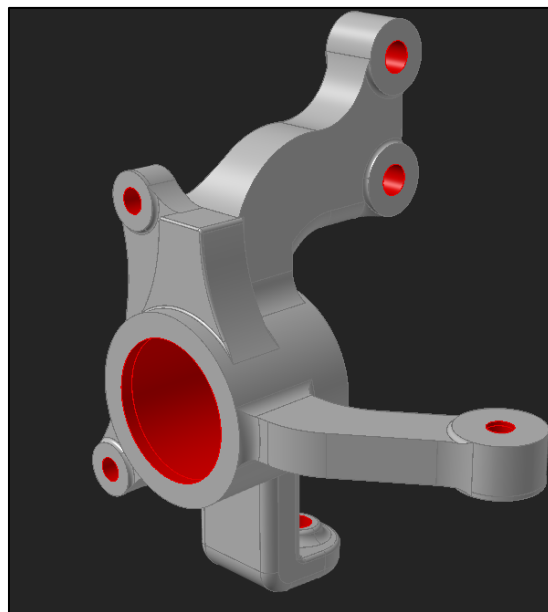


Figure 3.29: Partition on Steering Knuckle

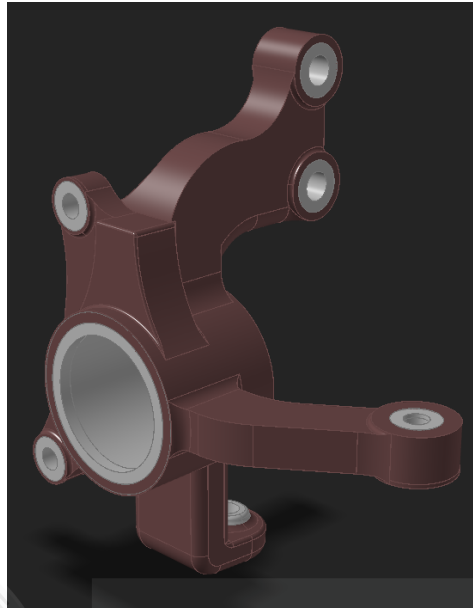


Figure 3.30: Design Space on Steering Knuckle

Once the design space was partitioned, as shown in figures 3.29 and 3.30, boundary conditions and loading were given. Fixed support was applied to specific points to prevent unreasonable movement and thereby allow for an accurate simulation of the model's deformation. Thus, loading conditions were further pegged on the Base Model, specifying the forces acting on the model. This arrangement made it so that, if higher loading was specified, the optimization results would be able to reflect the performance of the design under the specified loading conditions and would be capable of precisely distributing material and reducing weight while ensuring the needed strength.

## Setup The Topology Optimization

Table 3.7:Run Optimization Parameter

Parameter	Selection
Name file	Load Case 1
Type	Topology
Objective	Maximize Stiffness
Mass target	30% ,40%, 50%
Frequency constraints	None
Thickness constraints	None
Speed/accuracy	Faster
Gravity	No
Load cases	<ul style="list-style-type: none"> <li>- Load Case 30%</li> <li>- Load Case 40%</li> <li>- Load Case 50%</li> </ul>

Table 3.7 shows the parameter settings for the optimization process. The analysis thus began after selecting a file named "Load Case 30%, Load Case 40%," and Load case 50%;" topology optimization was subsequently noted as the selected type. The objective was defined as maximizing stiffness, while the material mass limits were set between 30 and 50%. No constraints were set on the frequency or the thickness to provide some freedom with the desired results. For speed in setup and efficiency in analyses, gravity effects were neglected. Load cases were sequentially applied at 30, 40, and 50% to assess the design under different scenarios.

To conduct the optimization method, the process developed the initial model by defining geometric and material properties. Then, the type of topology optimization and stiffness objective was defined, followed by setting the values for mass reduction. The topology optimization setup allows a greater degree of freedom to achieve an optimal design because it includes no frequency or thickness constraints. The speed and accuracy setting were set in a favourable way to compute the results rapidly. In this case, gravity effects were also neglected, allowing the simulation to concentrate on the load conditions solely. Finally, the load cases defined were applied sequentially to allow for an evaluation of the model performance under each load case. Finally, the results were examined at the end of the analysis to ensure that the objectives were achieved.

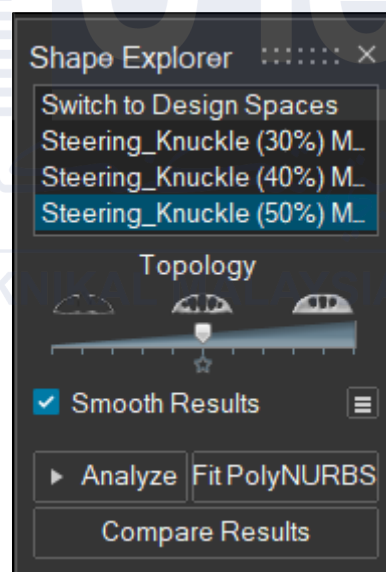


Figure 3.31: Shape Explorer

Shape Explorer interface in Figure 3.31 allows the view of topological optimization outputs of steering knuckle across three design iterations of 30%, 40%, and 50% material removal. The smooth results option allows enhancing the visualization, while analyze, fit PolyNURBS, and compare results functionalities accord detailed evaluation and improvement of the designs. It also has a topology slide that allows smooth

exploration of the geometry changes across iterations. In short, these would graphically show the integration of simulation progress tracking with detailed topology optimization analysis.

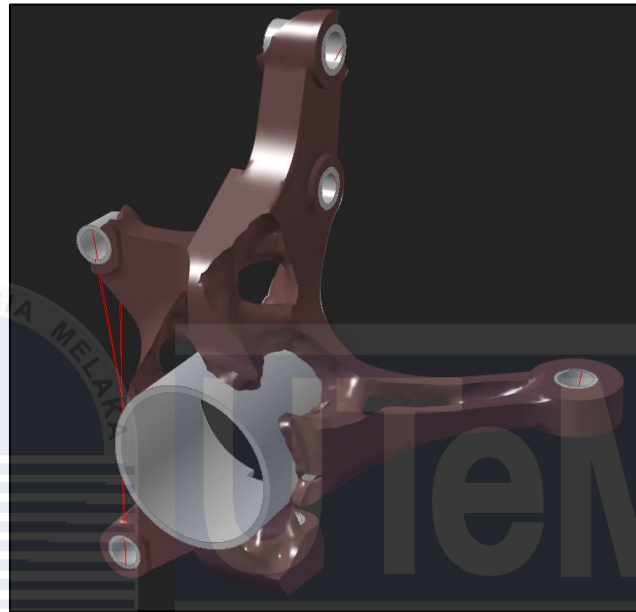


Figure 3.32: Optimized Steering Knuckle

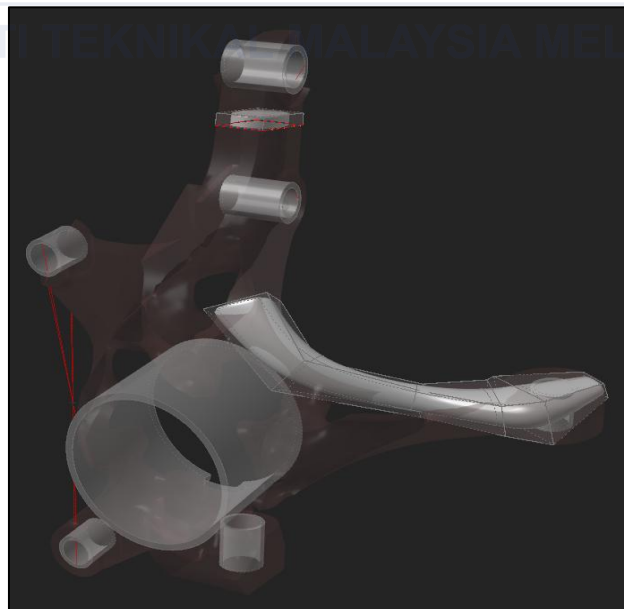


Figure 3.33: PolyNURBS Shape After Optimized

The last steps of the optimization process for the steering knuckle are illustrated in Figures 3.32 and 3.33. Figure 3.32 shows the optimized steering knuckle geometry obtained after the topology optimization, where unnecessary material is removed while ensuring the structural integrity and performance requirements are maintained. This optimization results in a lightweight design capable of withstanding the specified load cases.

In Figure 3.33 shows the PolyNURBS shape generated from the optimized topology. The PolyNURBS process refines and smooths the raw topology, creating a manufacturable and production-ready design while preserving the structural characteristics achieved during optimization. Together, these figures represent the transition from raw optimization results to a finalized, practical design in load case for 30%, 40% and 50%.



### 3.7.3 Lattice Structure Optimization

After using topology optimization to determine the most optimal element structure, Altair Inspire lattice structure optimization is applied to modify the design and maintain structural integrity. The methodology replaces solid sections with lightweight lattice designs, retaining the needed strength while using less weight. By simulating load conditions and analysing stress distributions, lattice parameters can be optimized to achieve the optimal balance between performance, reliability, and manufacturability. This methodology ensures efficient and innovative designs, which are ideal for complex technological uses and additive manufacturing processes.



Figure 3.34: Lattice Icon (Altair Inspire, 2023)

Figure 3.34 presents three types of lattice structures surface, planar, and strut lattices. Surface lattices, which are continuous porous structures, are used in applications such as heat exchangers and biomedical implants (Sağbaş & Gürkan, 2021). The planar lattice, which has repeating, flat grid-like patterns, is intended for directional strength and stability (Soyarslan et al., 2023). The chosen strut lattice, which consists of connecting rod-like parts, is widely used in aircraft components and composite panel lattices (Pan et al., 2020). These lattice options have importance for design optimization in additive manufacturing.

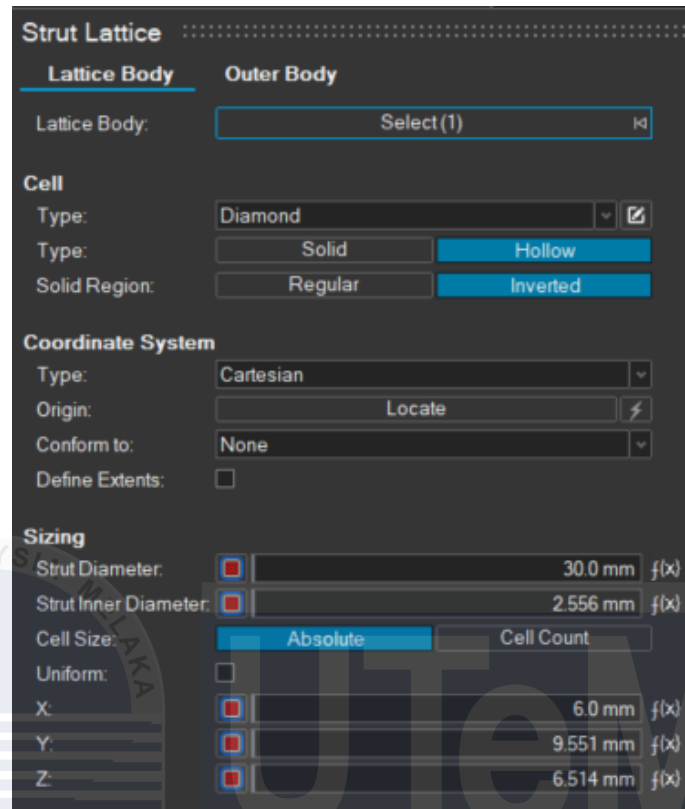


Figure 3.35: Strut Lattice Body Selection

Figure 3.35 Strut Lattice Body Selection shows a selection interface showing adjustable parameters for a diamond-shaped lattice design. The interface allows manipulation of lattice characteristics such as cell type, coordinate system, and dimensional parameters. The value input parameters for strut diameter (30.0 mm), inner diameter (2.555 mm), and absolute cell dimensions along the X (4.0 mm), Y (10.115 mm), and Z (20 mm) axes. Additional options facilitate the toggling between hollow and solid structures, as well as conventional and inverted solid parts.

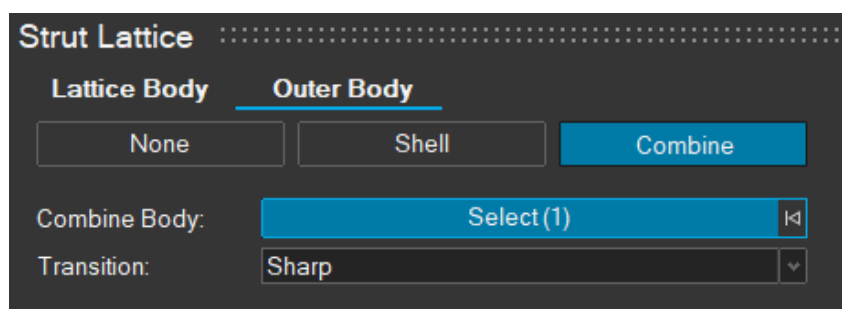


Figure 3.36: Sturt Lattice Outer Body

Figure 3.36 Strut Lattice Outer Body is shown to contain three selectable options: None, Shell, and Combine. The Combine option is selected to be merged with the partition selection, through which a unified body part can be generated. The interface is complemented by a transition parameter that is set to "Sharp," and a combine body field where specific selections can be made.



Figure 3.37: Steering Knuckle With lattice body

Figure 3.37 Steering Knuckle with Lattice Body is shown as an automotive component where a complex lattice structure has been integrated into its design. The original solid geometry is preserved at critical mounting points, while the main body is replaced by an intricate diamond-pattern lattice structure. The component's structural integrity is maintained through strategically placed solid sections, which are seamlessly connected to the lattice-filled regions. Additional options allow toggling between hollow solid structures and regular inverted solid regions, which can then be converted into triangle mesh representation for further analysis.

For the analysis, the loading conditions and boundary constraints remain identical to those defined in Load Case 1. After that, the steering knuckle with the strut lattice structure was subjected to finite element analysis (FEA) using Altair Inspire software to evaluate its mechanical performance under the applied loading conditions.

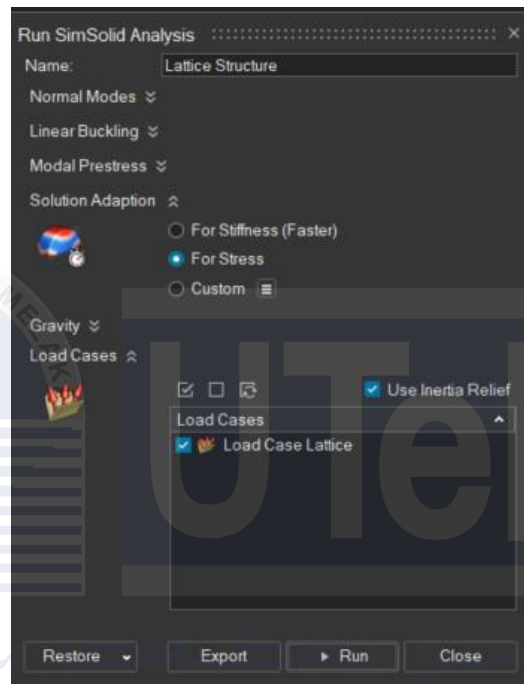


Figure 3.38: Run Analysis Model of Lattice Structure

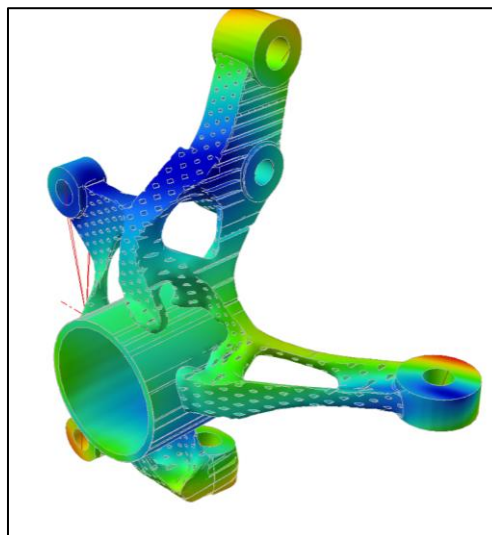


Figure 3.39: Analysis Process Completed

Figure 3.38 shows the Run Analysis setup interface, showing the configuration settings used for the lattice structure analysis. The analysis was conducted expressly for stress assessment, as indicated by the chosen option in the Solution Adaptation section. Furthermore, Inertia Relief was activated to address dynamic effects, and a designated load case referred to as Load Case Lattice was implemented.

Figure 3.39 shows the results of the completed analysis, showing the stress distribution and deformation patterns on the lattice-structured steering knuckle. Different color gradients depict the variation of stress intensity and displacement through the component. The warm colors represent regions of high stress concentration, while the cooler areas signify reduced stress levels. The analysis provided information on the lattice structure exposed to operational stress that helped identify critical areas and performance limitations.

### 3.8 Summary

The chapter presents a comprehensive methodology for optimizing the design of knuckles with advanced scanning and analysis software. The physical model is scanned using the EinScan Pro HD scanner, while detailed geometry is collected in 3D via point cloud data. This data is then cleaned up and edited before being converted into CAD models using Generative Shape Design (GSD) and Part Design features within CATIA V5. The model's accuracy has been validated, as the mass of the basic model is within 5% of that of the real model, a difference of 4.56%.

The methodology then continues to analysing at the steering knuckle's using the Altair software. Altair Motion View simulates the front suspension system and determines static load situations resulting in actual force estimates at several component positions. This data is transmitted into Altair Inspire, which performs static structural analysis on the Aluminium 6061-T6 material properties. The method finishes with two optimisation approaches to be specific is topology optimization, which aims to reduce weight by 30-50% while retaining structural integrity, and lattice structure optimization, which replaces solid parts with lightweight lattice designs. Throughout each stage, the process ensures that performance requirements and structural integrity are fulfilled while achieving weight reduction objectives.

## CHAPTER 4

### RESULTS AND DISCUSSION

#### 4.1 Introduction

In this chapter, simulation results from Finite Element Analysis in Altair Inspire 2024 are discussed topology optimization and lattice optimization. The results and discussion will focus on the analysis data and optimization such as Displacement, max shear stress, Von Mises Stress and Safety Factor. Data are presented in graphs and pictures in the appendix.

#### 4.2 Static Structural Analysis Base Model

This study used the Toyota Vios steering knuckle as a base model and conducted a static structural analysis of the steering knuckle. The analysis was performed using Altair Inspire software. Among the important performance indicators, the study focused on analyzing included displacement, von Mises stress, and safety factors. By means of comparison with the Toyota Vios steering knuckle, the analysis guarantees adherence to industry standards and offers a reliable source of performance evaluation reference.

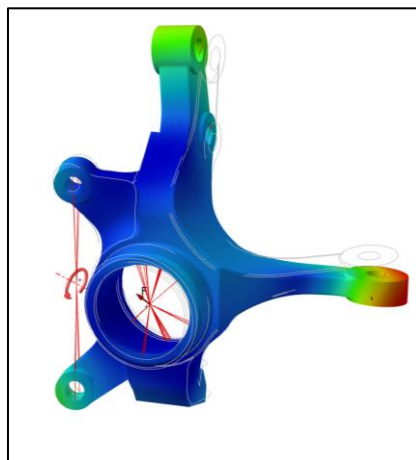


Figure 4.1: Base Model Analysis

Figure 4.1 Base Model Analysis displays stress distribution results that are visualized through a colour gradient, where red regions indicate areas of high stress concentration and blue regions represent areas of lower stress.

Table 4.1:Result of Base Model

Parameter	Range	Value	Figure
Displacement (mm)	Maximum	$3.43 \times 10^{-1}$	Figure 4.2
	Minimum	$3.34 \times 10^{-3}$	
Von Mises Stress (MPa)	Maximum	$9.35 \times 10^1$	Figure 4.3
	Minimum	$1.40 \times 10^{-1}$	
Factor of Safety		2.6	Figure 4.4

The results from Table 4.1 reveal important insights into the model's structural performance. The displacement, ranging from 0.00334 mm to 0.343 mm, shows that the model undergoes minimal deformation, with the maximum displacement remaining within acceptable limits in figure 4.2. The Von Mises stress has indicated a maximum of 93.5 MPa and a minimum of 0.140 MPa as represented in figure 4.3, thus calling for deep consideration of the material's strength especially where stress concentration is high. A safety factor of 2.6 indicates that there is a fair safety margin, which suggests that under the given load the model is safe but would perform better with further optimization, as can be inferred from figure 4.4.



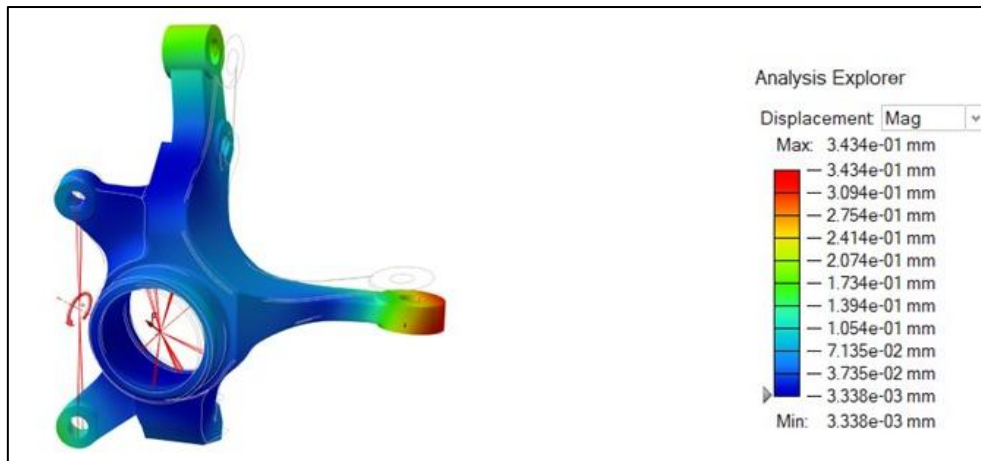


Figure 4.2: Displacement of Base Model

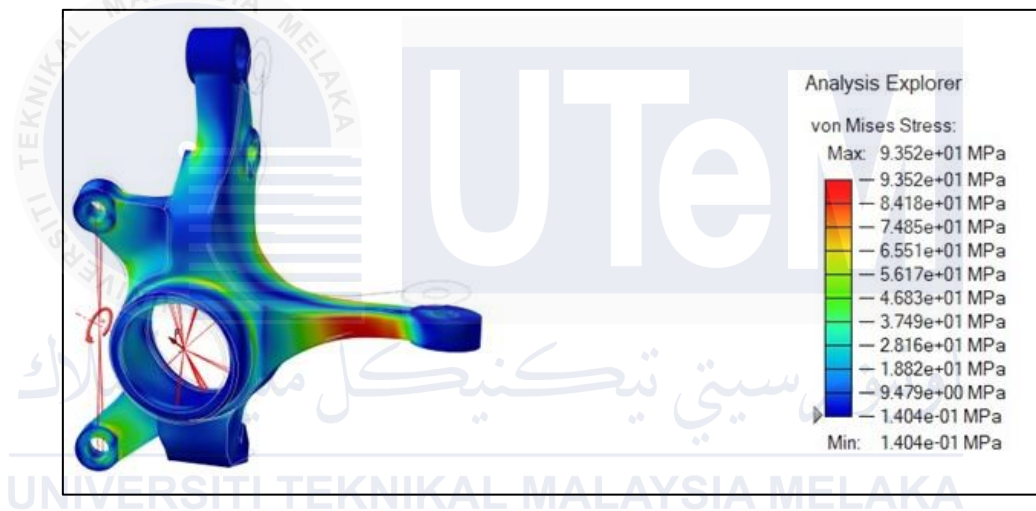


Figure 4.3: Von Mises Stress of Base Model

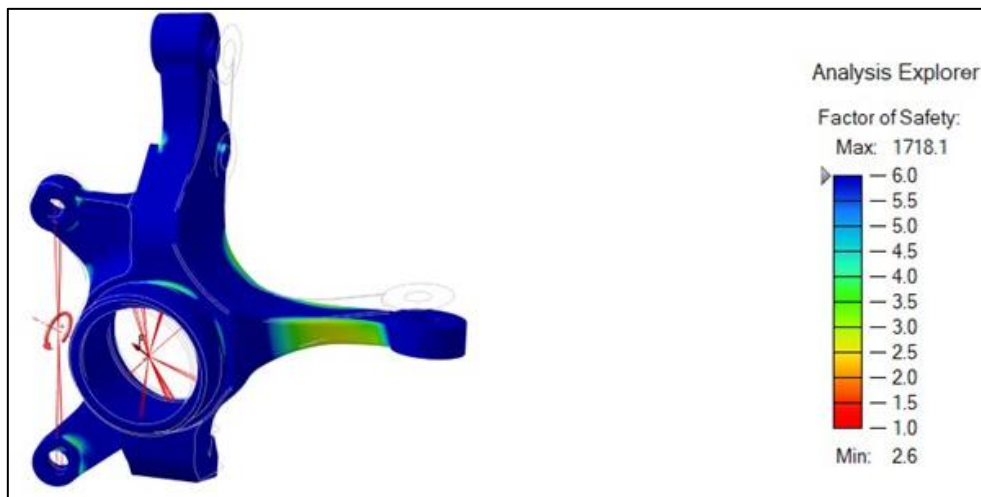


Figure 4.4 : Factor of Safety of Base Model

### 4.3 Topology Analysis and Optimization

In this subtopic, the results of topology optimization conducted on the steering knuckle are presented, focusing on reducing its shape and weight while maintaining structural integrity. The analysis assesses the effects of Weight Reduction Models (WRM) at 30%, 40%, and 50% levels on key parameters, including displacement, Von Mises Stress, and the factor of safety. These findings are used to provide valuable insights for optimizing the steering knuckle design by minimizing weight without compromising performance.

#### 4.3.1 Topology Optimized 30%



Figure 4.5: Steering Knuckle 30%

Figure 4.5 shows the steering knuckle optimized for 30% weight reduction using Altair Inspire. The design intent revolves around removing material from lower stress regions while providing enough structural integrity to maintain high loads in more loaded areas. Compared to the previous iterations, this model has a more lightweight structure that indicates a relatively substantial reduction in weight occurred while not having a very severe impact on functionality during typical operational conditions.

Table 4.2: Result of WRM 30%

Parameter	Range	Value	Figure
Displacement (mm)	Maximum	$3.98 \times 10^{-1}$	Figure 4.6
	Minimum	$2.40 \times 10^{-3}$	
Von Mises Stress (MPa)	Maximum	$1.36 \times 10^2$	Figure 4.7
	Minimum	$8.48 \times 10^{-2}$	
Factor of Safety		1.8	Figure 4.8

In Table 4.2, the analysis data for the 30% WRM are presented. The maximum displacement is recorded at 0.398 mm, while the minimum displacement is 0.00240 mm, as shown in figure 4.6. Regarding the von Mises stress, the range is between 0.0848 MPa to a peak of 136 MPa as shown in figure 4.7. As seen in the figure 4.8, a safety factor of 1.8 is classified as within an acceptable margin of 1.0 to 3.0 (Hoffenson, 2012). The results prove and render it competent that this design is maintaining structural performance at a weight reduction of 50%.

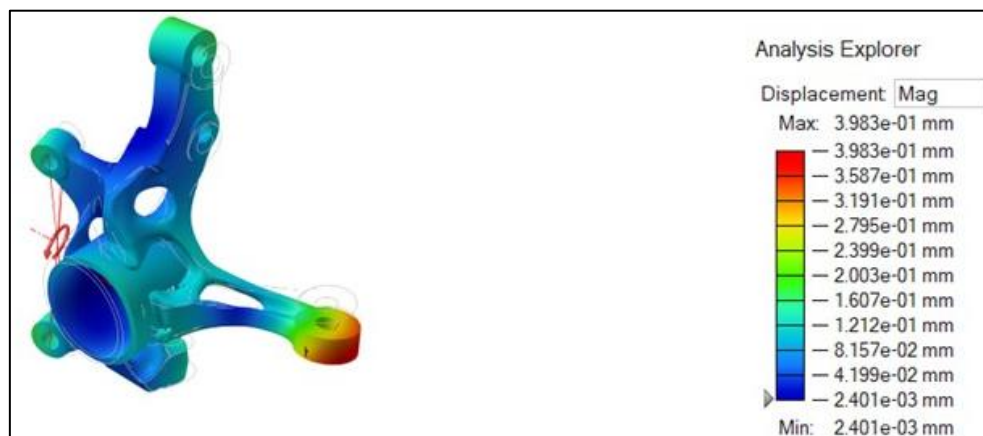


Figure 4.6: WRM 30% Displacement

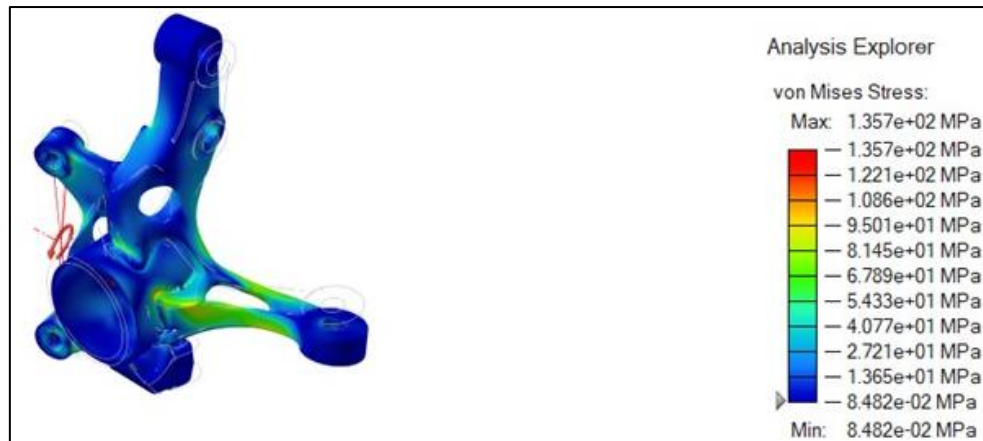


Figure 4.7: WRM 30% Von Mises Stress



Figure 4.8: WRM 30% Factor of Safety

#### 4.3.2 Topology Optimized 40%



Figure 4.9: Steering Knuckle 40%

Figure 4.9 shows the steering knuckle design optimized for a 40% weight reduction by carrying out topology optimization using Altair Inspire. This version, in contrast to the 50% model, incorporates additional weight-saving measures by getting rid of material in areas considered to be less critical and not affecting the strength necessary for load-bearing regions. The refined geometry highlights the potential for enhanced weight efficiency without significantly compromising the structural performance of the component.

Table 4 3 :Result of WRM 40%

Parameter	Range	Value	Figure
Displacement (mm)	Maximum	$4.28 \times 10^{-1}$	Figure 4.10
	Minimum	$3.42 \times 10^{-3}$	
Von Mises Stress (MPa)	Maximum	$1.31 \times 10^2$	Figure 4.11
	Minimum	$7.48 \times 10^{-2}$	
Factor of Safety		1.8	Figure 4.12

Table 4.3 provides the performance results for the 40% weight reduction model. The maximum displacement is recorded at 0.428 mm, while the minimum displacement is 0.00342 mm, as referenced in figure 4.10. The von Mises stress ranges between 0.0748 MPa and 131 MPa, documented in figure 4.11. The factor of safety, calculated at 1.8 as shown in figure 4.12, is well within the acceptable range of 1.0 to 3.0, indicating that this design meets the required safety standards while achieving significant weight reduction (Hoffenson, 2012).



Figure 4.10: WRM 40% Displacement

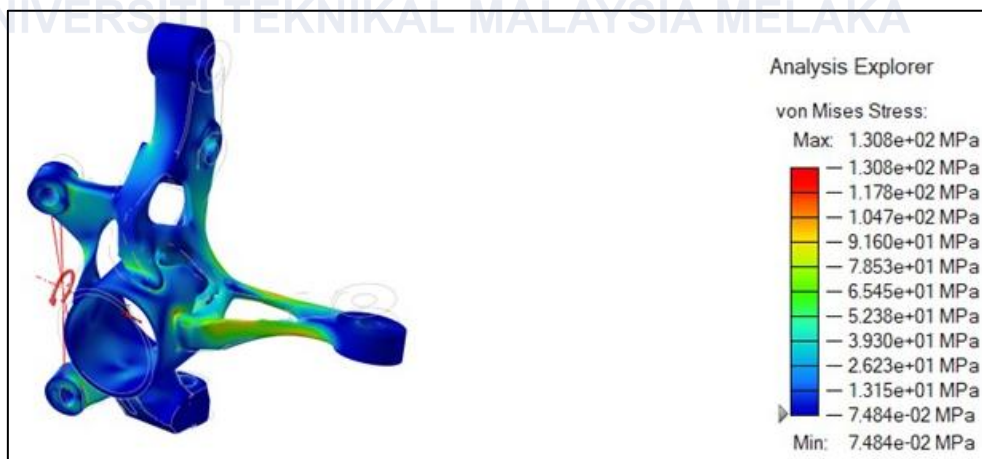


Figure 4.11: WRM 40% Von Mises Stress

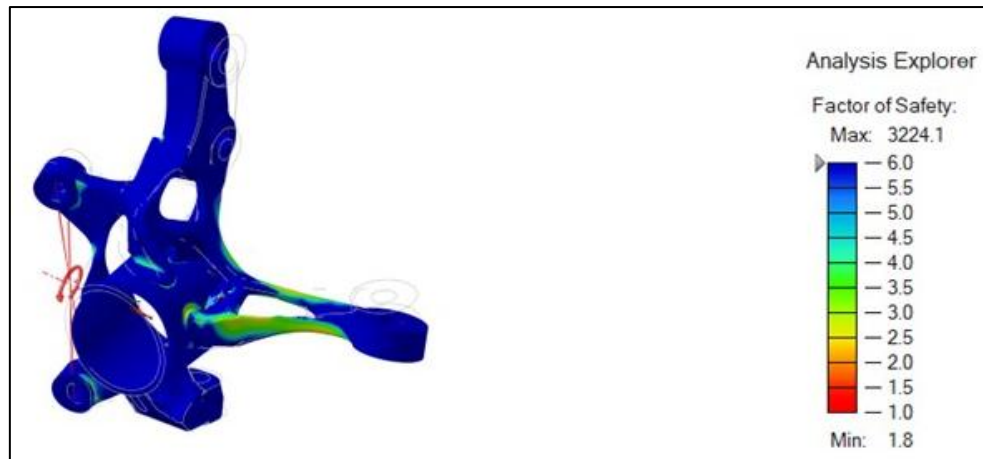


Figure 4.12: WRM 40% Factor of Safety



### 4.3.3 Topology Optimized 50%

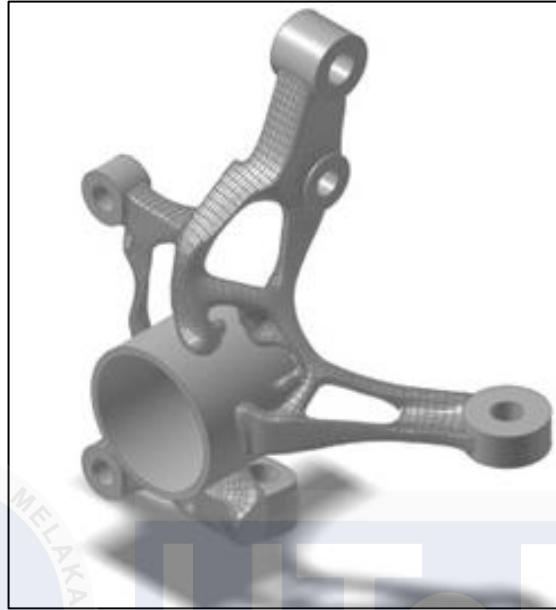


Figure 4.13: Steering Knuckle 50%

Figure 4.13 illustrates the optimized steering knuckle design after a 50% weight reduction, generated through topology optimization using Altair Inspire. The design shows significant material removal in non-critical areas while maintaining the structural integrity of the component. The lightweight structure emphasizes efficient material usage while ensuring performance under operational loads. This optimized model demonstrates the potential for reducing the overall weight of the steering knuckle, contributing to better fuel efficiency.

Table 4.4: Result of WRM 50%

Parameter	Range	Value	Figure
Displacement (mm)	Maximum	$1.22 \times 10^0$	Figure 4.14
	Minimum	$6.17 \times 10^{-2}$	
Von Mises Stress (MPa)	Maximum	$2.86 \times 10^2$	Figure 4.15
	Minimum	$7.74 \times 10^{-2}$	
Factor of Safety		0.8	Figure 4.16



Table 4.2 summarizes the findings for the 50% weight loss model. The maximum displacement is 1.22 mm, with a minimum displacement of 0.0617 mm, as shown in figure 4.14. The von Mises stress ranges from 0.0774 MPa to 286 MPa, as stated in figure 4.15. However, the factor of safety is assessed to be 0.8 as shown in figure 4.16, which is lower than the permissible range of 1.0 to 3.0 (Hoffenson, 2012). This result indicates that the design accomplishes the minimal safety criteria and requires additional optimization to handle stress concentrations and assure structural reliability.



Figure 4.14: WRM 50% Displacement

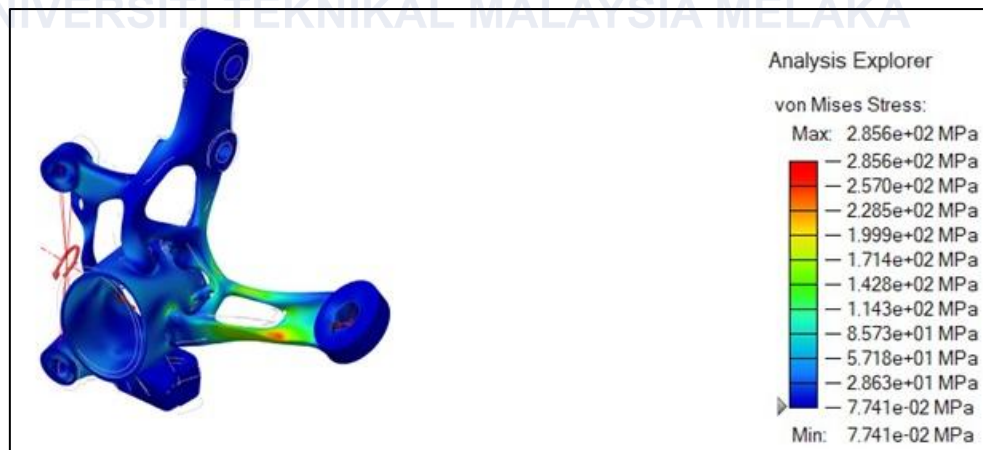


Figure 4.15: WRM 50% Von Mises Stress

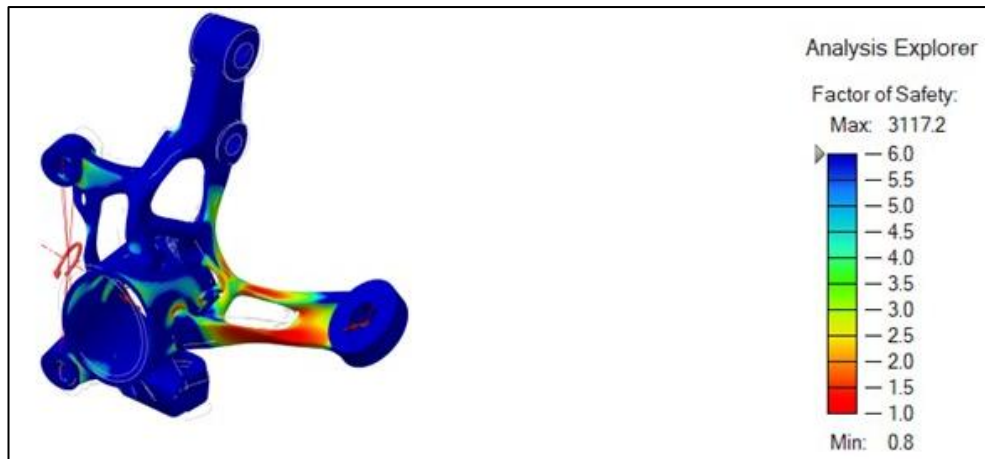


Figure 4.16: WRM 50% Factor of Safety



اونيورسيتي تېكنيكل مليسيا ملاك

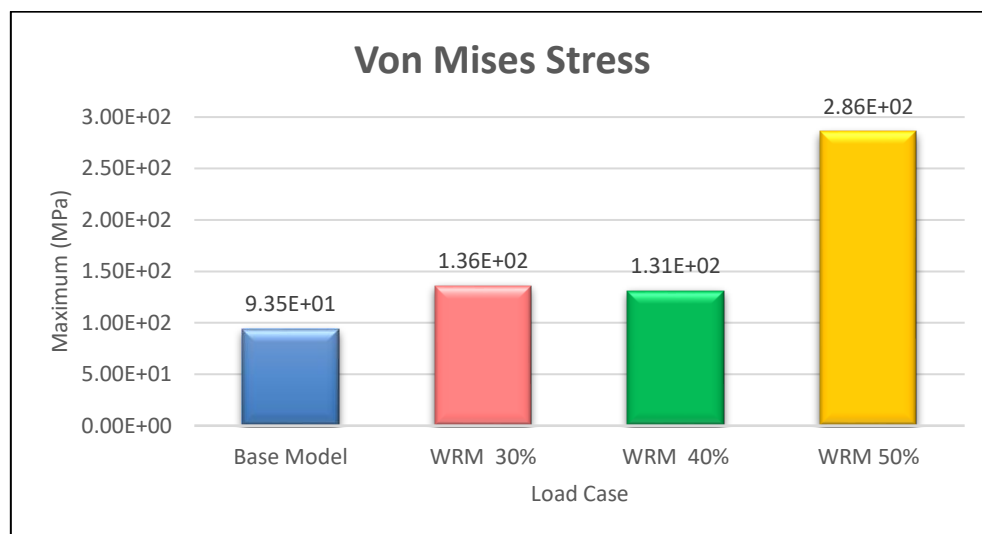
UNIVERSITI TEKNIKAL MALAYSIA MELAKA

#### 4.4 Comparison Analysis Between Base Model And 3 Topology Model

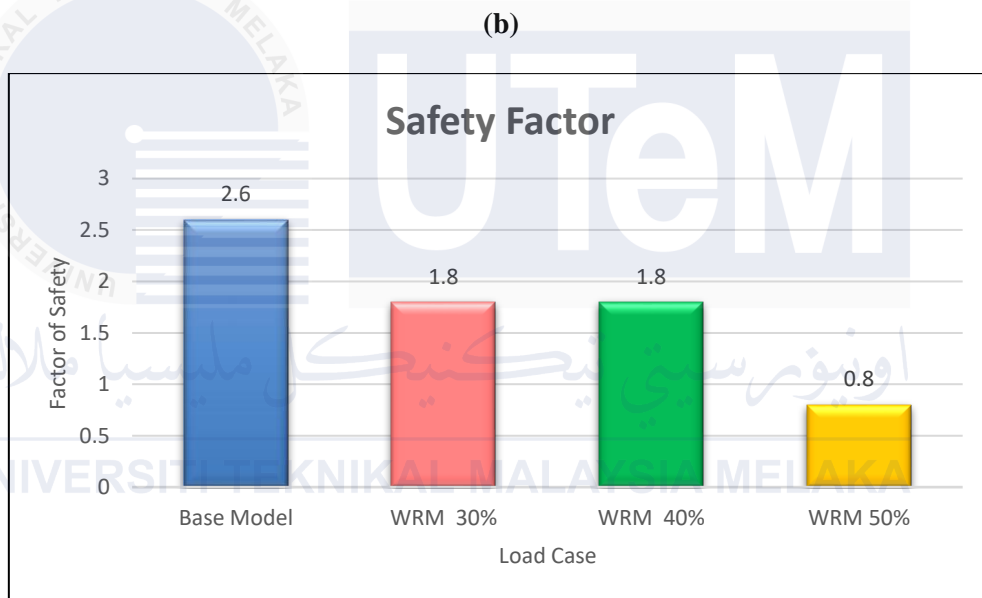
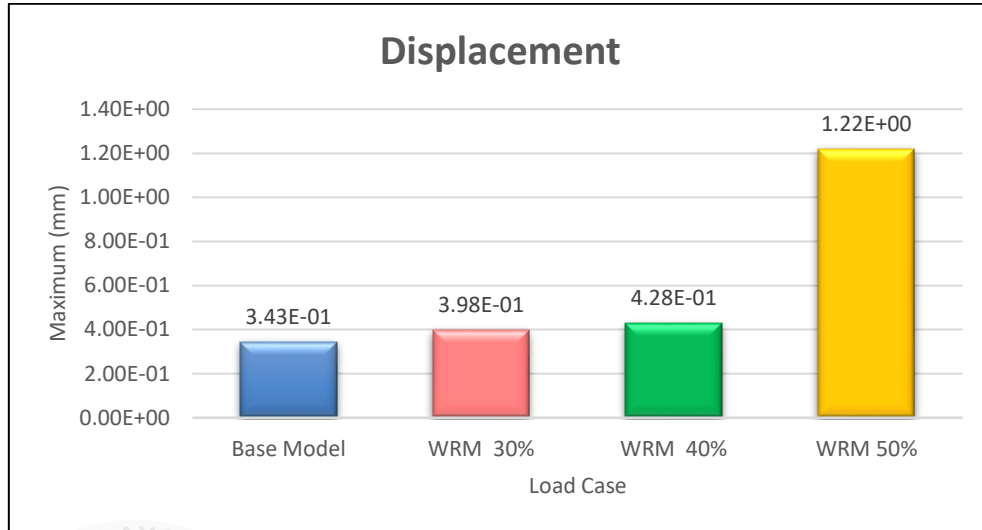
This results section compares the Base Model with three topology-optimized models featuring shape modifications of 30%, 40%, and 50%. The 50% Topology Model shows a moderate reshaping of the geometry, improving structural efficiency while maintaining strength. The 40% Topology Model introduces a more pronounced shape change, optimizing load paths with slight reductions in stiffness. The 30% Topology Model demonstrates the most aggressive shape modification, leading to significant weight savings but with noticeable reductions in both strength and stiffness. These results highlight the effect of shape optimization on the balance between structural performance and design efficiency. Table 4.5 shows the comparison weight (Kg) among WRM.

Table 4.5: Comparison for all WRM

Base Model & WRM	Weight (Kg)
Base Model	1.023
WRM 30 %	0.717
WRM 40%	0.63
WRM 50%	0.541



(a)



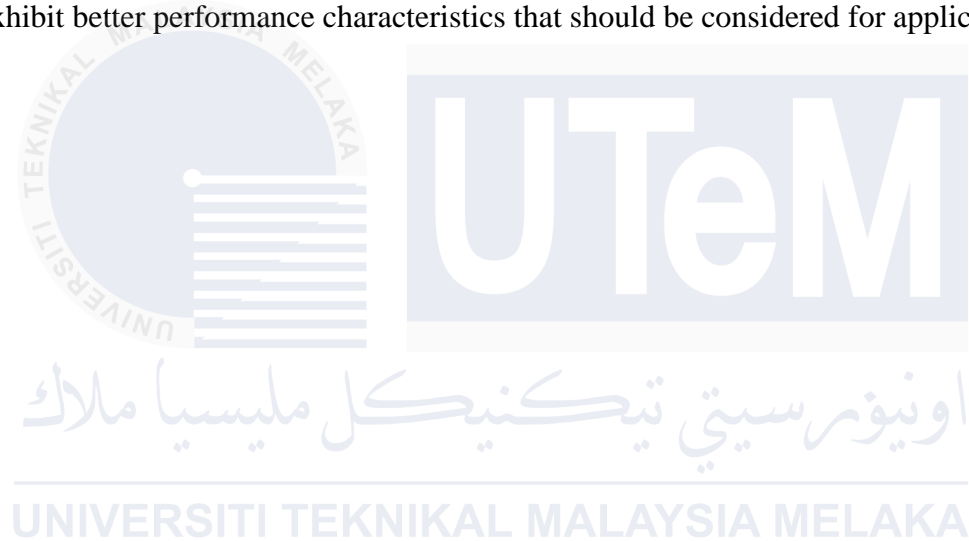
(c)

Figure 4.17: Comparison Analysis Data (a) Von Mises Stress (b) Displacement (c) Factor of Safety

Figure 4.17 presents a thorough comparative analysis through three distinct graphs each shows the structural behaviors under various load cases. In the Von Mises stress analysis, the highest recorded stress is 286 MPa for WRM 50%. On the other hand, WRM 40% and 30% exhibit lower stress values of 131 MPa and 136 MPa, respectively, compared to the base model's stress of 93.5 MPa. Additionally, the displacement graph indicates that the maximum deformation of 1.22 mm occurs in WRM 50%.

The Factor of Safety (FoS) analysis reveals an inverse correlation with stress values. The base model has the highest safety factor at 2.6, while WRM 50% has the lowest at 0.8, categorizing it as unsafe since it falls below the minimum safety threshold of 1.0. WRM 40% and 30% show safety factors of 1.8, suggesting that these configurations are more appropriate for structural design.

The findings indicate that WRM 50% demonstrates significant stress and displacement values along with an inadequate safety factor, whereas WRM 40% and 30% exhibit better performance characteristics that should be considered for application.



#### 4.5 Lattice Structure Analysis

In modern vehicle design, the steering knuckle provides support to the suspension and steering system, requiring a mix of strength, durability, and weight efficiency. Conventional solid constructions, while durable, may contribute to increased mass, which impacts vehicle performance. A lattice structure design, specifically using the 40% model, has been employed to provide an optimal shape that minimizes weight while maintaining structural integrity through a connected system of struts and nodes. The 40% model was chosen for lattice structure analysis because it balances between weight reduction and strength. This section provides an examination of the lattice-structured steering knuckle using Finite Element examination (FEA), assessing critical performance metrics like displacement, shear stress, Von Mises stress, and the safety factor. The results clarify the component's mechanical performance under operating stresses, highlighting crucial areas and confirming adherence to design specifications.

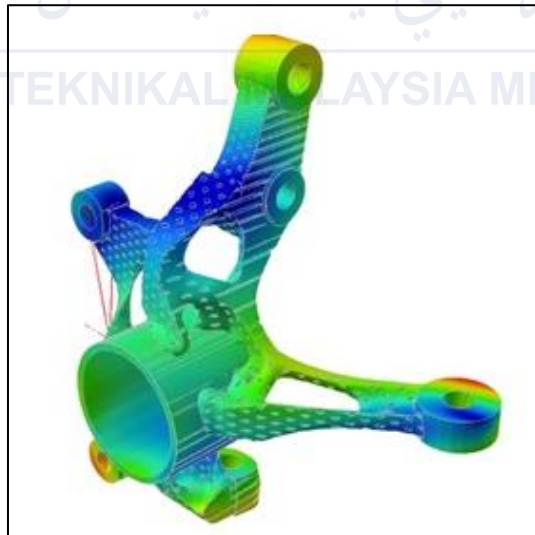


Figure 4.18: Steering Knuckle Lattice Structure Analysis

Figure 4.18 shows the result of steering knuckle lattice structure performed on analysis. Various colors represent the distribution of stress, displacement, and safety factors across the component. Areas of high stress and displacement are indicated by warmer colors, while cooler colors denote regions of lower intensity. The lattice structure is strategically optimized to balance strength and weight reduction, ensuring efficient mechanical performance under operational loads.

Table 4.6:Result Data of LSM

Parameter	Range	Value	Figure
Displacement (mm)	Maximum	$3.14 \times 10^{-1}$	Figure 4.19
	Minimum	$1.22 \times 10^{-2}$	
Von Mises Stress (MPa)	Maximum	$9.10 \times 10^2$	Figure 4.20
	Minimum	$1.63 \times 10^{-1}$	
Factor of Safety		0.3	Figure 4.21

Table 4.6 represents quantitative results generated by the finite element analysis of the steering knuckle lattice structure. Displacement values range from a minimum of  $1.22 \times 10^{-2}$  mm to a high of  $3.14 \times 10^{-1}$ mm, reflecting the degree of deformation under applied stresses as shown in figure 4.19. The Von Mises stress values range from 0.163 MPa to 910 MPa, indicating the comprehensive stress condition throughout the structure as illustrated in figure 4.20. The factor of safety is indicated as 0.3, indicating that the component functions around its material strength limits under the specified stress circumstances as shown in figure 4.21. The referenced appendices provide additional insights into the analysis results.

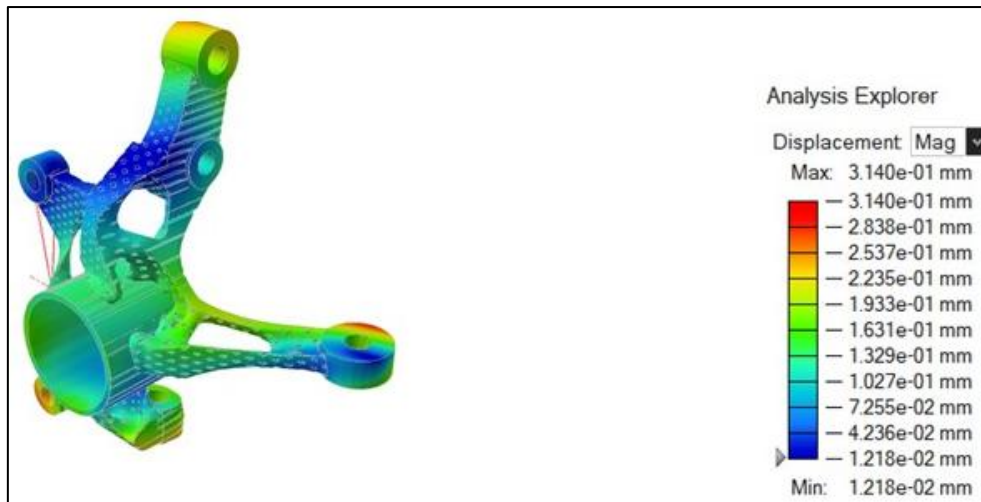


Figure 4.19: LSM Displacement



Figure 4.20: LSM Von Mises Stress

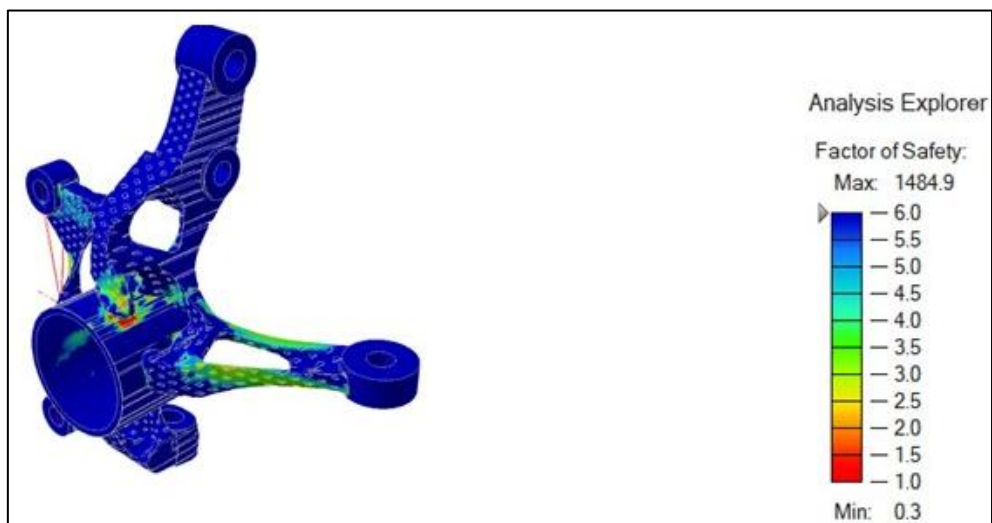


Figure 4.21: LSM Factor of Safety



#### 4.6 Comparison Between Base Model, Optimized and Lattice Structure

The last part of this study focuses on comparing the finite element analysis (FEA) results for the three design variations of the steering knuckle: the base model, the Weight Reduction Model with a 40% weight reduction, and the Lattice Structure Model. Table 4.7 summarizes key parameters, including weight, maximum displacement, maximum Von Mises stress, and the factor of safety. Through this comparison, the effects of structural optimization and lattice integration on the mechanical performance of the steering knuckle are evaluated systematically.

The base model, weight is 1.023 kg, showed the minimal maximum displacement of  $3.43 \times 10^{-1}$  mm and the greatest safety factor of 2.6. However, this design requires a slightly great mass, therefore increasing the total weight of the vehicle. However, the improved WRM, which produced a 40% reduction in weight (0.63 kg), showed a little increase in displacement to  $4.28 \times 10^{-1}$  mm and a decrease in the factor of safety to 1.8. Although these compromises, the improved model proficiently balances weight reduction with structural performance.

The LSM, with a mass of 0.588 kg, represents the lightest design among the three variations. It showed a maximum displacement of 0.314 mm, which is less than the optimized model but slightly better than the base model. The maximum Von Mises stress in the lattice structure reached 910 MPa, but the factor of safety dropped dramatically to 0.3, meaning that the component functions closer to its material limits. The lattice design provided significant weight reduction and acceptable displacement; even though the compromise in safety margins requires cautious analysis in high-stress scenarios. By analyzing different models, this study reveals the critical connection between design selection and performance outcomes as shown in figure 4.22.

Table 4.7: Comparison Analysis Data of Base Model, WRM 40% and LSM

Model	Weight (Kg)	Max Displacement	Max Von Mises Stress (MPa)	Factor Of Safety
Base Model	1.023	$3.43 \times 10^{-1}$	$9.35 \times 10^1$	2.6
WRM 40%	0.63	$4.28 \times 10^{-1}$	$1.31 \times 10^2$	1.8
LSM	0.588	$3.14 \times 10^{-1}$	$9.10 \times 10^2$	0.3

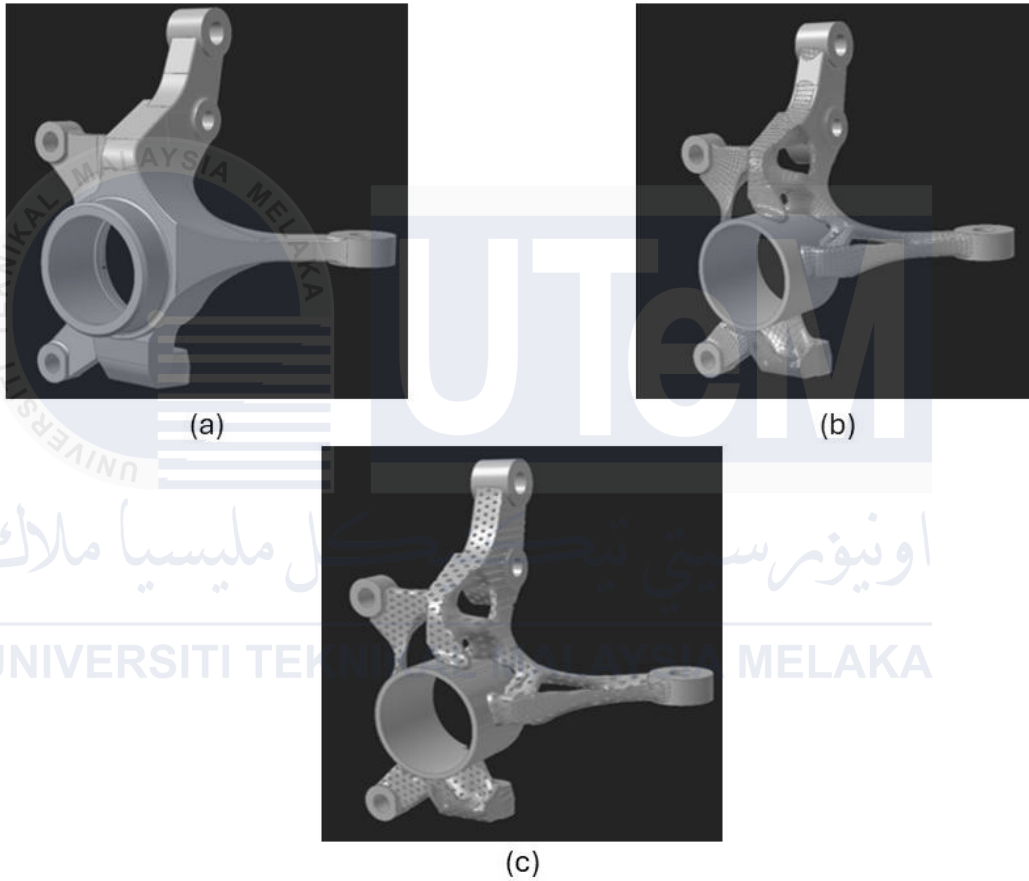


Figure 4.22: (a) Base Model (b) WRM 40% (c) LSM

## 4.7 Summary

The research analyzed the Toyota Vios steering knuckle using Finite Element Analysis in Altair Inspire 2024. The study begins with the base model, which showed good performance with a maximum displacement of 0.343 mm, a maximum Von Mises stress of 93.5 MPa, and a safety factor of 2.6, providing a strong benchmark.

Three topology-optimized designs were analyzed, with weight reduction of 30%, 40%, and 50%. The 30% and 40% WRM accomplished successfully with safety factors of 1.8, however the 50% WRM showed reduced structural integrity with a safety factor of 0.8, falling below the acceptable range of safety factor standard. A lattice structure model was constructed as well using the 40% WRM design, obtaining the lowest weight of 0.588 kg but showing concerned stress values with a safety factor of only 0.3. The final comparison of the base model, 40% WRM, and LSM revealed that the 40% WRM design achieved the best balance of weight reduction and structural integrity while maintaining acceptable safety margins whereas reducing the original weight by 38.4%.

## CONCLUSION & RECOMMENDATION

### 5.1 Conclusion

This research applied Altair Inspire to optimize the topology of the automotive part, which is steering knuckles, results in a lightweight while structurally efficient design. The objective of this research is to minimize the mass of the steering knuckle while maintaining its structural integrity under static loads analysis. The optimized design achieved a weight reduction of 40%, reducing the material usage without compromising the strength and stiffness required for vehicle safety. Stress and displacement analysis confirmed that the optimized model met the performance criteria under simulated loading conditions. Furthermore, the optimization process highlighted the critical load paths and areas for potential material removal, providing valuable insights for future component design. Overall, the research effectively proved the capacity of topology optimization to improve the efficiency of automotive components, so contributing to the main objective.

UNIVERSITI TEKNIKAL MALAYSIA MELAKA

## **5.2 Recommendations**

Based on the findings of this study, several recommendations are proposed to guide future research and industry applications.

### **5.2.1 Future Research**

Future study could focus on expanding topology optimization to other important automotive parts, such as suspension systems or engine mounts, to identify potential uses in vehicle design. Furthermore, the use of various materials, such as composites or high-strength metallic compounds, may improve the performance and efficiency of optimized designs. Implementing dynamic loading scenarios and analysis of fatigue will provide data regarding the long-term strength of optimized components. Furthermore, combining topology optimization with additive manufacturing techniques allows for the manufacture of complex geometry that is not limited by standard manufacturing limitations.

Lattice structure design has huge potential for future developments in automotive engineering. Future study may focus on multi-scale lattice optimization, in which micro and macro-scale lattice designs are combined to obtain the best balance of strength, stiffness, and manufacturability. Furthermore, the application of smart materials, such as shape-memory alloys or adaptive materials, might enable lattice structures to exhibit flexible stiffness features. Furthermore, bio-inspired lattice designs inspired by natural structures like honeycombs and bones provide interesting avenues for developing highly efficient geometries that specialize in weight reduction and load distribution. By increasing research in these areas, lattice structures have the potential to revolutionize automotive design by providing lighter, stronger, and more sustainable components for future vehicles.

## REFERENCES

- A Review on Steering Knuckle Analysis. (2019, June 1)
- Aakash, Amarnath., Amudhan, A., N., Manoj, K, V. (2023). Empowering Digital Twin Development: A Profound Exploration with Altair Tools. 1146-1153. doi: 10.1109/icssas57918.2023.10331675
- Blatnický, M., Sága, M., Dižo, J., & Brůna, M. (2020, February 11). Application of Light Metal Alloy EN AW 6063 to Vehicle Frame Construction with an Innovated Steering Mechanism. *Materials*, 13(4), 817-817. <https://doi.org/10.3390/ma13040817>
- Chen, J., Shen, X., & Zeng, Z. (2021, January 1). The structure design and performance analysis of a racing welded steering knuckle. <https://doi.org/10.25236/iccemm.2021.009>
- Chen, S., & Zhang, S. (2022, November 28). A structural optimization algorithm with stochastic forces and stresses. *Nature Computational Science*, 2(11), 736–744. <https://doi.org/10.1038/s43588-022-00350-w>
- Chen, Y.-C., Huang, H.-H., & Weng, C.-W.. (2019). Failure analysis of a re-design knuckle using topology optimization. 10(2). <https://doi.org/10.5194/MS-10-465-2019>
- Dalpadulo, E., Pini, F., & Leali, F.. (2021). Assessment of Computer-Aided Design Tools for Topology Optimization of Additively Manufactured Automotive Components. 11(22). <https://doi.org/10.3390/APP112210980>
- DeFelice, S. (2023, January 1). Complex geometries are possible with 3D printing. <https://www.eos.info/en/industrial-3d-printing/advantages/complex-geometries>
- Deshpande, A M., Ekabote, N., Sridhar, A., & Vernekar, A. (2020, December 1). Design cycle implementation on a customized steering knuckle for a competition ATV. <https://doi.org/10.1088/1742-6596/1706/1/012207>
- Deshpande, P., et al. (2020). “Static Analysis of Steering Knuckle and Its Shape Optimization.” *IOSR Journal of Mechanical and Civil Engineering (IOSR-JMCE)*, 1.
- Dusane, S. V., Dipke, M. K., & Kumbhalkar, M. A.. (2016). Analysis of Steering Knuckle of All Terrain Vehicles (ATV) Using Finite Element Analysis. 149(1). <https://doi.org/10.1088/1757-899X/149/1/012133>
- Farhatnia, F., Eftekhari, S A., Pakzad, A., & Oveissi, S. (2019, January 1). Optimizing the buckling characteristics and weight of functionally graded circular plates using the multi-objective Pareto archived simulated annealing algorithm (PASA). <https://doi.org/10.1051/smdo/2019014>

- Ferede, N. (2020). Topology Optimization of Automotive sheet metal part using Altair Inspire. *International Journal of Engineering and Management Sciences*, 5(3), 143–150. <https://doi.org/10.21791/ijems.2020.3.15>
- Georgantzia, E., Gkantou, M., & Kamaris, G S. (2021, January 1). Aluminium alloys as structural material: A review of research. <https://doi.org/10.1016/j.engstruct.2020.111372>
- Ghungarde, V., Awachar, S., Vaidya, N K., & Jagadeesha, T. (2019, October 1). Design optimization of steering knuckle by adopting bionic design approach. *IOP conference series. Materials science and engineering*, 624(1), 012023-012023. <https://doi.org/10.1088/1757-899x/624/1/012023>
- Goenka, M., Nihal, C., Ramanathan, R., Gupta, P., Parashar, A., & Joel, J. (2020, January 1). Automobile Parts Casting-Methods and Materials Used: A Review. *Materials today: proceedings*, 22, 2525-2531. <https://doi.org/10.1016/j.matpr.2020.03.381>
- Gulanová, J., Lonek, S., & Gulan, L. (2018, March 7). Comparison of two different approaches of a class-A surface creation and quality verification. <https://doi.org/10.1080/16864360.2018.1441242>
- Gupta, H., Shan, S., Rajvardhan, & Singh, N. K. (2021). Design and analysis of steering knuckle of hybrid metal matrix composite for the fsae vehicle. *Materials Today: Proceedings*, 46, 10551–10557. <https://doi.org/10.1016/j.matpr.2021.01.104>
- Heißing, B., & Ersoy, M. (2011). *Chassis Handbook: Fundamentals, Driving Dynamics, Components, Mechatronics, Perspectives*. Springer Vieweg.
- Hoffenson, S. (2012). Safety considerations in optimal automotive vehicle design. <https://deepblue.lib.umich.edu/handle/2027.42/91402>
- Ioana, B M., & Oancea, G. (2019, January 1). Parametric design of a complex part in a FEM environment. <https://doi.org/10.1051/mateconf/201929903005>
- Jeon, G T., Kim, K Y., Moon, J., Lee, C., Kim, W., & Kim, S J. (2018, October 20). Effect of Al 6061 Alloy Compositions on Mechanical Properties of the Automotive Steering Knuckle Made by Novel Casting Process. <https://doi.org/10.3390/met8100857>
- Jhala, P. R. L., Kothari, K. D., & Khandare, D. S. S.. (2010). *Geometry and Size Optimization for a Steering Knuckle with no change in attachment Geometry by reducing Production Cost and Weight*. 7. [https://www.researchgate.net/publication/266522603\\_Geometry\\_and\\_Size\\_Optimization\\_for\\_a\\_Steering\\_Knuckle\\_with\\_no\\_change\\_in\\_attachment\\_Geometry\\_by\\_reducing\\_Production\\_Cost\\_and\\_Weight](https://www.researchgate.net/publication/266522603_Geometry_and_Size_Optimization_for_a_Steering_Knuckle_with_no_change_in_attachment_Geometry_by_reducing_Production_Cost_and_Weight)

- Kashyzadeh, K R., Farrahi, G., Shariyat, M., & Ahmadian, M. (2018, September 1). The Role of Wheel Alignment Over the Fatigue Damage Accumulation in Vehicle Steering Knuckle. <https://doi.org/10.22084/jrstan.2018.15722.1042>
- Kashyzadeh, K. R.. (2023). Failure Strength of Automotive Steering Knuckle Made of Metal Matrix Composite. 4(1). <https://doi.org/10.3390/applmech4010012>
- Kentli, A. (2020, March 4). Topology Optimization Applications on Engineering Structures. <https://doi.org/10.5772/intechopen.90474>
- Khan, S., Khan, N., & Quadir, A.. (2018). Shape optimization of knuckle joint for different material using cae tools. 5(6).
- Kumar, D., & Mondal, S. (2021, March 1). A Review on Modelling, Design and Optimization of Forging Process. IOP conference series. Materials science and engineering, 1126(1), 012001-012001. <https://doi.org/10.1088/1757-899x/1126/1/012001>
- Kumar, L R., Sivalingam, S., Prashanth, K., & Rajkumar, K. (2020, February 28). Design, analysis and optimization of steering knuckle for all terrain vehicles. <https://pubs.aip.org/aip/acp/article/972940>
- Lee, D., & Rahman, S.. (2021). Robust design optimization under dependent random variables by a generalized polynomial chaos expansion. 63(5). <https://doi.org/10.1007/S00158-020-02820-Z>
- Li, G X., Zhang, M., Zhao, C., Jin, X., & Luo, W. (2019, November 1). Design Method of Function-Structure Integrated Lattice Structure. <https://doi.org/10.1088/1757-899x/686/1/012009>
- Matsimbi, M., Nziu, P. K., Masu, L. M., & Maringa, M.. (2021). <i>Topology Optimization of Automotive Body Structures: A review</i>. <i>13</i>, 15.
- Murr, L. E., Gaytan, S. M., Ceylan, A., Martinez, E., Martinez, J. L., Hernandez, D. H., ... & Wicker, R. B. (2010). Additive manufacturing of biomaterials: Opportunities and challenges. \*Journal of Materials Research, 25\*(12), 2336–2347. <https://doi.org/10.1557/JMR.2010.0026>
- Pan, C., Han, Y., & Lu, J. (2020, September 13). Design and Optimization of Lattice Structures: A Review. <https://doi.org/10.3390/app10186374>
- Product Re-Engineering by Topology Optimization for Forged Component. (2021, September 8). International Journal of Emerging Trends in Engineering Research, 9(9), 1266–1270. <https://doi.org/10.30534/ijeter/2021/10992021>
- Pugazhenth, R., Anbuhezhiyan, G., Muthuraman, R., Vignesh, M., & Ponshanmugakumar, A. (2021, January 1). Optimization of fatigue life and fractography analysis of knuckle joint. <https://doi.org/10.1016/j.matpr.2021.04.018>



- Qaralleh, A., Maciolek, A., Weichert, J., Möller, B., & Melza, T. (2024, January 1). Fatigue Analysis of Steering Knuckles Using the Local Strain Approach. <https://doi.org/10.1016/j.prostr.2024.03.072>
- Rajesh kumar, L., Sivalingam, S., Prashanth, K., & Rajkumar, K.. (2020). Design, analysis and optimization of steering knuckle for all terrain vehicles. 10. <https://doi.org/https://doi.org/10.1063/5.0000044>
- Rashwan, A.. (2019). Topology optimization and rim design.4(4). <https://doi.org/10.21791/IJEMS.2019.4.10>
- Remigio-Reyes, J. O., Garduño, I. E., Rojas-García, J. C., Arcos-Gutierrez, H., Ortigosa, R.. (2022). Topology optimization-driven design of added rib architecture system for enhanced free vibration response of thin-wall plastic components used in the automotive industry.123(3-4).<https://doi.org/10.1007/s00170-022-10219-x>
- Research on Aluminum Alloy Materials and Application Technology for Automotive Lightweighting. (2023, January 1). <https://doi.org/10.25236/ajmc.2023.040601>
- Santana, C E., Reyes, L A., Orona-Hinojos, J M., Huerta, L., Ríos, A., & Zambrano-Robledo, P D C. (2024, March 10). Numerical Study of Reinforced Aluminum Composites for Steering Knuckles in Last-Mile Electric Vehicles. <https://doi.org/10.3390/wevj15030109>
- Sathishkumar, S., & Kanna, M R R. (2019, January 1). TOPOLOGY OPTIMIZATION OF INTEGRATED COMBUSTION ENGINE PISTON USING FEA METHOD (CAE TOOLS). <https://doi.org/10.26480/amm.01.2019.01.05>
- Shirsat, V G., & More, O A. (2021, August 1). Design Calculations and Analysis of ALTO 800 Steering Knuckle Using Fea
- Soyarslan, C., Gleadall, A., Yan, J., Argeso, H., & Sozumert, E. (2023). Elastostatics of star-polygon tile-based architected planar lattices. *Materials & Design*, 226, 111580. <https://doi.org/10.1016/j.matdes.2022.111580>
- Srivastava, S. P., Salunkhe, S., Pande, S., & Kapadiya, B. (2020). Topology optimization of steering knuckle structure. *International Journal for Simulation and Multidisciplinary Design Optimization*, 11, 4. <https://doi.org/10.1051/smdo/2019018>
- Sun, D., Zhang, L., Xiong, Y., & Ren, F. (2019, July 1). Cost-effective New Alloy Cast Iron. <https://hvalidate.perfdribe.com/fb803c746e9148689b3984a31fccd902//>
- Sun, Y., Yao, S. & Alexandersen, J. Topography optimisation using a reduced-dimensional model for convective heat transfer between plates with varying channel height and constant temperature. *Struct Multidisc Optim* 66, 206 (2023). <https://doi.org/10.1007/s00158-023-03661-2>

- Tagade, P. P., Sahu, A. R., & Kutarmare, H. C. (2015). Optimization and finite element analysis of steering knuckle. *International Journal of Computer Applications*.  
<https://research.ijcaonline.org/icquest2015/number4/icquest2844.pdf>
- Terrile, R. J., Aghazarian, H., Ferguson, M. I., Fink, W., Huntsberger, T. L., Keymeulen, D., Klimeck, G., Kordon, M. A., Lee, S., & Allmen, P. von .. (2004). *Evolutionary Computation Technologies for the Automated Design of Space Systems*. 8.  
<https://doi.org/10.1109/EH.2005.24>
- Tharazi, I., Halim, N. H. A., Salleh, F. M., Manurung, Y. H., Sabtu, A. S., Zulkifli, Z., & Khalit, M. I. (2024). Sheet Metal Forming Analysis of Aluminium Alloy AA6061 using |Altair INSPIRE Form Simulation. *Jurnal Kejuruteraan*, 36(3), 1237–1247.  
[https://doi.org/10.17576/jkukm-2024-36\(3\)-33](https://doi.org/10.17576/jkukm-2024-36(3)-33)
- Tisza, M., & Czinege, I. (2018, December 1). Comparative study of the application of steels and aluminium in lightweight production of automotive parts.  
<https://doi.org/10.1016/j.ijlmm.2018.09.001>
- Tyflopoulos, E., Lien, M., & Steinert, M. (2021, February 5). Optimization of Brake Calipers Using Topology Optimization for Additive Manufacturing. <https://doi.org/10.3390/app11041437>
- Velmanirajan, K., & Anuradha, K. (2020, March 4). Aluminium and Its Interlinking Properties.  
<https://doi.org/10.5772/intechopen.86553>
- W. Tao and M. C. Leu, "Design of lattice structure for additive manufacturing," 2016 International Symposium on Flexible Automation (ISFA), Cleveland, OH, USA, 2016, pp. 325-332, doi: 10.1109/ISFA.2016.7790182. keywords: {Lattices;Design automation;Design methodology;Geometry;Automation;Aerospace engineering},
- Wang, J., Lu, K., Zheng, Q., Ma, W., Peng, P., Chen, C., Li, J., Li, P., & Zheng, D. (2019, August 1). Study on Low-Pressure Casting Technique and Mold Design of the Aluminum Wheel. <https://doi.org/10.1109/icma.2019.8816222>
- Xu, Kuangdi. (2022).Simulation of Sand-Casting Process Using Altair Inspire Cast. 447-456. doi: 10.1007/978-981-19-3895-5\_36
- Yang, Z.. (2023). Topography Optimization of a Sheet Metal Assembly of Repetitive Features.  
<https://doi.org/10.4271/2023-01-0032>
- Yunjun, Z., Shi-jin, C., Huang, M., Yan, Y., Deng, Q., Li, S., Xia, J., Deng, L., Jin, J., Chen, T., & Yang, J. (2020, January 1). Research and application of precision forging forming process for flat thin flash of automobile disc steering knuckle. *Elsevier BV*, 50, 32-36.  
<https://doi.org/10.1016/j.promfg.2020.08.007>

Zhu, J., Zhou, H., Wang, C., Lü, Z., Yuan, S., & Zhang, W. (2021, January 1). A review of topology optimization for additive manufacturing: Status and challenges. Chinese journal of aeronautics/Chinese Journal of Aeronautics, 34(1), 91-110.  
<https://doi.org/10.1016/j.cja.2020.09.020>



## APPENDICES

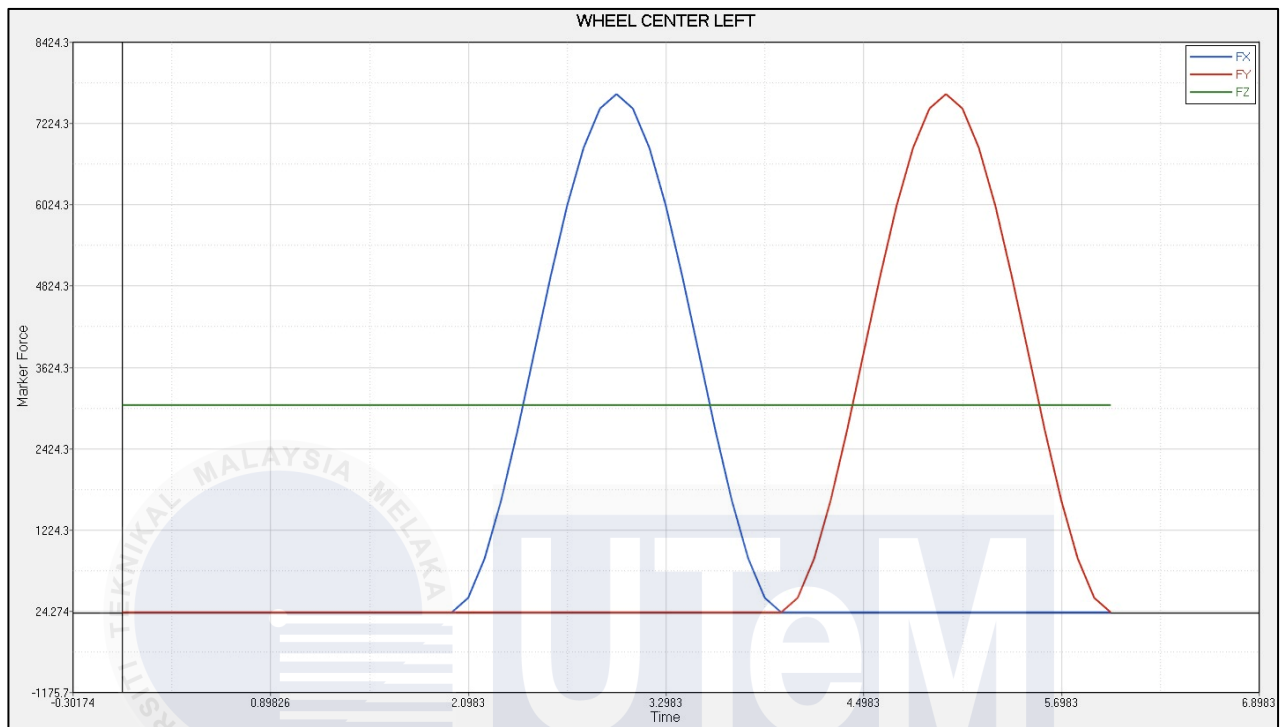
Gant Chart for PSM 1

Activity Project	PROJEK SARJANA MUDA 1 (PSM 1)														
	Week (Semester 6)														
	1	2	3	4	5	6	7	8	9	10	11	12	13	14	15
Briefing PSM 1															
Chapter 1															
Project problem statement, objective and scope identification															
Chapter 2 Literature finding (Journal, article, paper)															
Literature writing															
Data Scan at laboratory															
Chapter 3 Methodology															
Chapter 4 Preliminary result, analysis and summary writing															
Report Review 1															
BDP 1 submission report															
BDP1 presentation															

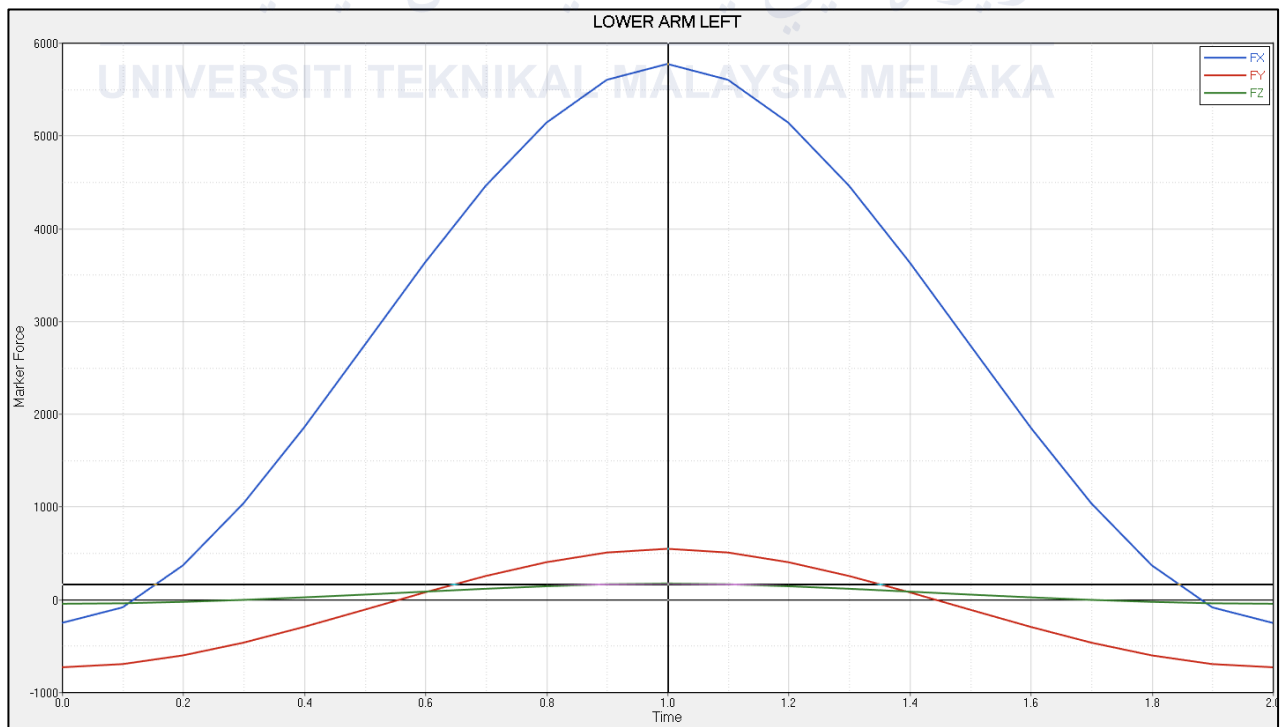
**Table Gant Chart for PSM 2**

Activity Project	PROJEK SARJANA MUDA 2 (PSM 2)														
	Week (Semester 7)														
	1	2	3	4	5	6	7	8	9	10	11	12	13	14	15
Briefing PSM 2															
Chapter 3 Adjustment															
Altair Motion View															
Identify the Loading & Boundary Condition															
Analysis of Topology Optimization															
Analysis of Lattice Structure															
Chapter 4 outcome result, analysis summary writing															
Report Review 2															
BDP 2 submission report															
BDP 2 presentation															

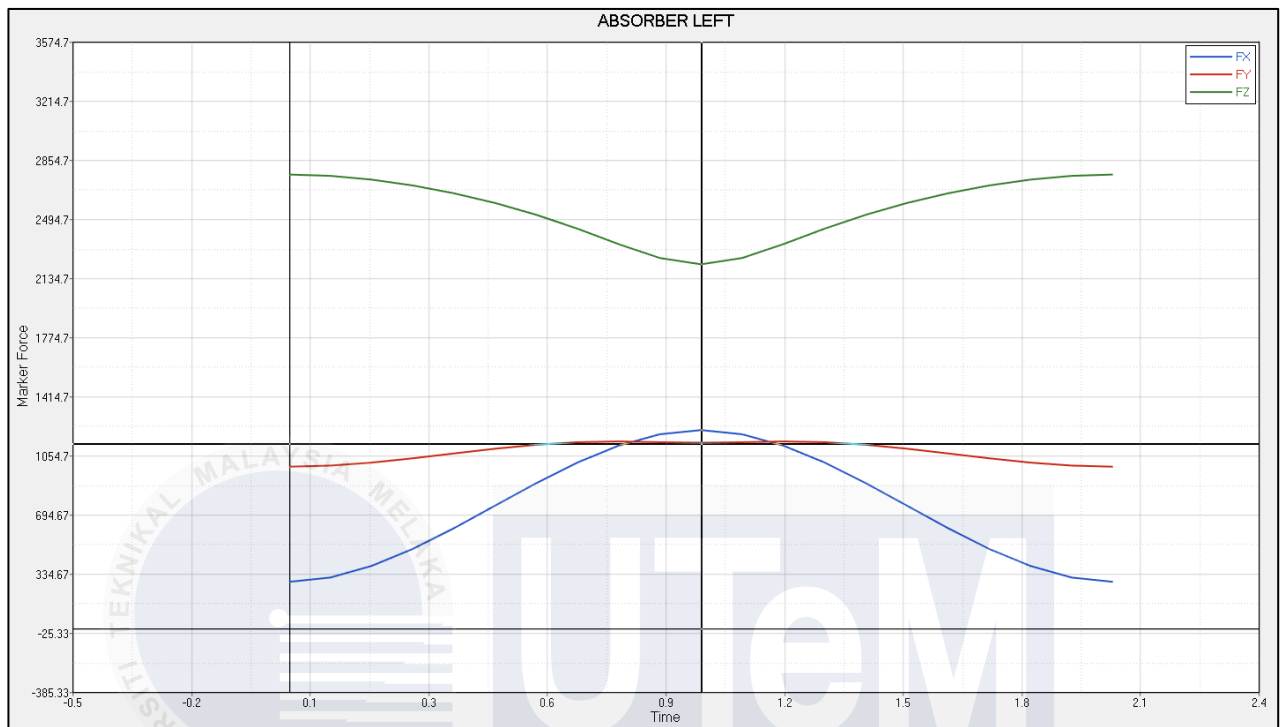
## Appendix A Graph Wheel Centre Left



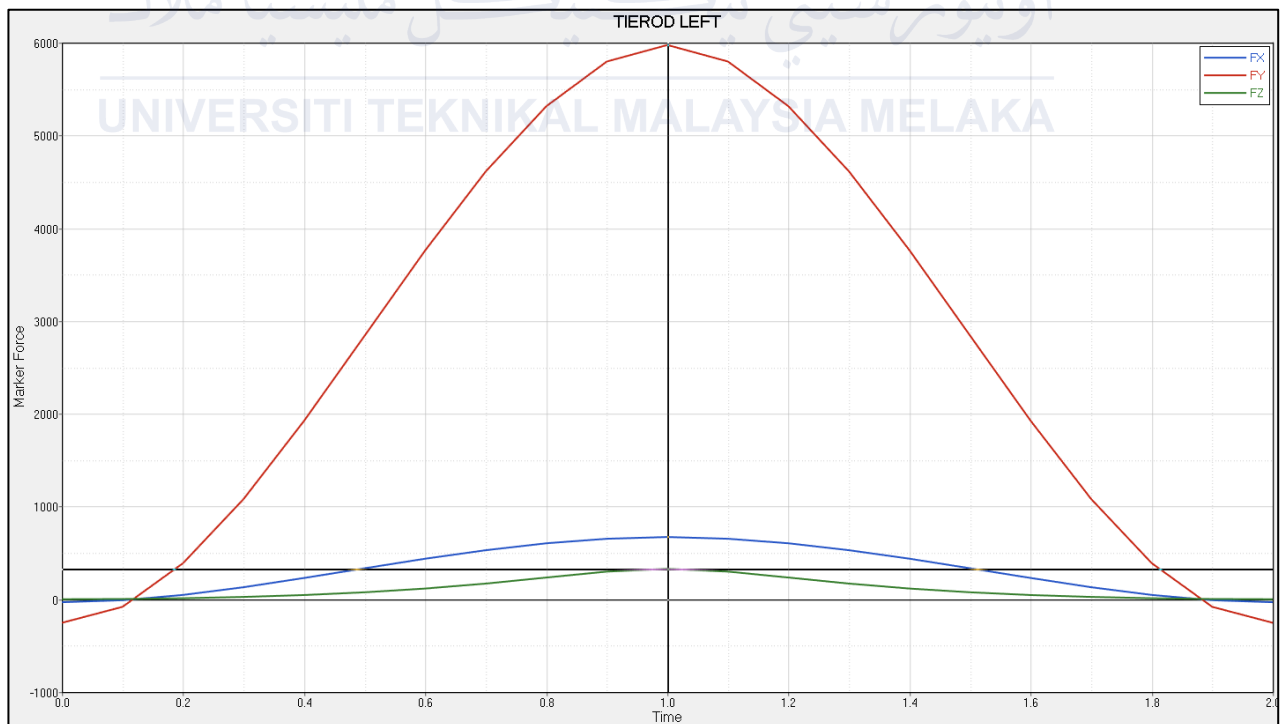
## Appendix B Graph Lower Arm Left



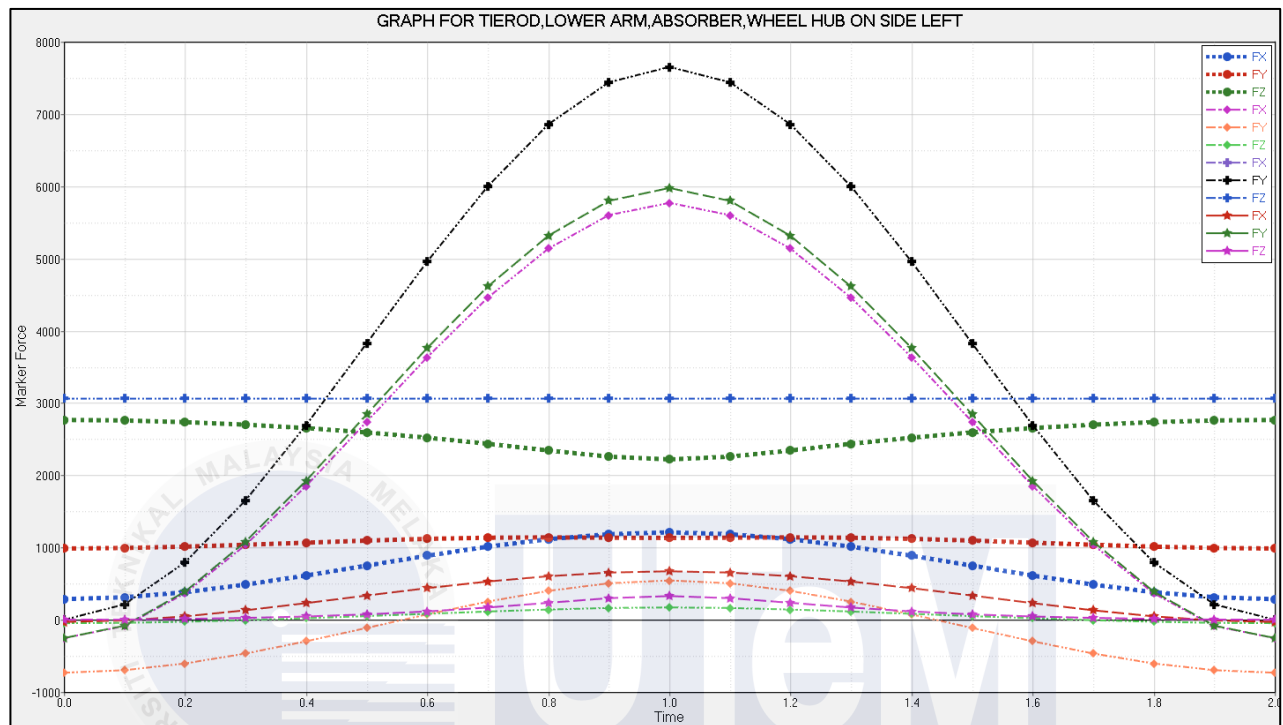
### Appendix C Graph Absorber Left



### Appendix D Graph Tie Rod Left



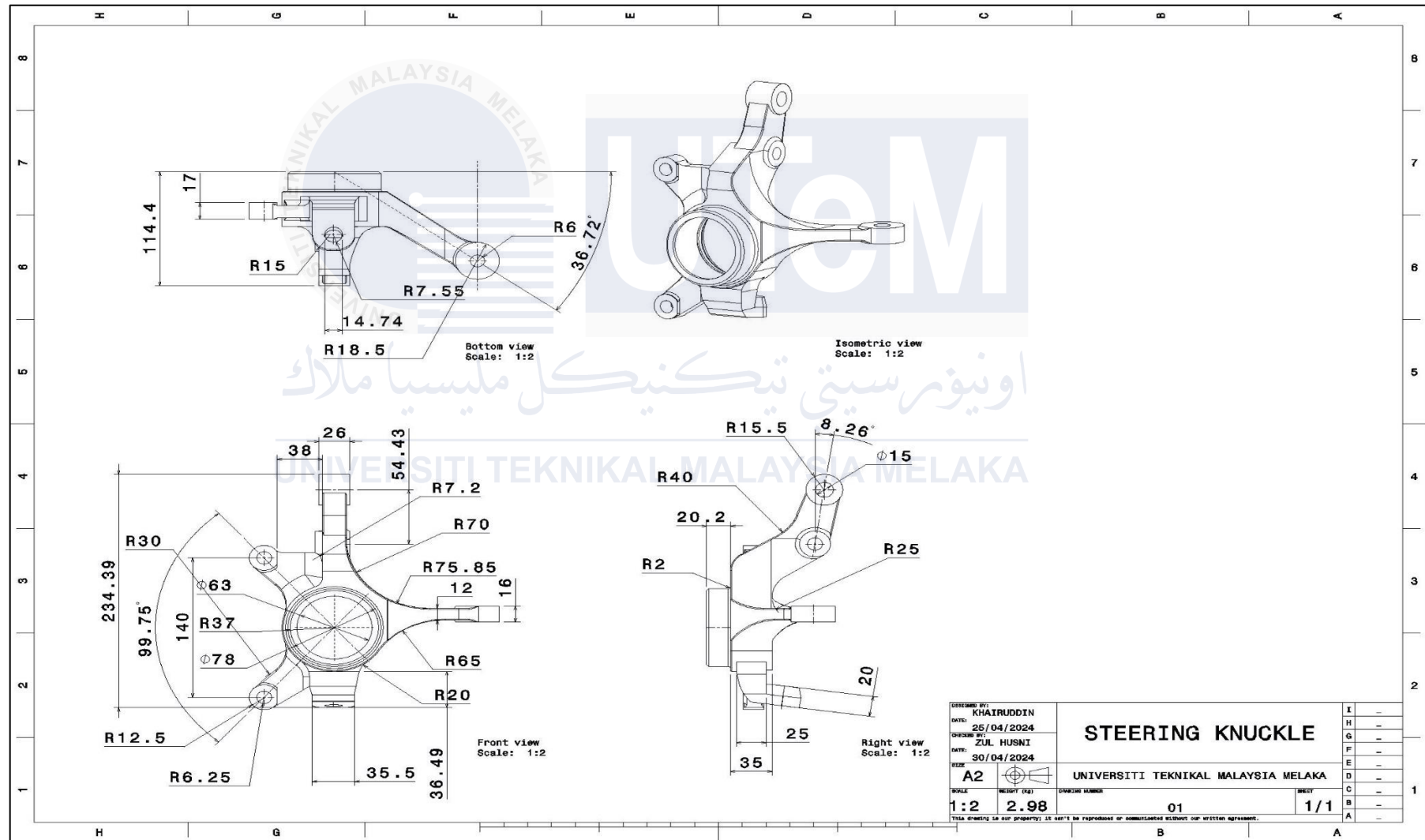
## Appendix E Graph For 4 Parts in Left Side



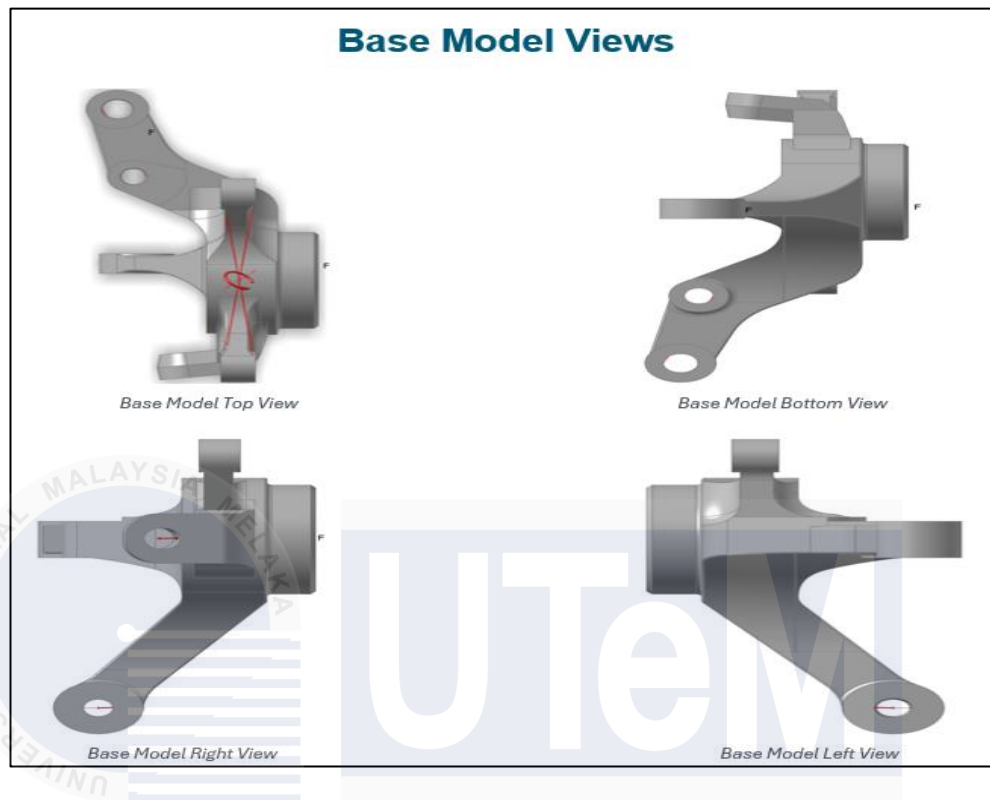
اونيورسيتي تېكنيكل مليسيا ملاك  
UNIVERSITI TEKNIKAL MALAYSIA MELAKA



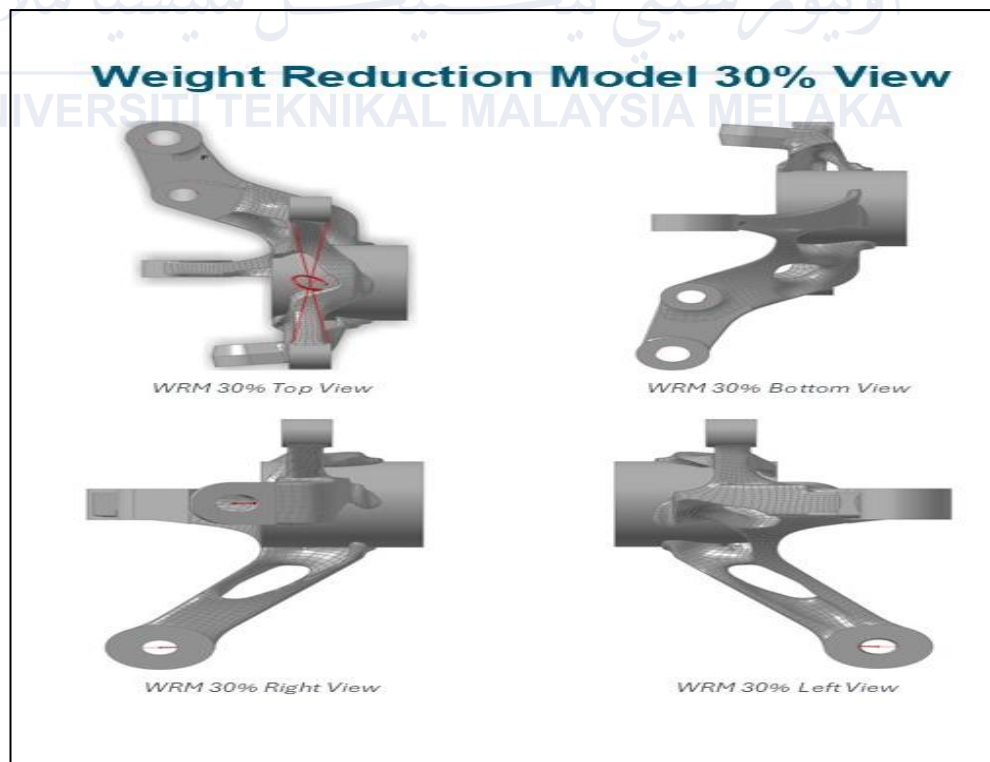
## Appendix F Technical Drawing of Base Model (Load Case 1)



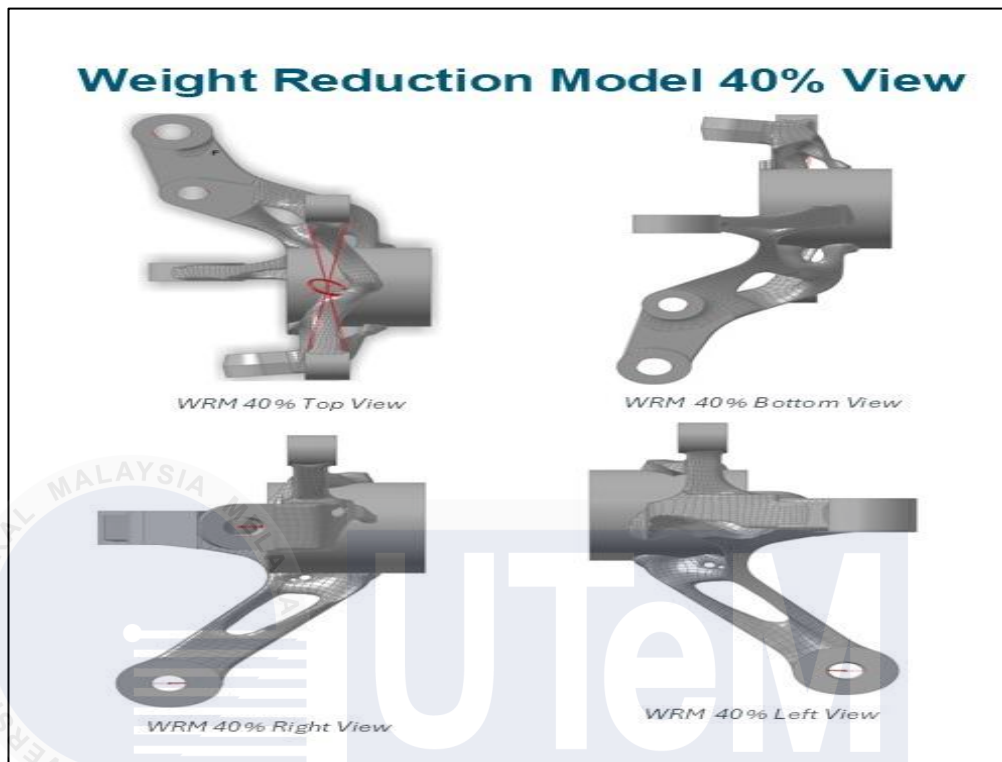
## Appendix G Base Model



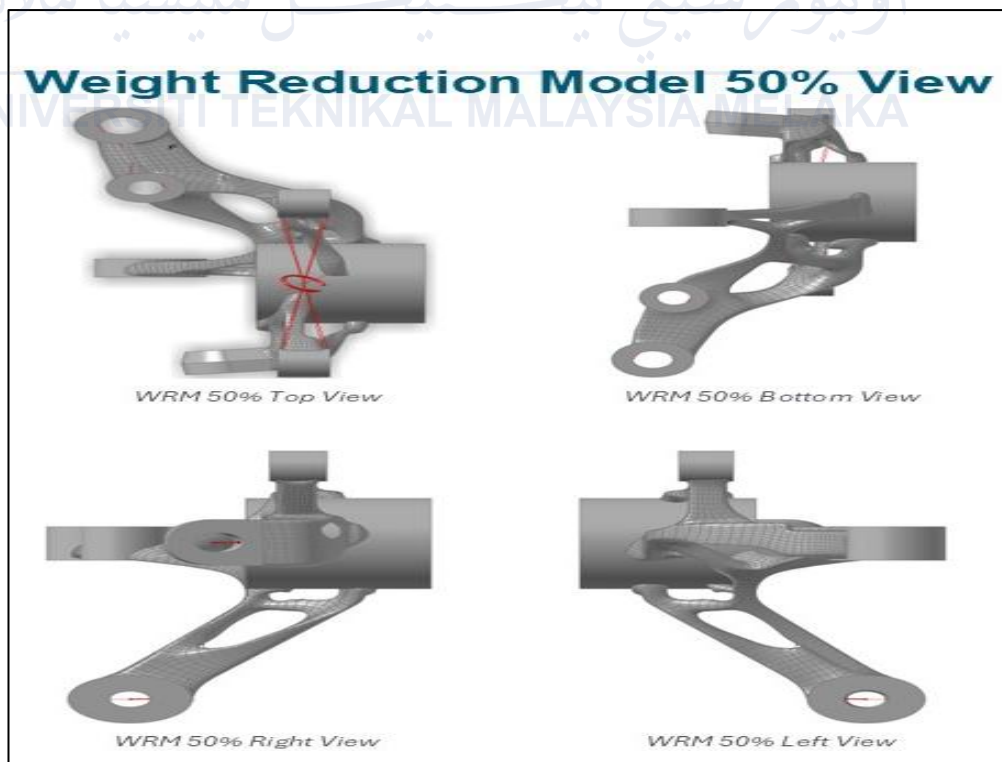
## Appendix H WRM 30%



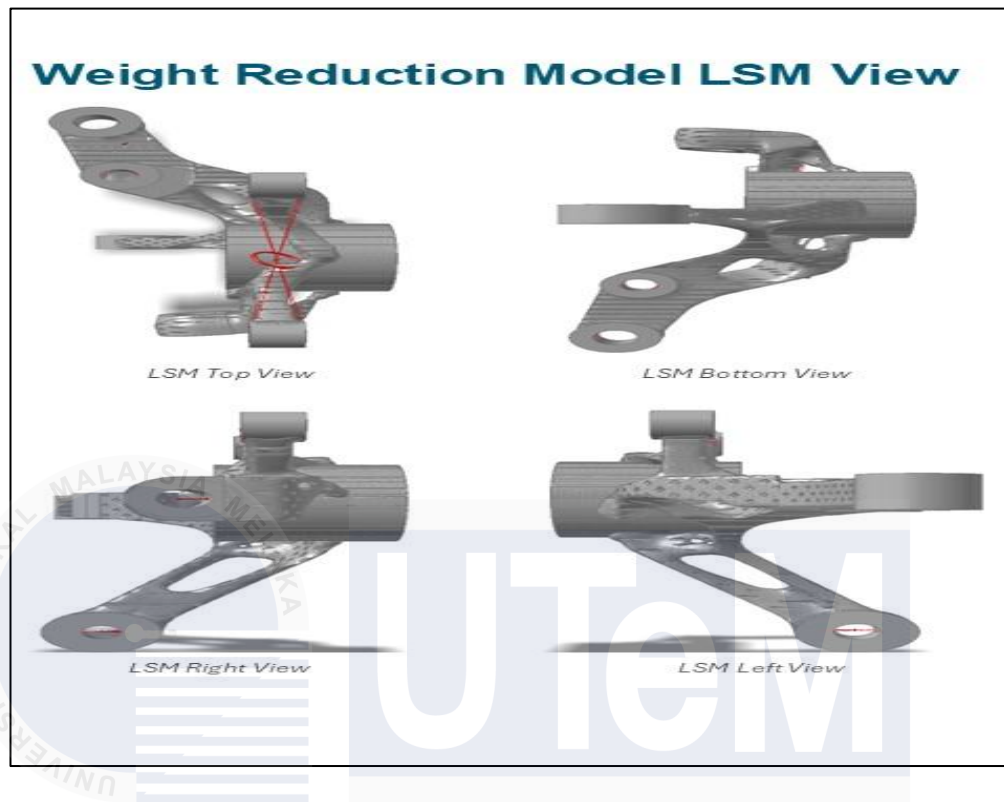
## Appendix I WRM 40%



## Appendix J WRM 50%



## Appendix K Model (Lattice Structure)



## Appendix L Base Model Fabrication



#### Appendix M WRM 40% Fabrication



TOPOLOGY MODEL 40%

#### Appendix N Lattice Structure Model Fabrication



LATTICE STRUCTURE MODEL 40%